

Information measures, entanglement and quantum evolution



Claudia Zander

Faculty of Natural & Agricultural Sciences

University of Pretoria

Pretoria

Submitted in partial fulfilment of the requirements for the degree

Magister Scientiae

April 2007

I declare that the thesis, which I hereby submit for the degree Magister Scientiae in Physics at the University of Pretoria, is my own work and has not previously been submitted by me for a degree at this or any other tertiary institution.

Acknowledgements

I would like to thank Prof. Plastino for being an excellent supervisor and my family and friends for their wonderful support. The financial assistance of the National Research Foundation (NRF) towards this research is hereby acknowledged. Opinions expressed and conclusions arrived at, are those of the authors and are not necessarily to be attributed to the NRF.

*I said to my soul, be still and wait without hope
For hope would be hope for the wrong thing;
Wait without love for love would be love of the wrong thing;
There is yet faith but the faith and the love and
The hope are all in the waiting.
Wait without thought, for you are not ready for thought:
So the darkness shall be the light, and the stillness the dancing.
T.S. Eliot*

Information measures, entanglement and quantum evolution

Claudia Zander

Supervised by Prof. A.R. Plastino

Department of Physics

Submitted for the degree: MSc (Physics)

Summary

Due to its great importance, both from the fundamental and from the practical points of view, it is imperative that the concept of entanglement is explored. In this thesis I investigate the connection between information measures, entanglement and the “speed” of quantum evolution.

In Chapter 1 a brief review of the different information and entanglement measures as well as of the concept of “speed” of quantum evolution is given. An illustration of the quantum no-cloning theorem in connection with closed timelike curves is also provided.

The work leading up to this thesis has resulted in the following three publications and in one conference proceeding:

- (A) C. Zander and A.R. Plastino, “Composite systems with extensive S_q (power-law) entropies”, *Physica A* **364**, (2006) pp. 145-156
- (B) S. Curilef, C. Zander and A.R. Plastino, “Two particles in a double well: illustrating the connection between entanglement and the speed of quantum evolution”, *Eur. J. Phys.* **27**, (2006) pp. 1193-1203
- (C) C. Zander, A.R. Plastino, A. Plastino and M. Casas, “Entanglement and the speed of evolution of multi-partite quantum systems”, *J. Phys. A: Math. Theor.* **40** (11), (2007) pp. 2861-2872

- (D) A.R. Plastino and C. Zander, “Would Closed Timelike Curves Help to Do Quantum Cloning?”, *AIP Conference Proceedings: A century of relativity physics*, *ERE* **841**, (2005) pp. 570-573.

Chapter 2 is based on (A) and is an application of the S_q (power-law) entropy. A family of models for the probability occupancy of phase space exhibiting an extensive behaviour of S_q and allowing for an explicit analysis of the thermodynamic limit is proposed.

Chapter 3 is based on (B). The connection between entanglement and the speed of quantum evolution as measured by the time needed to reach an orthogonal state is discussed in the case of two quantum particles moving in a one-dimensional double well. This illustration is meant to be incorporated into the teaching of quantum entanglement.

Chapter 4 is based on (C). The role of entanglement in time evolution is investigated in the cases of two-, three- and N -qubit systems. A clear correlation is seen between entanglement and the speed of evolution. States saturating the speed bound are explored in detail.

Chapter 5 summarizes the conclusions drawn in the previous chapters.

Contents

1	Introduction	1
1.0.1	Information and entropic measures	3
1.0.1.1	Shannon entropy	3
1.0.1.2	Rényi entropy	5
1.0.1.3	S_q power-law entropies	5
1.0.1.4	Mixed states in quantum mechanics	6
1.0.1.5	Quantum entropic measures	8
1.0.2	Entanglement	10
1.0.2.1	Entropy of entanglement	13
1.0.2.2	Entanglement measure based upon the linear entropy	14
1.0.2.3	Entanglement of formation	14
1.0.2.4	Negativity	16
1.0.2.5	Multi-partite entanglement measures	17
1.0.2.6	Application: superdense coding	18
1.0.2.7	Application: quantum teleportation	19
1.0.3	Speed of quantum evolution	21
1.0.4	Quantum no-cloning and CTC	22
1.0.4.1	Properties of the fidelity distance	23
1.0.4.2	CTC and quantum cloning	24
2	Composite Systems with Extensive S_q (Power-Law) Entropies	28
2.1	Overview	28
2.2	A discrete binary system	30
2.3	Comparison of the (p, λ) and the (p, κ) binary models	38

2.4	Quantum mechanical version of the binary system	40
2.5	A continuous system	44
2.6	Conclusions	48
3	Two Particles in a Double Well: Illustrating the Connection Between Entanglement and the Speed of Quantum Evolution	49
3.1	Overview	49
3.2	Two particles in a double well: separable vs entangled states . . .	50
3.3	Entanglement and the speed of quantum evolution	55
3.3.1	The speed of quantum evolution and its lower bound . . .	55
3.3.2	Comparing a separable state and a maximally entangled state	55
3.3.3	More general states	59
3.4	Conclusions	62
4	Entanglement and the Speed of Evolution of Multi-Partite Quantum Systems	64
4.1	Overview	64
4.2	Independent bi-partite systems	65
4.2.1	β -case	68
4.2.2	s -case	70
4.3	Interacting bi-partite systems	75
4.3.1	$\omega = \omega_0$	77
4.3.2	$\omega_0 = 0$	78
4.3.3	$\omega = 3\omega_0$	79
4.3.3.1	β -case	79
4.3.3.2	s -case	82
4.4	Entanglement and the speed of quantum evolution of three-partite systems	86
4.4.1	$\{\alpha, r\}$ -case	89
4.4.2	$\{r_1, r_2\}$ -case	99
4.5	N -qubits ESSLE states saturating the quantum speed limit	103
4.6	Role of entanglement in time-optimal quantum evolution	112
4.7	Conclusions	116

5	Conclusions	118
A	Numerical Search for Highly Entangled Multi-Qubit States	122
A.1	Overview	122
A.2	Pure state multi-partite entanglement measures based on the degree of mixedness of subsystems	123
A.3	Search for multi-qubit states of high entanglement	124
A.3.1	Searching algorithm	124
A.3.2	Results yielded by the searching algorithm	126
A.3.2.1	Four qubits	127
A.3.2.2	Five qubits	129
A.3.2.3	Six qubits	129
A.3.2.4	Seven qubits	130
A.3.2.5	The single-qubit reduced states conjecture	131
A.4	Conclusions	131
A.5	Search algorithm (MATHEMATICA)	133
A.6	The End	137
	References	138

Chapter 1

Introduction

“The difference between theory and practice is that in theory, there is no difference between practice and theory, but in practice, there is.”

In recent years the physics of information [1; 2; 3; 4] has received increasing attention [5; 6; 7; 8; 9; 10; 11; 12; 13; 14; 15; 16]. There is a growing consensus that information is endowed with physical reality, not in the least because the ultimate limits of any physical device that processes or transmits information are determined by the fundamental laws of physics [6; 11; 12; 13; 14]. That is, the physics of information and computation is an interdisciplinary field which has promoted our understanding of how the underlying physics influences our ability to both manipulate and use information. By the same token a plenitude of theoretical developments indicate that the concept of information constitutes an essential ingredient for a deep understanding of physical systems and processes [1; 2; 3; 4; 5; 6]. Landauer’s principle is one of the most fundamental results in the physics of information and is generally associated with the statement “information is physical”. It constitutes a historical turning point in the field by directly connecting information processing with (more) conventional physical quantities [17]. According to Landauer’s principle a minimal amount of energy is required to be dissipated in order to erase a bit of information in a computing device working at temperature T . This minimum energy is given by $kT \ln 2$, where k denotes Boltzmann’s constant [18; 19; 20]. Landauer’s principle has deep implications, as it allows for the derivation of several important results in classical and

quantum information theory [21]. It also constitutes a rather useful heuristic tool for establishing new links between, or obtaining new derivations of, fundamental aspects of thermodynamics and other areas of physics [22].

Information is something that is encoded in a physical state of a system and a computation is something that can be carried out on a physically realizable device. In order to quantify information one will need a measure of how much information is encoded in a system or process. Shannon entropy, Rényi entropy (which is a generalization of Shannon entropy) and S_q power-law entropies will be discussed. Since the universe is quantum mechanical at a fundamental level, the question naturally arises as to how quantum theory can enhance our insight into the nature of information.

Entanglement is one of the most fundamental aspects of quantum physics. It constitutes a physical resource that allows quantum systems to perform information tasks not possible within the classical domain. That is, quantum information is typically encoded in non-local correlations between the different parts of a physical system and these correlations have no classical counterpart. One of the aims of quantum information theory is to understand how entanglement can be used as a resource in communication and other information processes. Two spectacular applications of entanglement are quantum teleportation and superdense coding, which will be discussed in more detail.

Another important aspect of entanglement is its influence on the “speed” of quantum evolution of both independent and interacting systems and hence the possibility exists that it could speed up quantum computation and other quantum information processes.

Since the outcome of a quantum mechanical measurement has a random element, we are unable to infer the initial state of the system from the measurement outcome. This basic property of quantum measurements is connected with another important distinction between quantum and classical information: quantum information cannot be copied with perfect fidelity. This is called the no-cloning principle. If it were possible to make a perfect copy of a quantum state, one could

then measure an observable of the copy (in fact, we could perform measurements on as many copies as necessary) without disturbing the original, thereby defeating, for instance, the principle that two non-orthogonal quantum states cannot be distinguished with certainty [23]. Perfect quantum cloning would also allow the second principle of thermodynamics [23] to be defeated. It has also been proved that quantum cloning would allow (via EPR-type experiments [24]) information to be transmitted faster than the speed of light.

1.0.1 Information and entropic measures

Entropy is an extremely important concept in information theory and in other fields as well. The entropy of a probability distribution can be interpreted not only as a measure of uncertainty, but also as a measure of information. The amount of information which one obtains by observing the result of an experiment depending on chance, can be taken numerically equal to the amount of uncertainty concerning the outcome of the experiment before carrying it out [25]. The Shannon entropy, introduced by Claude E. Shannon, is a fundamental measure in information theory.

1.0.1.1 Shannon entropy

This is the unique, unambiguous criterion for the amount of uncertainty represented by a discrete probability distribution, that is, the amount of uncertainty concerning the outcome of an experiment:

$$H_{Shannon}(p_1, p_2, \dots, p_n) = -k \sum_{i=1}^n p_i \log_2 p_i, \quad (1.1)$$

where p_i is the probability that the discrete variable x will assume the value x_i and k is a positive constant which when set to one gives the unit “bits” for the entropy.

The three conditions which give rise to the above expression, are [26]

1. H is a continuous function of the p_i

-
2. If all p_i 's are equal, then $H(1/n, 1/n, \dots, 1/n)$ is a monotonic increasing function of n
 3. The composition law:

$$H(p_1, p_2, \dots, p_n) = H(w_1, w_2, \dots, w_r) + w_1 H(p_1/w_1, \dots, p_k/w_1) + w_2 H(p_{k+1}/w_2, \dots, p_{k+m}/w_2) + \dots, \quad (1.2)$$

where $w_1 = (p_1 + \dots + p_k)$, $w_2 = (p_{k+1} + \dots + p_{k+m})$, etc.

In the view of Jaynes [26; 27; 28], the relationship between thermodynamic and informational entropy is, that thermodynamics should be seen as an application of Shannon's information theory. Thermodynamic entropy is then interpreted as being an estimate of the amount of information that remains uncommunicated by a description solely in terms of the macroscopic variables of classical thermodynamics and that would be needed to define the detailed microscopic state of the system. The increase in entropy characteristic of irreversibility always signifies, both in quantum mechanics and classical theory, a loss of information.

One of the most important property of entropy is its additivity, that is, given two probability distributions $P = (p_1, p_2, \dots, p_n)$ and $Q = (q_1, q_2, \dots, q_m)$,

$$H_{Shannon}[P * Q] = H_{Shannon}[P] + H_{Shannon}[Q], \quad (1.3)$$

where by $P * Q$ we denote the direct product of the distributions. Now, one cannot replace condition 3 with eq. (1.3), since the latter condition is much weaker. Actually, there are several quantities other than eq. (1.1) which satisfy conditions 1, 2 and eq. (1.3). The following is one generalization of the Shannon entropy.

1.0.1.2 Rényi entropy

The *entropy of order α* of the distribution $P = (p_1, p_2, \dots, p_n)$ is defined to be [25]

$$R_\alpha(p_1, p_2, \dots, p_n) = \frac{1}{1 - \alpha} \log_2 \left(\sum_{k=1}^n p_k^\alpha \right), \quad (1.4)$$

where $\alpha \geq 0$, $\alpha \neq 1$ and R_α is measured in units of bits. That is, the above expression can be regarded as a measure of the entropy of the distribution P and in the limiting case $\alpha \rightarrow 1$ we recover the Shannon entropy:

$$\lim_{\alpha \rightarrow 1} R_\alpha(p_1, p_2, \dots, p_n) = \sum_{k=1}^n p_k \log_2 \frac{1}{p_k}. \quad (1.5)$$

An interpretation of Rényi entropy is, that the greater the parameter α the greater the dependence of the entropy on the probabilities of the more probable values and hence less on the improbable ones.

Closely related to Rényi entropy is another generalization of Shannon's entropy that has been the subject of much interest recently, the S_q power-law entropy.

1.0.1.3 S_q power-law entropies

The power-law S_q entropies, advanced by Tsallis, are non-extensive entropic functionals given by [29; 30; 31],

$$\begin{aligned} S_q(p) &= \frac{1}{q-1} \left(1 - \sum_i p_i^q \right) && \text{(discrete case)} \\ S_q(p) &= \frac{1}{q-1} \left(1 - \int p^q(x) dx \right) && \text{(continuous case)} \end{aligned} \quad (1.6)$$

where p denotes the probability distribution and the parameter q is any real number (characterizing a particular statistics), $q \neq 1$. The Tsallis entropy possesses the usual properties of positivity, equiprobability, concavity, irreversibility and it generalizes the standard additivity (eq. (1.3)) as well as the Shannon additivity

(eq. (1.2)) [30]. The normal Boltzmann-Gibbs entropy is recovered in the limit $q \rightarrow 1$.

The non-extensive thermo-statistical formalism based upon the S_q entropies has been applied to a variegated family of problems in physics, astronomy, biology and economics [32]. In particular, the case $q = 2$ constitutes a powerful tool for the study of quantum entanglement (see Chapters 3 and 4 of this dissertation). Tsallis entropy can also be regarded as a one-parameter generalization of the Shannon entropy.

The characteristic property of Tsallis entropy is *pseudoadditivity*,

$$S_q(A, B) = S_q(A) + S_q(B) + (1 - q)S_q(A)S_q(B), \quad (1.7)$$

with A and B being two mutually independent finite event systems whose joint probability distribution satisfies

$$p(A, B) = p(A)p(B). \quad (1.8)$$

From this it is evident that q is a measure of the non-extensivity of the system.

1.0.1.4 Mixed states in quantum mechanics

The density operator language gives a description of quantum mechanics that does not take as its foundation the state vector. A quantum system whose state $|\psi\rangle$ is known exactly is said to be in a pure state. In this case the density operator is simply $\rho = |\psi\rangle\langle\psi|$. Otherwise, ρ is in a mixed state and it is said to be a mixture of the different pure states in the ensemble for ρ . That is, suppose a quantum system is in one of a number of states $|\psi_i\rangle$ (where i is an index) with respective probabilities p_i ; the ensemble of pure states is then denoted by $\{p_i, |\psi_i\rangle\}$. It is important to note that the states $|\psi_i\rangle$ do not need to be orthogonal to each other. The density operator for the system is then defined by

$$\rho \equiv \sum_i p_i |\psi_i\rangle\langle\psi_i|, \quad (1.9)$$

where $\sum_i p_i = 1$. Now an operator ρ is the density operator associated with an ensemble $\{p_i, |\psi_i\rangle\}$ if and only if it satisfies the conditions:

- (a) Hermiticity condition: ρ is Hermitian, that is, $\rho^\dagger = \rho$
- (b) Normalization condition: ρ has trace equal to one
- (c) Positivity condition: ρ is a positive operator.

The above conditions provide a characterization of density operators that is intrinsic to the operator itself: one can define a density operator to be a positive Hermitian operator ρ which has trace equal to one.

Given a density matrix ρ , the decomposition in equation (1.9) is not unique. One may have different $\{p_i, |\psi_i\rangle\}$ leading to the same ρ :

$$\sum_i p'_i |\psi'_i\rangle\langle\psi'_i| = \sum_i p_i |\psi_i\rangle\langle\psi_i|. \quad (1.10)$$

As an illustration consider for instance two decompositions

$$\begin{aligned} \rho &= \begin{pmatrix} \frac{1}{4} & 0 & 0 & 0 \\ 0 & \frac{1}{4} & 0 & 0 \\ 0 & 0 & \frac{1}{4} & 0 \\ 0 & 0 & 0 & \frac{1}{4} \end{pmatrix} = \frac{1}{4} |00\rangle\langle 00| + \frac{1}{4} |01\rangle\langle 01| + \frac{1}{4} |10\rangle\langle 10| + \frac{1}{4} |11\rangle\langle 11| \\ &= \frac{1}{8} (|00\rangle + |11\rangle)(\langle 00| + \langle 11|) + \frac{1}{8} (|00\rangle - |11\rangle)(\langle 00| - \langle 11|) \\ &\quad + \frac{1}{8} (|01\rangle + |10\rangle)(\langle 01| + \langle 10|) + \frac{1}{8} (|01\rangle - |10\rangle)(\langle 01| - \langle 10|). \end{aligned} \quad (1.11)$$

This non-unique character of the decomposition of ρ as a “mixture” of pure states is very relevant for the discussion of the concept of “entanglement of formation”, see equations (1.28) and (1.29).

The main applications of the density operator formalism are the descriptions of quantum systems whose state is only partially known, and the description of subsystems of a composite quantum system, where the latter description is provided by the reduced density operator. The density matrices for the description of subsystems form the basis of the description of the phenomenon of quantum entanglement.

1.0.1.5 Quantum entropic measures

The following quantum entropic measures are invariant under unitary transformation, since the trace is invariant under unitary transformation:

1. von Neumann entropy
2. Tsallis entropy
3. Rényi entropy.

A proper extension of Shannon's entropy to the quantum case is given by the von Neumann entropy, defined as

$$S(\rho) = -\text{Tr}(\rho \log_2 \rho), \quad (1.12)$$

where ρ is the density matrix of the system. Thus quantum states are described by replacing probability distributions with density operators. In order to compute $S(\rho)$, one has to write ρ in terms of its eigenbasis. Since $\lim_{p \rightarrow 0} p \log_2 p = 0$ is well defined, we can set $0 \log_2 0 = 0$ by continuity.

If the system is finite (finite dimensional matrix representation) the entropy (1.12) describes the departure of our system from a pure state. In other words, it measures the degree of mixture of our state describing a given finite system.

The following are properties of the von Neumann entropy [33]:

- $S(\rho)$ is only zero for pure states.
- $S(\rho)$ is maximal and equal to $\log_2 N$ for a maximally mixed state, N being the dimension of the Hilbert space.
- $S(\rho)$ is invariant under a change of basis of ρ , that is, $S(\rho) = S(U \rho U^\dagger)$, with U a unitary transformation.
- Given two density matrices ρ_I, ρ_{II} describing independent systems I and II , we have that $S(\rho)$ is additive: $S(\rho_I \otimes \rho_{II}) = S(\rho_I) + S(\rho_{II})$.

-
- If ρ_A and ρ_B are the reduced (marginal) density matrices of the general state ρ_{AB} , then

$$S(\rho_{AB}) \leq S(\rho_A) + S(\rho_B). \quad (1.13)$$

The last property is known as subadditivity and also holds for the Shannon entropy. However, some properties of the Shannon entropy do not hold for the von Neumann entropy, thus leading to many interesting consequences for quantum information theory. While in Shannon's theory the entropy of a composite system can never be lower than the entropy of any of its parts, in quantum theory this is not the case and can actually be seen as an indicator of an entangled state ρ_{AB} .

In the framework of quantum information theory the von Neumann entropy is extensively used in different forms such as conditional and relative entropies. Due to the inadequacy of the Shannon information measure in certain situations, the von Neumann entropy is likewise not adequate as an appropriate quantum generalization of Shannon entropy. In classical measurements the Shannon information measure is a natural measure of our ignorance about the properties of a system, whose existence is independent of measurement. Conversely, quantum measurement cannot claim to reveal the properties of a system that existed before the measurement was made. This argument has encouraged the introduction of the non-additivity property of Tsallis' entropy as the main reason for recovering a true quantal information measure in the quantum context, thus claiming that non-local correlations ought to be described because of the particularity of Tsallis' entropy.

In the quantum case the Tsallis entropy becomes

$$S_q(\rho) = \frac{1}{q-1} [1 - \text{Tr}(\rho^q)] \quad (1.14)$$

and the Rényi entropy

$$R_\alpha(\rho) = \frac{1}{1-\alpha} \log_2 [\text{Tr}(\rho^\alpha)]. \quad (1.15)$$

1.0.2 Entanglement

A bipartite pure state $|\psi\rangle_{AB}$ is entangled if it cannot be expressed as a direct product,

$$|\psi\rangle_{AB} = |\phi\rangle_A |\varphi\rangle_B. \quad (1.16)$$

Pure states that can be factorized as (1.16) are called separable or non-entangled. The marginal density matrices $\rho_A = \text{Tr}_B(|\psi\rangle_{AB}\langle\psi|)$ and $\rho_B = \text{Tr}_A(|\psi\rangle_{AB}\langle\psi|)$ associated with an entangled pure state correspond to mixed states. This means that the joint state can be completely known, yet the subsystems are in mixed states and hence we do not have maximal knowledge concerning them. A classic example is the singlet state of two spin- $\frac{1}{2}$ particles, $\frac{1}{\sqrt{2}}(|\uparrow\downarrow\rangle - |\downarrow\uparrow\rangle)$, in which neither particle has a definite spin direction, but when one is observed to be spin-up, the other one will always be observed to be spin-down and vice-versa. This is the case despite the fact that it is impossible to predict (using quantum mechanics) which set of measurement results will be observed. As a consequence, measurements performed on one system seem to be instantaneously influencing other systems entangled with it. If the state is separable then subsystems A and B are with certainty in the pure states $|\phi\rangle_A$ and $|\varphi\rangle_B$ respectively.

The general idea behind the most important entanglement measures of pure bipartite states is the following. The more “mixed” the marginal density matrices associated with the subsystems are, the more entangled is the global state of the bi-partite system. Consequently, any appropriate measure of the degree of mixedness of a subsystem’s marginal density matrix provides a measure of the amount of entanglement exhibited by the global, bi-partite pure state.

A bi-partite mixed state of a composite quantum system is entangled if it cannot be represented as a mixture of factorizable pure states,

$$\rho_{AB} = \sum_i p_i |\alpha_i\rangle\langle\alpha_i| \otimes |\beta_i\rangle\langle\beta_i|, \quad (1.17)$$

where $\sum_i p_i = 1$, and $|\alpha_i\rangle$ and $|\beta_i\rangle$ are pure states of subsystems A and B respectively. It is also of considerable interest to quantify the entanglement of general bi-partite mixed states, but unfortunately mixed-state entanglement is not as well understood as pure-state entanglement and is often very difficult to compute. One reason for the interest in mixed-state entanglement is a connection with the transmission of quantum information through noisy quantum channels [34].

Entanglement can be regarded as a physical resource which is associated with the peculiar non-classical correlations that are possible between separated quantum systems. Entanglement lies at the basis of important quantum information processes such as quantum cryptographic key distribution [35], quantum teleportation [36], superdense coding [37] and quantum computation [38]. The experimental implementation of these processes could lead to a deep revolution in both the communication and computational technologies. There are several valid measures of entanglement, some more useful and practical than others, depending on the type of analysis to be performed and on the specific application or system being analyzed.

Entangled states cannot be prepared locally by acting on each subsystem individually [39]. This property is directly related to entanglement being invariant under local unitary transformation: one can perform a unitary operation on a subsystem without changing the entanglement of the global system. As an illustration consider a system consisting of two subsystems A and B . A local unitary operator is then defined to be $U = U_A \otimes U_B$ where the unitary operators U_A and U_B solely act on A and B respectively. A bi-partite pure state can be expressed in a standard form (the Schmidt decomposition) that is often useful. That is, according to the Schmidt decomposition an arbitrary state $|\psi\rangle_{AB}$ in the Hilbert space $\mathcal{H} = \mathcal{H}_A \otimes \mathcal{H}_B$ of the composite system can be expressed as follows

$$|\psi\rangle_{AB} = \sum_i \sqrt{\lambda_i} |\phi_i^{(A)}\rangle |\phi_i^{(B)}\rangle \quad (1.18)$$

in terms of particular orthonormal bases $\{|\phi_i^{(A)}\rangle\}$ and $\{|\phi_j^{(B)}\rangle\}$ in \mathcal{H}_A and \mathcal{H}_B respectively. The summation over the index in the Schmidt decomposition goes to the smaller of the dimensionalities of the two Hilbert spaces \mathcal{H}_A and \mathcal{H}_B [40]. The λ_i 's are non-negative real numbers satisfying $\sum_i \lambda_i = 1$. It is important to note that the Schmidt decomposition of a given quantum state is not unique and that the Schmidt decomposition pertains to a specific state of the composite system, so for two different states we have two different Schmidt decompositions [40]. The marginal density matrices for ρ_A and ρ_B are given by

$$\begin{aligned} \rho_A &= \text{Tr}_B[|\psi\rangle_{AB}\langle\psi|] \\ &= \sum_i \lambda_i |\phi_i^{(A)}\rangle\langle\phi_i^{(A)}| \end{aligned} \quad (1.19)$$

$$\rho_B = \sum_i \lambda_i |\phi_i^{(B)}\rangle\langle\phi_i^{(B)}|. \quad (1.20)$$

From this it is clear that ρ_A and ρ_B have the same non-zero eigenvalues. If the subsystems A and B have different dimensions, then the number of zero eigenvalues of ρ_A and ρ_B differ. The number of non-zero eigenvalues in ρ_A (or ρ_B) and hence the number of terms in the Schmidt decomposition of $|\psi\rangle_{AB}$ is called the Schmidt number for the state $|\psi\rangle_{AB}$. In terms of this quantity one can define what it means for a bi-partite pure state to be entangled: $|\psi\rangle_{AB}$ is entangled if its Schmidt number is greater than one, otherwise it is separable.

From equations (1.19) and (1.20), the von Neumann entropy of $|\psi\rangle_{AB}$ is then

$$S_{vN}(\rho_A) = - \sum_i \lambda_i \log_2 \lambda_i = S_{vN}(\rho_B). \quad (1.21)$$

Acting on $|\psi\rangle_{AB}$ with the local unitary operator U results in the state $|\psi'\rangle_{AB}$,

$$[U_A \otimes U_B]|\psi\rangle_{AB} = \sum_i \sqrt{\lambda_i} \left(U_A |\phi_i^{(A)}\rangle \otimes U_B |\phi_i^{(B)}\rangle \right). \quad (1.22)$$

The marginal density matrix for subsystem A then becomes

$$\rho'_A = \text{Tr}_B \left([U_A \otimes U_B]|\psi\rangle_{AB}\langle\psi|[U_A^\dagger \otimes U_B^\dagger] \right) \quad (1.23)$$

and so the von Neumann entropy is

$$S_{vN}[\rho_A] = S_{vN}[\rho'_A] = - \sum_i \lambda_i \log_2 \lambda_i \quad (1.24)$$

which implies that the entanglement remains constant under local unitary operation. This means that the only way to entangle A and B is for the two subsystems to directly interact with one another, that is, one has to apply a collective or global unitary transformation to the state. It is a law of entanglement theory (which can be derived as a theorem of quantum mechanics [41]) that the entanglement between two spatially separated systems cannot, on average, be increased by carrying out local operations and classical communications (LOCC) protocols [42].

1.0.2.1 Entropy of entanglement

The entropy of entanglement is given by the von Neumann entropy of the marginal density matrices. This is an operational measure: it gives the number of ebits that are needed to create a pure entangled state in the laboratory. An “ebit” or entanglement bit is a unit of entanglement and is defined as the amount of entanglement in a Bell pair $|\beta_{00}\rangle, |\beta_{01}\rangle, |\beta_{10}\rangle$ or $|\beta_{11}\rangle$, see equations (1.41). These states and any related to them by local unitary operations can be used to perform a variety of non-classical feats such as superdense coding and quantum teleportation and are thus a valuable resource [42].

For each pure state $|\psi\rangle_{AB}$, the entanglement is defined as the von Neumann entropy of either of the two subsystems A and B [43],

$$E(|\psi\rangle_{AB}) = -\text{Tr}(\rho_A \log_2 \rho_A) = -\text{Tr}(\rho_B \log_2 \rho_B), \quad (1.25)$$

where ρ_A and ρ_B are the marginal density matrices of the subsystems:

$$\begin{aligned} \rho_A &= \text{Tr}_B(|\psi\rangle_{AB}\langle\psi|) \\ \rho_B &= \text{Tr}_A(|\psi\rangle_{AB}\langle\psi|). \end{aligned} \quad (1.26)$$

1.0.2.2 Entanglement measure based upon the linear entropy

Another useful entanglement measure which gives the degree of mixedness of the density matrix ρ and which is easy to compute (since there is no need to diagonalize ρ) is given by the linear entropy,

$$S(\rho) = 1 - \text{Tr}(\rho^2). \quad (1.27)$$

This entropic measure coincides (up to a constant multiplicative factor) with the quantum power-law entropy S_q with Tsallis' parameter $q = 2$. Similar to the von Neumann entropy, for each pure state $|\psi\rangle_{AB}$ the entanglement is defined as the linear entropy of either of the two subsystems A and B . The linear entropy does not stem from an operational point of view, but it gives a good idea of how much entanglement is present when one is not interested in the detailed resources needed to create these states in a laboratory.

1.0.2.3 Entanglement of formation

This is a physically motivated measure of entanglement for mixed states which is intended to quantify the resources needed to create a given entangled state [44]. That is, from an “engineering” point of view this measure gives the minimum number of ebits that are needed to create entangled states. Since entanglement is a valuable resource one wants to minimize the amount of ebits needed.

The entanglement of formation is defined as follows [44; 45]: given a density matrix ρ of a pair of quantum systems A and B , consider all possible pure-state decompositions of ρ , that is, all ensembles of states $|\psi_i\rangle$ with probabilities p_i such that

$$\rho = \sum_i p_i |\psi_i\rangle\langle\psi_i|. \quad (1.28)$$

This non-unique character of the decomposition of ρ has been discussed in Section 1.0.1.4.

For each pure state, the entanglement E is defined as the von Neumann entropy of either of the two subsystems A and B (see (1.25)). The entanglement of

formation of the mixed state ρ is then defined as the average entanglement of the pure states of the decomposition, minimized over all decompositions of ρ :

$$\mathbf{E}(\rho) = \min \sum_i p_i E(\psi_i). \quad (1.29)$$

In other words, the entanglement of formation of a mixed state ρ is defined as the minimum average entanglement of an ensemble of pure states that represents ρ . Of particular interest is the “entanglement of formation” (EOF) for mixed states of a two-qubit system. In that special case an explicit formula for the entanglement of formation has been discovered. For bi-partite states of higher dimension or for three and more qubits one has to resort to numerical optimization routines which are computationally expensive and often extremely hard to compute. In the latter instance one then has to use other measures such as the negativity discussed in Section 1.0.2.4. To obtain the EOF of an arbitrary state of two qubits, one has to follow the procedure by Wootters [44]. For a general state ρ of two qubits, the spin-flipped state is

$$\tilde{\rho} = (\sigma_y \otimes \sigma_y) \rho^* (\sigma_y \otimes \sigma_y), \quad (1.30)$$

where ρ^* is the complex conjugate of ρ taken in the standard basis and σ_y is the usual Pauli matrix. The EOF is then given by

$$\mathbf{E}(\rho) = \mathcal{E}(C(\rho)), \quad (1.31)$$

where the function \mathcal{E} is

$$\begin{aligned} \mathcal{E}(C) &= h\left(\frac{1 + \sqrt{1 - C^2}}{2}\right), \\ h(x) &= -x \log_2 x - (1 - x) \log_2 (1 - x) \end{aligned} \quad (1.32)$$

and the “concurrence” C is defined as

$$C(\rho) = \max\{0, \lambda_1 - \lambda_2 - \lambda_3 - \lambda_4\}, \quad (1.33)$$

with the λ_i 's being the eigenvalues, in decreasing order, of the Hermitian matrix $R = \sqrt{\sqrt{\rho} \tilde{\rho} \sqrt{\rho}}$. This procedure clearly also holds for bi-partite pure states $|\phi\rangle$

and in that case the EOF can be interpreted roughly as the number of qubits that must have been exchanged between two observers in order for them to share the state $|\phi\rangle$ [44].

1.0.2.4 Negativity

The partial transpose of a density matrix ρ can be used to determine whether the mixed quantum state represented by ρ is separable [46] and can therefore also be used to detect entanglement in ρ [47; 48]. This entanglement measure is effective in numerical explorations of multi-partite mixed states due to its relative simplicity and computability [49].

Consider an N -qubit state of the form

$$|\psi\rangle = \sum_{k=0}^{2^N-1} c_k |k\rangle, \quad (1.34)$$

where the c_k satisfy the normalization condition and each $|k\rangle$ is a basis state $|a_1 a_2 \dots a_N\rangle$ with $a_1 a_2 \dots a_N$ being the binary representation of the integer k , $a_i \in \{0, 1\}$. A density operator of a mixed state ρ can be written in terms of pure states having the same form as $|\psi\rangle$:

$$\begin{aligned} \rho &= \sum_{j=1}^n p_j |\psi_j\rangle \langle \psi_j| \\ &= \sum_{j=1}^n p_j \sum_{a_1, a_2, \dots, a_N=0}^1 c_{a_1 a_2 \dots a_N}^j |a_1 a_2 \dots a_N\rangle \sum_{a'_1, a'_2, \dots, a'_N=0}^1 c_{a'_1 a'_2 \dots a'_N}^{j*} \langle a'_1 a'_2 \dots a'_N| \\ &= \sum_{j=1}^n p_j \sum_{\substack{a_1, a_2, \dots, a_N=0 \\ a'_1, a'_2, \dots, a'_N=0}}^1 d_{a_1 a_2 \dots a_N a'_1 a'_2 \dots a'_N}^j |a_1 a_2 \dots a_N\rangle \langle a'_1 a'_2 \dots a'_N|, \end{aligned} \quad (1.35)$$

$d_{a_1 a_2 \dots a_N a'_1 a'_2 \dots a'_N}^j = c_{a_1 a_2 \dots a_N}^j c_{a'_1 a'_2 \dots a'_N}^{j*}$. To construct the partial transpose of ρ with respect to the index i (corresponding to the cut set $\{i\}$), we have to transpose the bits a_i and a'_i in the basis states:

$$\begin{aligned}
\rho^{T_{\{i\}}} &= \sum_{j=1}^n p_j \sum_{\substack{a_1, a_2, \dots, a_N=0 \\ a'_1, a'_2, \dots, a'_N=0}}^1 d_{a_1 \dots a_i \dots a_N a'_1 \dots a'_i \dots a'_N}^j |a_1 \dots a_i \dots a_N\rangle \langle a'_1 \dots a_i \dots a'_N| \\
&= \sum_{j=1}^n p_j \sum_{\substack{a_1, a_2, \dots, a_N=0 \\ a'_1, a'_2, \dots, a'_N=0}}^1 d_{a_1 \dots a'_i \dots a_N a'_1 \dots a_i \dots a'_N}^j |a_1 \dots a_i \dots a_N\rangle \langle a'_1 \dots a'_i \dots a'_N| \quad (1.36)
\end{aligned}$$

The partial transpose with respect to a larger set of indices (larger cut set) is constructed in a similar way by transposing the bits corresponding to each index in the set. To obtain the entanglement of the mixed state (1.35) we need to consider all unique cut sets and then sum the negative eigenvalues of the corresponding partially transposed matrices. As entanglement measure one then takes the negation of the aforementioned sum. The number of unique cut sets is $2^{N-1} - 1$, since the complimentary cut sets result in partially transposed matrices which have the same eigenvalues and the trivial partial transpose with respect to the empty cut gives the original density matrix which has no negative eigenvalues. [47; 48; 49]

1.0.2.5 Multi-partite entanglement measures

Due to its great relevance, both from the fundamental and from the practical points of view, it is imperative to explore and characterize all aspects of the quantum entanglement of multi-partite quantum systems [50; 51]. There are several possible N -qubit entanglement measures for pure states $|\phi\rangle$, one being the average of all the single-qubit linear entropies,

$$Q(|\phi\rangle) = 2 \left(1 - \frac{1}{N} \sum_{k=1}^N \text{Tr}(\rho_k^2) \right). \quad (1.37)$$

Here ρ_k , $k = 1, \dots, N$, stands for the marginal density matrix describing the k th qubit of the system after tracing out the rest. This quantity, often referred to as “global entanglement” (GE), measures the average entanglement of each qubit of the system with the remaining $(N-1)$ -qubits.

The GE measure can be generalized by using the average values of the linear entropies associated with more general partitions of the N -qubit system into two

subsystems (and not only the partitions of the system into a 1-qubit subsystem and an $(N - 1)$ -qubit subsystem). A particular generalization is given by the following family of multi-qubit entanglement measures,

$$Q_m(|\phi\rangle) = \frac{2^m}{2^m - 1} \left(1 - \frac{m!(N - m)!}{N!} \sum_s \text{Tr}(\rho_s^2) \right), \quad m = 1, \dots, [N/2], \quad (1.38)$$

where the sum runs over all the subsystems s consisting of m qubits, ρ_s are the corresponding marginal density matrices and $[x]$ denotes the integer part of x . The quantities Q_m measure the average entanglement between all the subsystems consisting of m qubits and the remaining $(N - m)$ qubits. Another way of characterizing the global amount of entanglement exhibited by an N -qubit state is provided by the sum of the (bi-partite) entanglement measures associated with all the possible bi-partitions of the N -qubits system [49]. These entanglement measures are given, essentially, by the degree of mixedness of the marginal density matrices associated with each bi-partition. These degrees of mixedness can be, in turn, evaluated in several ways. For instance, we can use the von Neumann entropy, the linear entropy or a Rényi entropy of index q [50; 51]. There has recently been great interest in the search for highly entangled multi-qubit states [49; 51]. The results of such a numerical search are reported in the Appendix.

1.0.2.6 Application: superdense coding

For superdense coding we require two parties, conventionally known as ‘Alice’ and ‘Bob’, who are far from each other. Alice can send two classical bits of information to Bob by sending him a single qubit, if they initially share a pair of qubits in the entangled state:

$$|\psi\rangle = \frac{|00\rangle + |11\rangle}{\sqrt{2}}. \quad (1.39)$$

The state $|\psi\rangle$ is fixed (no qubits need to be sent in order to prepare the state) with Alice and Bob being in possession of the first and second qubit respectively. The procedure Alice uses to send two bits of classical information via her qubit is as follows [33]: if she intends to send the bit string ‘00’ to Bob then she does

nothing to her qubit. To send ‘01’ she applies the phase flip Z to her qubit. If she wishes to send ‘10’ then she applies the quantum NOT gate, X , to her qubit and to send ‘11’ she applies the iY gate. The X , Y and Z gates are given by

$$X = \begin{pmatrix} 0 & 1 \\ 1 & 0 \end{pmatrix} \quad Y = \begin{pmatrix} 0 & -i \\ i & 0 \end{pmatrix} \quad Z = \begin{pmatrix} 1 & 0 \\ 0 & -1 \end{pmatrix}. \quad (1.40)$$

The four resulting states are the Bell states:

$$\begin{aligned} 00 : |\psi\rangle &\rightarrow |\beta_{00}\rangle = \frac{|00\rangle + |11\rangle}{\sqrt{2}} \\ 01 : |\psi\rangle &\rightarrow |\beta_{01}\rangle = \frac{|00\rangle - |11\rangle}{\sqrt{2}} \\ 10 : |\psi\rangle &\rightarrow |\beta_{10}\rangle = \frac{|10\rangle + |01\rangle}{\sqrt{2}} \\ 11 : |\psi\rangle &\rightarrow |\beta_{11}\rangle = \frac{|01\rangle - |10\rangle}{\sqrt{2}}, \end{aligned} \quad (1.41)$$

which are orthonormal and can thus be distinguished by an appropriate quantum measurement. Once Bob has received Alice’s qubit he can perform a measurement in the Bell basis and determine which of the four possible bit strings Alice sent. Thus superdense coding is achieved by transmitting two bits of information through the interaction of a single qubit. This illustrates that information is indeed physical and that quantum mechanics can predict surprising information processing abilities [33].

1.0.2.7 Application: quantum teleportation

As for superdense coding, we need two separated parties Alice and Bob sharing the entangled EPR state $|\beta_{00}\rangle$. Alice wants to send Bob the unknown state $|\psi\rangle = \alpha|0\rangle + \beta|1\rangle$ (α and β are not known) by making use of the EPR pair and sending classical information to Bob. She accomplishes this by interacting the qubit $|\psi\rangle$ with her half of the EPR pair and then sending her two qubits of the resultant state (the first two qubits denote Alice’s)

$$|\psi_0\rangle = |\psi\rangle|\beta_{00}\rangle = \frac{1}{\sqrt{2}} [\alpha|0\rangle(|00\rangle + |11\rangle) + \beta|1\rangle(|00\rangle + |11\rangle)] \quad (1.42)$$

through a CNOT gate

$$U_{CN} = \begin{pmatrix} 1 & 0 & 0 & 0 \\ 0 & 1 & 0 & 0 \\ 0 & 0 & 0 & 1 \\ 0 & 0 & 1 & 0 \end{pmatrix}, \quad (1.43)$$

obtaining the state

$$|\psi_1\rangle = \frac{1}{\sqrt{2}} [\alpha|0\rangle(|00\rangle + |11\rangle) + \beta|1\rangle(|10\rangle + |01\rangle)]. \quad (1.44)$$

She then sends her first qubit through a Hadamard gate

$$H_d = \begin{pmatrix} 1 & 1 \\ 1 & -1 \end{pmatrix}, \quad (1.45)$$

obtaining

$$|\psi_2\rangle = \frac{1}{2} [|00\rangle(\alpha|0\rangle + \beta|1\rangle) + |01\rangle(\alpha|1\rangle + \beta|0\rangle) + |10\rangle(\alpha|0\rangle - \beta|1\rangle) + |11\rangle(\alpha|1\rangle - \beta|0\rangle)]. \quad (1.46)$$

From the first term in the above expression it can be seen that when Alice's qubits are in the state $|00\rangle$ then Bob's qubit is in the state $|\psi\rangle$. Thus when Alice performs a measurement and obtains the result 00, Bob's post-measurement state will be $|\psi\rangle$. In a similar way we can determine the state of Bob's system given Alice's measurement outcomes:

$$\begin{aligned} 00 &\longmapsto |\psi_3(00)\rangle = \alpha|0\rangle + \beta|1\rangle \\ 01 &\longmapsto |\psi_3(01)\rangle = \alpha|1\rangle + \beta|0\rangle \\ 10 &\longmapsto |\psi_3(10)\rangle = \alpha|0\rangle - \beta|1\rangle \\ 11 &\longmapsto |\psi_3(11)\rangle = \alpha|1\rangle - \beta|0\rangle. \end{aligned} \quad (1.47)$$

Alice now sends Bob the classical information of her outcome, thereby telling him in which one of the four possible states his qubit has ended up. This classical information enables him to recover the state $|\psi\rangle$ by either doing nothing when the outcome is 00, applying the gate X when he receives 01, the Z gate when getting

10 or first applying an X and then a Z gate when the information 11 reaches him. Since classical information needs to be exchanged, quantum teleportation does not enable faster than light communication. Quantum teleportation illustrates that different resources in quantum mechanics can be interchanged: one shared EPR pair together with two classical bits of communication is a resource at least the equal of one qubit of communication [33].

1.0.3 Speed of quantum evolution

The problem of the “speed” of quantum evolution is relevant in connection with the physical limits imposed by the basic laws of quantum mechanics on the speed of information processing and information transmission [13; 14; 52]. When processing information, the output state of the computer device has to be reasonably distinct from the input state [52]. In quantum mechanics two states are distinguishable if they are orthogonal, thus basic computational steps involve moving from one quantum state to an orthogonal one. Consequently, lower bounds on the time needed to reach an orthogonal state also provide estimations on how fast one can perform elementary computation operations [14]. These, in turn, can be used to estimate fundamental limits on how fast a physical computer can run [14; 52].

A natural measure for the “speed” of quantum evolution governed by the Hamiltonian H is provided by the time interval τ that a given initial state $|\psi(t_0)\rangle$ takes to evolve into an orthogonal state [52; 53; 54],

$$\langle\psi(t_0)|\psi(t_0 + \tau)\rangle = 0. \quad (1.48)$$

Let E denote the energy’s expectation value,

$$E = \langle H \rangle, \quad (1.49)$$

and ΔE the energy’s uncertainty,

$$\Delta E = \sqrt{\langle H^2 \rangle - \langle H \rangle^2}. \quad (1.50)$$

Two fundamental lower bounds for τ , in terms of E and ΔE , are given by (see [54], [55] and references therein)

$$\frac{\pi\hbar}{2\Delta E} \tag{1.51}$$

and

$$\frac{\pi\hbar}{2E}. \tag{1.52}$$

The latter bound was derived by Margolus and Levitin in [52]. These two bounds can be combined as (see [53]),

$$\tau_{min} = \max\left(\frac{\pi\hbar}{2E}, \frac{\pi\hbar}{2\Delta E}\right), \tag{1.53}$$

which constitutes a lower limit for the evolution time τ to an orthogonal state.

The problem of the minimum time necessary to reach an orthogonal state is also relevant in connection with the energy-time Heisenberg uncertainty principle [14], which can be formulated in terms of the minimum time that a system with a given spread in energy requires to evolve to a distinguishable state (that is, to an orthogonal state).

My main focus will be on the speed of the evolution which can be regarded as the ratio of the absolute time taken and the minimum possible time imposed by equation (1.53). If the ratio is one, it implies optimum usage of the energy resources. On the other hand, the greater the ratio, the less “efficient” the energy resources are being used. Thus τ/τ_{min} can be viewed as a measure of how efficiently the energy resources are being used to evolve to an orthogonal state.

1.0.4 Quantum no-cloning and CTC

The quantum no-cloning theorem constitutes a hallmark feature of quantum information. It states that quantum information cannot be cloned: an unknown quantum state of a given (source) system cannot be perfectly duplicated while

leaving the state of the source system unperturbed [56; 57]. No unitary (quantum mechanical) transformation exists that can perform the process

$$|\psi\rangle \otimes |0\rangle \otimes |\Sigma\rangle \longrightarrow |\psi\rangle \otimes |\psi\rangle \otimes |\Sigma_\psi\rangle, \quad (1.54)$$

for arbitrary source states $|\psi\rangle$. In the above equation $|0\rangle$ and $|\Sigma\rangle$ denote, respectively, the initial standard states of the target qubit and of the copy machine, and $|\Sigma_\psi\rangle$ is the final state of the copy machine. In other words, universal quantum cloning is not permitted by the basic laws of quantum mechanics. The impossibility of universal quantum cloning can be proved in two different ways. One can show that it is not compatible with the linearity of quantum evolution or that it is not compatible with the unitarity of quantum evolution.

In [58] I have explored the possibility of performing quantum cloning operations in the presence of closed timelike curves. In a Lorentzian manifold, a closed timelike curve (CTC) is a worldline of a material particle in spacetime that is closed. CTCs appear in some exact solutions to the Einstein field equation of general relativity [59].

1.0.4.1 Properties of the fidelity distance

In our discussion of the cloning process in the presence of closed timelike curves (CTC) we are going to use the fidelity distance between two quantum states (represented by two density matrices) of a given quantum system. The main properties of this measure that we are going to use are briefly reviewed: the fidelity distance between two quantum states is given by [33]

$$F[\rho, \sigma] = \text{Tr} \sqrt{\rho^{1/2} \sigma \rho^{1/2}}. \quad (1.55)$$

In the particular case that one of the states is pure, we have

$$F[|\psi\rangle, \rho] = \sqrt{\langle \psi | \rho | \psi \rangle}. \quad (1.56)$$

A fundamental property of the fidelity measure is that it remains constant under unitary transformations,

$$F[U\rho U^\dagger, U\sigma U^\dagger] = F[\rho, \sigma]. \quad (1.57)$$

If we have a composite system AB , the distance between two density matrices describing two states of the composite system is smaller or equal to the distance between the marginal density matrices associated with one of the subsystems,

$$F[\rho_{AB}, \sigma_{AB}] \leq F[\rho_A, \sigma_A]. \quad (1.58)$$

Finally, the distance between two factorizable density matrices complies with

$$F[\rho_0 \otimes \sigma_0, \rho_1 \otimes \sigma_1] = F[\rho_0, \rho_1] F[\sigma_0, \sigma_1]. \quad (1.59)$$

The fidelity distance is a number between zero and one, $F = 0$ corresponds to completely distinguishable density matrices, whereas $F = 1$ signifies that the density matrices are identical.

1.0.4.2 CTC and quantum cloning

The ideas and methods of quantum information theory [33] provide an interesting framework for the study of certain aspects of the physics of closed timelike curves [59]. Quantum computation processes with part of the quantum data traversing closed timelike curves lead to a new physical model of computation [60] and also to various physical effects with profound implications for the foundations of quantum theory [59]. It has been conjectured [59] that the nonlinear evolution of chronology respecting qubits interacting with closed timelike curve qubits may be used to overcome the celebrated quantum no-cloning theorem [56; 57]. We investigate the alluded to conjecture by recourse to the analysis of specific models of the cloning process [58].

We consider a quantum cloning process where the copy machine is a composite system consisting of two subsystems A and B , as Figure 1.1 illustrates.

The subsystem B is allowed to traverse a closed timelike curve. The joint density matrix describing the state of the source qubit, target qubit and the subsystem A of the copy machine (all three assumed to be chronology respecting) evolves, due to their interaction with subsystem B , nonlinearly. A successful cloning process would be of the form,

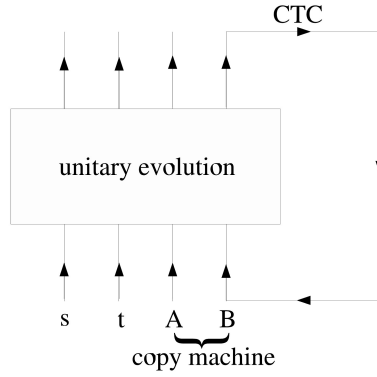


Figure 1.1: Diagram depicting the quantum evolution of our set-up.

$$|\psi_i\rangle \otimes |0\rangle \otimes \rho_A \otimes \rho_B^{(i)} \longrightarrow |\psi_i\rangle \otimes |\psi_i\rangle \otimes \sigma_{AB}^{(i)}, \quad (1.60)$$

where $|0\rangle$ and ρ_A are, respectively, the standard initial states of the target qubit and the subsystem A of the copy machine. The process (1.60) is assumed to be described by a unitary transformation.

The subsystem B (traversing a closed timelike curve) verifies the consistency condition [59],

$$\rho_B^{(i)} = \text{Tr}_A \left(\sigma_{AB}^{(i)} \right). \quad (1.61)$$

Notice that this consistency condition implies that the initial state of the subsystem B (traversing a closed timelike curve) is not independent of the initial state of the source qubit. Furthermore, due to the aforementioned consistency

condition the evolution of the source and target qubits (as well as the subsystem A of the copy machine) is nonlinear. Consequently, the usual argument for the quantum no-cloning theorem based on the linearity of quantum evolution cannot be applied here. Instead, we consider the behaviour of the fidelity distance between two realizations of the cloning process. The fidelity distance between density matrices is given by equation (1.55).

We assume that two different states $\langle\psi_1|$ and $\langle\psi_2|$ can be successfully cloned. Since the unitary evolution for both initial states is the same, the fidelity distance between the initial states of the cloning process has to be equal to the fidelity distance between the final states of the cloning process (property (1.57)). Using the basic properties of the fidelity distance mentioned in Section 1.0.4.1, one then gets

$$\begin{aligned}
 |\langle\psi_1|\psi_2\rangle| F\left[\rho_B^{(1)}, \rho_B^{(2)}\right] &= |\langle\psi_1|\psi_2\rangle|^2 F\left[\sigma_{AB}^{(1)}, \sigma_{AB}^{(2)}\right] \\
 &\leq |\langle\psi_1|\psi_2\rangle|^2 F\left[\rho_B^{(1)}, \rho_B^{(2)}\right].
 \end{aligned}
 \tag{1.62}$$

In order to satisfy this inequality, at least one of the following conditions must be fulfilled:

- $\langle\psi_1|\psi_2\rangle = 0$
- $F\left[\rho_B^{(1)}, \rho_B^{(2)}\right] = 0$.

In the first case we have orthogonal source states which, as happens with standard linear quantum evolution, can be cloned. The second case can be realized for an appropriate choice of the unitary transformation (1.60). Consequently, it is possible to clone two non-orthogonal states in the presence of a closed timelike curve. However, if the subsystem B of the copy machine has a Hilbert space of finite dimension N , the maximum number of non-orthogonal states that can be cloned by the present scheme is N . It is important to emphasize that the cloning process based upon closed timelike curves cannot be used to implement faster than light signalling: due to the nonlinear character of the process we have just discussed, a mixture of two pure states of the target qubit does not evolve

into the corresponding mixture of the final states generated by those initial states separately [58].

Chapter 2

Composite Systems with Extensive S_q (Power-Law) Entropies

The problem of characterizing the kind of correlations leading to an extensive behaviour of the S_q (power-law) entropic measure has recently been considered by Tsallis, Gell-Mann and Sato (TGS) [61]. I propose a family of models for the probability occupancy of phase space exhibiting an extensive behaviour of S_q and allowing for an explicit analysis of the $N \rightarrow \infty$ (thermodynamic) limit [62].

2.1 Overview

The non-extensive thermo-statistical formalism [29; 61; 63] based upon the power-law entropic measure S_q (also referred to as the Tsallis entropy) [29] has been the focus of intensive research activity in recent years. There are several multi-disciplinary applications of S_q . In physics the S_q entropy has been applied (among other things) to:

A) Descriptions of meta-stable states of many-body systems with long-range interactions:

1. Meta-stable states of pure electron plasmas: [64].
2. Meta-stable states in astrophysical self-gravitating N -body systems: [65; 66].

B) Systems with fluctuating temperature: [67].

C) Other applications, for example: High T_c superconductivity [68].

Specific applications in physics and other fields such as biophysics [69] and econophysics [70] include the non-linear Fokker-Planck equations: [71; 72] (these equations are used to model several kinds of systems both in and outside physics).

The non-extensive q -entropy is defined as (1.6)

$$S_q = \frac{1}{q-1} \left[1 - \sum_{i=1}^W p_i^q \right], \quad (2.1)$$

where p_i is the probability associated with the i -microstate of the system under consideration, W is the total number of microstates, and q is an entropic index that may adopt any real value. In the limit $q \rightarrow 1$ the standard Boltzmann-Gibbs entropy is recovered,

$$S_1 = - \sum_{i=1}^W p_i \ln p_i. \quad (2.2)$$

When we have a composite system ($L + R$) consisting of two statistically independent subsystems L and R ,

$$\begin{aligned} p_{ij}^{(L+R)} &= p_i^{(L)} p_j^{(R)} \quad (\text{classical}) \\ \rho^{(L+R)} &= \rho^{(L)} \otimes \rho^{(R)} \quad (\text{quantum mechanical}), \end{aligned} \quad (2.3)$$

the total entropy $S_q^{(L+R)}$ is related to the entropies of the subsystems by (1.7)

$$S_q^{(L+R)} = S_q^{(L)} + S_q^{(R)} + (1-q)S_q^{(L)}S_q^{(R)}. \quad (2.4)$$

In the limit $q \rightarrow 1$, the standard extensive behaviour is recovered. **Here I am going to restrict my considerations to the range $q \in [0, 1]$.**

The non-extensive behaviour described by equation (2.4) holds, of course, only under very special circumstances: when both subsystems are statistically independent. Under those same circumstances the standard logarithmic entropy is extensive. From the physical point of view the extensivity of entropy is a desirable behaviour. Consequently, if a generalized entropic functional is going

2.2 A discrete binary system

to be used to describe physical systems, it is a physically relevant problem to characterize what kind of statistical correlations yield an extensive behaviour of the aforementioned entropic functional. In the case of the Tsallis measure S_q , the first steps towards such a characterization program were done by TGS in [61].

The aim of the present chapter is to discuss two new models of composite systems exhibiting an additive behaviour of S_q , and allowing for an explicit analysis of the $N \rightarrow \infty$ (thermodynamic) limit. This chapter is organized as follows. In Section 2.2 I analyze a discrete binary system exhibiting, for appropriate values of the relevant parameters, an extensive behaviour of S_q . In Section 2.3 we compare our model with the one advanced by TGS in [61]. A quantum version of our model is considered in Section 2.4. In Section 2.5 I investigate a continuous model. Finally, some conclusions are drawn in Section 2.6.

2.2 A discrete binary system

I am going to consider a classical composite system consisting of N identical (but distinguishable) subsystems each one having two possible states, 0 or 1. Our composite system has 2^N microstates. Each possible microstate corresponds to a string (of length N) of 0's and 1's. First we start with two equal and distinguishable binary subsystems, A and B ($N=2$). The associated joint probabilities are indicated in Table 2.1.

$A \setminus B$	0	1
0	$\lambda p + (1 - \lambda)p^2$	$p(1 - p)(1 - \lambda)$
1	$p(1 - p)(1 - \lambda)$	$(1 - p)\lambda + (1 - \lambda)(1 - p)^2$

Table 2.1: Joint probabilities for two binary subsystems A and B .

This joint probability distribution is described by two parameters $p, \lambda \in [0, 1]$. The parameter p gives the marginal probability distribution $\{p, 1 - p\}$, which is the same for both subsystems. The parameter λ is associated with the statistical correlations between both subsystems. For $\lambda = 0$ the subsystems are independent

2.2 A discrete binary system

whereas $\lambda = 1$ corresponds to the strongest possible degree of correlation. So far our construction is similar to the one corresponding to the discrete model discussed in [61]. In point of fact, comparing our Table 2.1 with Table 1 of [61], one can identify

$$\kappa = \lambda p(1 - p). \quad (2.5)$$

Thus, as far as the case of two subsystems is concerned, our construction can be regarded as a re-parametrization of the one employed by TGS. However, there is an important difference between these two parametrizations. In our case, the parameters p and λ can be chosen independently of each other: they can adopt any pair of values in the interval $[0, 1]$. Contrariwise, the parameters κ and p used by TGS cannot be chosen independently. The range of admissible values of κ (yielding positive joint probabilities) depends on the value of p (see Table 1 of [61]).

The next step is to construct an appropriate joint probability distribution for a system consisting of three equal and distinguishable binary subsystems A, B and C . We want this probability distribution to be such that the marginal distributions associated with each of the three possible bi-partite subsystems AB, AC or BC , be all equal to the probabilities listed in Table 2.1. In this case ($N=3$), a solution to the above problem is given by the probabilities in Table 2.2.

$A \setminus B$	0	1
0	$\lambda p + (1 - \lambda)p^3$ $[(1 - \lambda)p^2(1 - p)]$	$(1 - \lambda)p^2(1 - p)$ $[(1 - \lambda)p(1 - p)^2]$
1	$(1 - \lambda)p^2(1 - p)$ $[(1 - \lambda)p(1 - p)^2]$	$(1 - \lambda)p(1 - p)^2$ $[\lambda(1 - p) + (1 - \lambda)(1 - p)^3]$

Table 2.2: Joint probabilities for three binary subsystems A, B and C . The quantities without (within) $[]$ correspond to state 0 (state 1) of subsystem C .

At this step it is convenient to use the notation introduced by TGS [61],

$$r_{10} \equiv p_0^{(A)} = p$$

2.2 A discrete binary system

$$\begin{aligned}
r_{01} &\equiv p_1^{(A)} = (1 - p) \\
r_{20} &\equiv p_{00}^{(A+B)} = \lambda p + (1 - \lambda)p^2 \\
r_{11} &\equiv p_{01}^{(A+B)} = p_{10}^{A+B} = p(1 - p)(1 - \lambda) \\
r_{02} &\equiv p_{11}^{(A+B)} = (1 - p)^2 + \lambda p(1 - p),
\end{aligned} \tag{2.6}$$

and one can verify that this gives equation (3) of [61]:

$$\begin{aligned}
r_{20} + 2r_{11} + r_{02} &= 1 \\
r_{20} + r_{11} &= r_{10} = p \\
r_{11} + r_{02} &= r_{01} = 1 - p.
\end{aligned} \tag{2.7}$$

With the notation

$$\begin{aligned}
r_{30} &\equiv p_{000}^{(A+B+C)} \\
r_{21} &\equiv p_{001}^{(A+B+C)} = p_{010}^{(A+B+C)} = p_{100}^{(A+B+C)} \\
r_{12} &\equiv p_{110}^{(A+B+C)} = p_{101}^{(A+B+C)} = p_{011}^{(A+B+C)} \\
r_{03} &\equiv p_{111}^{(A+B+C)},
\end{aligned} \tag{2.8}$$

where by r_{ij} I imply that the microstate consists of i 0's and j 1's ($i + j = N$), one can verify

$$\begin{aligned}
r_{30} + 3r_{21} + 3r_{12} + r_{03} &= 1 \\
r_{30} + r_{21} &= r_{20} = \lambda p + (1 - \lambda)p^2 \\
r_{21} + r_{12} &= r_{11} = p(1 - p)(1 - \lambda) \\
r_{12} + r_{03} &= r_{02} = (1 - p)^2 + \lambda p(1 - p).
\end{aligned} \tag{2.9}$$

We want the marginal distribution for $(N - 1)$ -subsystems of our N -subsystems composite system to be equal to the distribution of the $(N - 1)$ -subsystems composite system. Following TGS, the generalization of the above procedure yields a general set of equations relating the probabilities of the N -subsystems case with the $(N - 1)$ -subsystems case,

2.2 A discrete binary system

$$r_{N-n,n} + r_{N-n-1,n+1} = r_{N-n-1,n} \quad (2.10)$$

$$\sum_{n=0}^N l_{N-n,n} r_{N-n,n} = 1 \quad (N = 0, 1, 2, \dots; \quad n = 0, 1, 2, \dots, N), \quad (2.11)$$

where $l_{N-n,n} = \binom{N}{n}$.

A solution of the recurrence relations (2.10) complying with the normalization condition (2.11) and providing a natural N -generalization of equations (2.8), is given by

$$\begin{aligned} r_{N,0} &= \lambda p + (1 - \lambda)p^N \\ r_{N-n,n} &= (1 - \lambda)p^{N-n}(1 - p)^n, \quad 1 \leq n \leq N - 1 \\ r_{0,N} &= \lambda(1 - p) + (1 - \lambda)(1 - p)^N, \end{aligned} \quad (2.12)$$

since they verify

$$\begin{aligned} r_{N,0} + r_{N-1,1} &= r_{N-1,0} \\ r_{N-n,n} + r_{N-n-1,n+1} &= r_{N-n-1,n} \quad 1 \leq n \leq N - 2 \\ r_{1,N-1} + r_{0,N} &= r_{0,N-1} \end{aligned} \quad (2.13)$$

and

$$\begin{aligned} \sum_{n=0}^N \binom{N}{n} r_{N-n,n} &= \lambda + (1 - \lambda) \sum_{n=0}^N \binom{N}{n} p^{N-n}(1 - p)^n \\ &= 1. \end{aligned} \quad (2.14)$$

It is important to realize that the solution (2.12) to the set of equations (2.10) is *not equivalent* to the one found by TGS in [61]. The fact that (2.12) constitutes a new solution to (2.10) can already be appreciated from Table 2.2 (case $N = 3$). For instance, we have from Table 2.2 that

$$\frac{p_{(010)}}{p_{(011)}} = \frac{p}{1 - p}. \quad (2.15)$$

2.2 A discrete binary system

However, the case $N = 3$ of TGS gives,

$$\left(\frac{p_{(010)}}{p_{(011)}} \right)_{\text{TGS}} = \frac{p^2(1-p) - \kappa(1+p)}{p(1-p)^2 + \kappa p}. \quad (2.16)$$

The quotients (2.15) and (2.16) are clearly different. The quotient (2.16) can be made equal to (2.15) for one particular value of κ , but for our set of probabilities expression (2.15) holds true for the complete range of admissible values of $\lambda \in [0, 1]$.

The probability distribution characterized by the equations (2.12) (which from here on we are going to call $p^{(c)}$) can be conveniently recast as

$$p^{(c)} = \lambda p^{(a)} + (1 - \lambda)p^{(b)}, \quad (0 \leq \lambda \leq 1), \quad (2.17)$$

in terms of two particular probability distributions, $p^{(a)}$ and $p^{(b)}$. The probability distribution $p^{(a)}$ is such that only two microscopic configurations have non-vanishing probabilities: the microstate with all subsystems in state 0 has probability p , and the microstate with all subsystems in state 1 has probability $(1 - p)$. Therefore

$$\begin{aligned} p_{(00\dots 0)}^{(a)} &= p \\ p_{(11\dots 1)}^{(a)} &= 1 - p \\ p_i^{(a)} &= 0, \quad i \neq 00\dots 0, 11\dots 1 \end{aligned} \quad (2.18)$$

where i denotes all possible 2^N combinations of 0's and 1's in the string. On the other hand, the probability distribution $p^{(b)}$ is completely factorizable: the probabilities of finding any of its subsystems in states 0 or 1 respectively are p and $(1 - p)$,

$$p_{i_1\dots i_N}^{(b)} = \prod_{k=1}^N [\delta_{0i_k} p + \delta_{1i_k} (1 - p)], \quad i_k = 0, 1 \quad (k = 1, \dots, N). \quad (2.19)$$

For both $p^{(a)}$ and $p^{(b)}$, as well as for any linear combination of them, the marginal probabilities associated with any of the N subsystems are p for state 0 and $(1 - p)$ for state 1.

2.2 A discrete binary system

To obtain the entropy of $p^{(b)}$, we need to apply eq. (2.4) recursively, that is

$$S_q[p^{(b)}; N] = S_q[p^{(b)}; N-1] + S_q[p^{(b)}; 1] + (1-q)S_q[p^{(b)}; N-1]S_q[p^{(b)}; 1]. \quad (2.20)$$

The entropy of $p^{(b)}$ is then

$$S_q[p^{(b)}; N] = \frac{1}{1-q} \{ [1 + (1-q)S_q[1]]^N - 1 \}, \quad N \geq 2, \quad (2.21)$$

where

$$S_q[p^{(c)}; 1] = S_q[1] = \frac{1 - p^q - (1-p)^q}{q-1} \quad (2.22)$$

is the entropy of the marginal probability distribution for one subsystem, which is the same for both $p^{(a)}$ and $p^{(b)}$, and thus also for $p^{(c)}$. Now

$$S_q[p^{(c)}; N](\lambda = 0) = S_q[p^{(b)}; N] \quad (2.23)$$

$$S_q[p^{(c)}; N](\lambda = 1) = S_q[p^{(a)}; N] = S_q[1]. \quad (2.24)$$

Since $S_q[p^{(b)}; N]$ increases exponentially with N and $NS_q[1]$ only linearly, it means that there exists an N from which onward $S_q[p^{(b)}; N] > NS_q[1] > S_q[1]$. Therefore, it follows from (2.23-2.24) that a λ exists for which

$$S_q[p^{(c)}; N](\lambda) = NS_q[1]. \quad (2.25)$$

From the general expression for the entropy $S_q[p^{(c)}; N]$,

$$S_q[p^{(c)}; N] = \frac{1}{q-1} \left[1 - \sum_{i=1}^{2^N} \delta_i^q \right], \quad (2.26)$$

it is possible to derive the following convenient expression for the q -entropy of $p^{(c)}$,

$$S_q[p^{(c)}; N] = \frac{1}{q-1} [1 - (1-\lambda)^q [1 + (1-q)S_q[1]]^N + (1-\lambda)^q p^{Nq} + (1-\lambda)^q (1-p)^{Nq} - [(1-\lambda)p^N + \lambda p]^q - [(1-\lambda)(1-p)^N + \lambda(1-p)]^q]. \quad (2.27)$$

2.2 A discrete binary system

The method used to obtain this expression is as follows: from Table 2.3 we have the probability distributions for $p^{(b)}$ and $p^{(c)}$ and so let $S_q^*[p^{(c)}; N]$ be the “entropy” from considering only the $(1 - \lambda)p_j$ contributions,

$$S_q^*[p^{(c)}; N] = \frac{1}{q-1} \left[1 - (1-\lambda)^q \sum_{j=1}^{2^N} p_j^q \right]. \quad (2.28)$$

Microstate	$p^{(b)}$	$p^{(c)}$
00...0	p_1	$(1-\lambda)p_1 + \lambda p$
10...0	p_2	$(1-\lambda)p_2$
\vdots	p_i	$(1-\lambda)p_i$
11...1	p_{2^N}	$(1-\lambda)p_{2^N} + \lambda(1-p)$

Table 2.3: Probability distributions for $p^{(b)}$ and $p^{(c)}$, with $i = 3, 4, \dots, 2^N - 1$.

Using the general expression for $S_q[p^{(b)}; N]$,

$$S_q[p^{(b)}; N] = \frac{1}{q-1} \left\{ 1 - \sum_{j=1}^{2^N} p_j^q \right\}, \quad (2.29)$$

for which we already have expression (2.21), results in $S_q^*[p^{(c)}; N]$ becoming

$$S_q^*[p^{(c)}; N] = \frac{1}{q-1} \left[1 - \underbrace{(1-\lambda)^q \left\{ 1 - (q-1)S_q[p^{(b)}; N] \right\}}_{\text{“sum”}} \right]. \quad (2.30)$$

Now we have to subtract $[(1-\lambda)p^N]^q$ and $[(1-\lambda)(1-p)^N]^q$ from the “sum” and add $[(1-\lambda)p^N + \lambda p]^q$ and $[(1-\lambda)(1-p)^N + \lambda(1-p)]^q$ in order to get $S_q[p^{(c)}; N]$. Doing that and substituting for the expression for $S_q[p^{(b)}; N]$ then results in eq. (2.27).

We want $NS_q[1] = S_q[p^{(c)}; N]$ and, as was already shown, for large enough N this relation can be fulfilled. Thus in this limit

2.2 A discrete binary system

$$p^{Nq}, (1-p)^{Nq}, p^N, (1-p)^N \rightarrow 0 \quad (\text{large } N) \quad p, q \in (0, 1) \quad (2.31)$$

and so

$$NS_q[1] \approx \frac{1}{1-q} [1 + (1-q)S_q[1]]^N (1-\lambda)^q. \quad (2.32)$$

Hence for large N ,

$$\lambda \approx 1 - \left\{ \frac{NS_q[1](1-q)}{[1 + (1-q)S_q[1]]^N} \right\}^{\frac{1}{q}}. \quad (2.33)$$

Therefore, in the thermodynamic limit λ tends to one and hence $p^{(c)}$ tends to $p^{(a)}$ which is maximally correlated. This means that as N increases the correlations have to become stronger and stronger in order to have an extensive behaviour for S_q .

In Tables 2.4 and 2.5 I give, for $p = 0.4$, $q = 0.95$ and $q = 0.5$, and for different values of N , the exact values of the parameter λ corresponding to an extensive behaviour of S_q , as well as the approximate values of λ provided by the asymptotic expression (2.33). We see that for both values of q , and as N increases, the exact λ approaches the asymptotic one given by expression (2.33), and both tend to 1.

N	λ [eq.(2.25)]	λ [eq.(2.33)]
2	0.216385	0.944547
10	0.24632	0.772787
50	0.641409	0.700808
100	0.892354	0.894677
200	0.993735	0.993708
400	0.999989	0.999989

Table 2.4: Exact and approximate solutions for $S_q[p^{(c)}; N](\lambda) = NS_q[1]; q = 0.95, p = 0.4$.

In Figures 2.1 and 2.2 we can see the behaviour of the quantity $D = S_q[p^{(c)}; N] - NS_q[1]$ as a function of λ , for different values of p , q and N .

2.3 Comparison of the (p, λ) and the (p, κ) binary models

N	λ [eq.(2.25)]	λ [eq.(2.33)]
2	0.739562	0.830909
5	0.890285	0.863812
10	0.985326	0.98209
50	≈ 1	≈ 1

Table 2.5: Exact and approximate solutions for $S_q[p^{(c)}; N](\lambda) = NS_q[1]; q = 0.5, p = 0.4$.

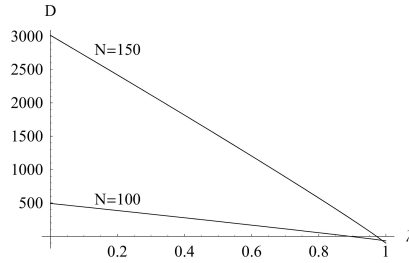


Figure 2.1: $S_q[p^{(c)}; N] - NS_q[1] = D$ as a function of λ ($q=0.95, p=0.4$).

2.3 Comparison of the (p, λ) and the (p, κ) binary models

As we have seen, in the (p, λ) model, it is possible to provide a *proof* that for any value $0 \leq p \leq 1$ and $0 < q \leq 1$, and for large enough N , there always exists a λ -value such that the total q -entropy of the composite system is equal to N times the entropy of one of the subsystems. Moreover, we also obtained an analytic asymptotic expression for λ , valid in the limit of large values of N .

On the other hand, in the (p, κ) model, it is not clear that there always exists, for large values of N , a κ -value leading to an extensive behaviour of S_q . Here we approached this problem numerically and obtained evidence indicating that for large enough values of N , such a κ -value does not exist.

Tables 2.6 and 2.7 were obtained by solving $S_q(N) = NS_q(1)$ (for two different values of q) using equation (5) from [61]. In the two tables, p_s is the approximate starting value of p from which onward solutions for κ exist. A cross (\times) denotes

2.3 Comparison of the (p, λ) and the (p, κ) binary models

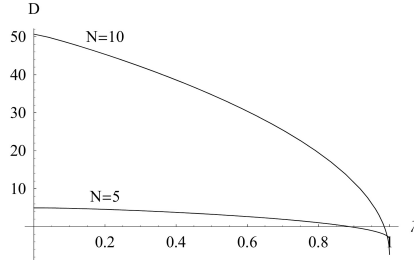


Figure 2.2: $S_q[p^{(c)}; N] - NS_q[1] = D$ as a function of λ ($q=0.5$, $p=0.4$).

that no solution for κ exists for those values of N and p .

N	p_s	$\kappa_{0.95}(p_s)$	$\kappa_{0.95}(p = 0.5)$	$\kappa_{0.95}(p = 0.8)$
2	1×10^{-6}	1.66×10^{-8}	± 0.0550153	0.0291402; -0.0212572
3	0.001	6.82877×10^{-7}	0.0356238; -0.0338204	0.0237656; -0.0194896
4	0.24	0.00800363	0.0242283	0.0197763; -0.0176847
5	0.49	0.0156661	0.0161904	0.016671; -0.0158311
6	0.63	0.0149745	×	0.0141553; -0.0138966
7	0.72	0.01261	×	0.0120335; -0.011793
8	0.78	0.0102438	×	0.0101443

Table 2.6: Solutions for κ that make S_q additive ($q = 0.95$). [61]

2.4 Quantum mechanical version of the binary system

N	p_s	$\kappa_{0.5}(p_s)$	$\kappa_{0.5}(p = 0.5)$	$\kappa_{0.5}(p = 0.8)$
2	0.0001	0.0000642983	± 0.185235	0.116236
3	0.47	0.0796122	0.0832543	0.0697844
4	0.75	-0.0593005	×	-0.0395967
5	0.8	-0.0388661	×	-0.0388661
6	0.84	-0.0253567	×	×
7	0.86	-0.0194571	×	×
8	0.88	-0.0143473	×	×

Table 2.7: Solutions for κ that make S_q additive ($q = 0.5$). [61]

2.4 Quantum mechanical version of the binary system

In this Section I am going to consider a quantum version of my binary model. The corresponding composite quantum system consists of N equal but distinguishable subsystems, each one described by a Hilbert space of dimension 2, with basis vectors $\{|0\rangle, |1\rangle\}$. In other words, I am going to deal with a system of N qubits. The so-called computational basis of the complete Hilbert space of the composite system is then $\{|00\dots 0\rangle, |10\dots 0\rangle, \dots, |11\dots 1\rangle\}$. We want the marginal (mixed) quantum state associated with each subsystem to be a statistical mixture of the basis states $\{|0\rangle\}$ and $\{|1\rangle\}$, with weights p and $(1 - p)$, respectively.

Consider

$$\rho^{(b)} = \underbrace{\rho_1 \otimes \rho_1 \otimes \dots \otimes \rho_1}_{N \text{ times}} \quad (2.34)$$

where

$$\rho_1 = p|0\rangle\langle 0| + (1 - p)|1\rangle\langle 1| \quad (2.35)$$

and let

$$\rho^{(a)} = p|00\dots 0\rangle\langle 0\dots 00| + (1 - p)|11\dots 1\rangle\langle 1\dots 11|. \quad (2.36)$$

Define $\rho^{(c)}$ to be

$$\rho^{(c)} = \lambda\rho^{(a)} + (1 - \lambda)\rho^{(b)}, \quad (0 \leq \lambda \leq 1). \quad (2.37)$$

2.4 Quantum mechanical version of the binary system

Since both $\rho^{(a)}$ and $\rho^{(b)}$ are diagonal in the computational basis (therefore not entangled), $\rho^{(c)}$ is also diagonal in that basis (hence unentangled). This means the diagonal elements are just the probability distributions. For density matrices the q -entropy is given by

$$S_q = \frac{1 - \text{Tr}(\rho^q)}{q - 1}, \quad (2.38)$$

hence all the equations for $p^{(c)}$ also hold for $\rho^{(c)}$: $S_q[\rho^{(c)}; N] = S_q[p^{(c)}; N]$.

Keeping the definitions for $\rho^{(b)}$ and $\rho^{(c)}$ the same but changing $\rho^{(a)}$ to the state

$$\rho^{(a)} = |\phi\rangle\langle\phi| \quad (2.39)$$

$$|\phi\rangle = \sqrt{p}|00\dots 0\rangle + \sqrt{(1-p)}|11\dots 1\rangle, \quad (2.40)$$

makes the system truly quantum mechanical ($|\phi\rangle$ is entangled), since now $\rho^{(a)}$ is not diagonal in the computational basis and consequently, neither is $\rho^{(c)}$.

The marginal density matrices of $\rho^{(a)}$ and $\rho^{(b)}$ are both equal to ρ_1 and thus the marginal density matrix of $\rho^{(c)}$ will be ρ_1 . Unlike the classical case, we now have $\rho_1 \neq \rho^{(c)}[N = 1]$. Actually, we have $\rho_m^{(c)} \neq \rho^{(c)}[N = m]$ which means the marginal density matrix for m subsystems is not the same as the density matrix for a composite system consisting of m subsystems.

The result obtained for $S_q[\rho^{(b)}; N]$, using the recursion (2.4)

$$S_q[\rho^{(b)}; N] = S_q[\rho^{(b)}; N - 1] + S_q[\rho^{(b)}; 1] + (1 - q)S_q[\rho^{(b)}; N - 1]S_q[\rho^{(b)}; 1], \quad (2.41)$$

is exactly the same as in the classical case, that is, $S_q[\rho^{(b)}; N]$ is equal to equation (2.21), with $S_q[1]$ also being equal to equation (2.22). Since $\rho^{(a)}$ is a projector and the trace is invariant under a change of basis (unitary transformation), it follows that $S_q[\rho^{(a)}; N] = 0$.

The marginal density matrix of m subsystems is obtained by tracing out the other $(N - m)$ subsystems. All the marginal density matrices of $\rho^{(c)}$ (for

2.4 Quantum mechanical version of the binary system

$m = 1, 2, \dots, N - 1$) are diagonal, which means that only the complete system is entangled.

The marginal density matrix of $\rho^{(c)}$ for two subsystems is

$$\rho_2^{(c)} = \begin{pmatrix} \lambda p + (1 - \lambda)p^2 & 0 & 0 & 0 \\ 0 & (1 - \lambda)p(1 - p) & 0 & 0 \\ 0 & 0 & (1 - \lambda)p(1 - p) & 0 \\ 0 & 0 & 0 & (1 - p)^2 + \lambda p(1 - p) \end{pmatrix}. \quad (2.42)$$

This gives rise to the same probability distributions as in Table 2.1. Now,

$$S_q[\rho^{(c)}; N](\lambda = 0) = S_q[\rho^{(b)}; N], \quad (2.43)$$

$$S_q[\rho^{(c)}; N](\lambda = 1) = S_q[\rho^{(a)}; N] = 0. \quad (2.44)$$

Using the same argument as for the classical case, there exists an N from which onward $S_q[\rho^{(b)}; N] > NS_q[1] > 0$ and thus a λ exists for which $S_q[\rho^{(c)}; N] = NS_q[1]$.

Once again, in order to determine $S_q[\rho^{(c)}; N]$ we use $S_q[\rho^{(b)}; N]$. For this purpose we employ a similar procedure as in the classical case. Since $\rho^{(b)}$ is diagonal,

$$\text{Tr}((\rho^{(b)})^q) = \sum_{j=1}^{2^N} \lambda_j^q, \quad (2.45)$$

where λ_j are the diagonal elements. By rearranging the computational basis to have $|11\dots 1\rangle$ in the second place and letting the rest stay in the same order, $\{|00\dots 0\rangle, |11\dots 1\rangle, \dots\}$, the matrix for $\rho^{(c)}$ becomes

$$\rho^{(c)} = \begin{pmatrix} \lambda p + (1 - \lambda)p^N & \lambda\sqrt{p(p-1)} & 0 & 0 & \dots & 0 \\ \lambda\sqrt{p(p-1)} & \lambda(1-p) + (1-\lambda)(1-p)^N & 0 & 0 & \dots & 0 \\ 0 & 0 & (1-\lambda)\lambda_2 & 0 & \dots & 0 \\ 0 & 0 & 0 & \ddots & \dots & 0 \\ \vdots & \vdots & \vdots & \vdots & \ddots & \vdots \\ 0 & 0 & 0 & 0 & \dots & (1-\lambda)\lambda_{2^{N-1}} \end{pmatrix}. \quad (2.46)$$

2.4 Quantum mechanical version of the binary system

Then

$$\begin{aligned}
S_q[\rho^{(c)}; N] &= \frac{1}{q-1} \left(1 - \left[\text{Tr} \left\{ ([1-\lambda]\rho^{(b)})^q \right\} - ([1-\lambda]p^N)^q \right. \right. \\
&\quad \left. \left. - ([1-\lambda][1-p]^N)^q + e_+^q + e_-^q \right] \right) \\
&= \frac{1}{q-1} \left\{ 1 - (1-\lambda)^q [1 + (1-q)S_q[1]]^N + (1-\lambda)^q p^{Nq} \right. \\
&\quad \left. + (1-\lambda)^q (1-p)^{Nq} - e_+^q - e_-^q \right\} \tag{2.47}
\end{aligned}$$

where

$$\begin{aligned}
e_{\pm} &= \frac{1}{2} \left\{ (1-p)^N - p^N(\lambda-1) + \lambda - (1-p)^N \lambda \right. \\
&\quad \left. \pm \sqrt{[(1-p)^N(\lambda-1) + p^N(\lambda-1) - \lambda]^2 - 4(\lambda-1)[-(p-1)p]^N(\lambda-1)} \right. \\
&\quad \left. - (1-p)^N p \lambda + (p-1)p^N \lambda \right\} \tag{2.48}
\end{aligned}$$

are the eigenvalues of the top left hand corner 2×2 matrix block.

For large N , $S_q[\rho^{(c)}; N] = NS_q[1]$ is also approximately equal to the right hand side of equation (2.32) and thus λ will again be given by equation (2.33).

It is worth considering the case $p = \frac{1}{2}$ separately. For this value of p the state $|\phi\rangle$ is a GHZ state [73],

$$|GHZ\rangle = \frac{1}{\sqrt{2}}(|00\dots 0\rangle + |11\dots 1\rangle), \tag{2.49}$$

which means we have,

$$\rho^{(c)} = \lambda|GHZ\rangle\langle GHZ| + \frac{1-\lambda}{2^N}I, \tag{2.50}$$

where I is the $2^N \times 2^N$ identity matrix. The state (2.50) is known to be separable if and only if [73]

$$0 \leq \lambda \leq \frac{1}{1 + 2^{N-1}}. \tag{2.51}$$

Comparing equation (2.33) with equation (2.51), it follows that in the thermodynamic limit the value of λ yielding an extensive S_q describes an entangled state.

2.5 A continuous system

We now consider a system where the phase space of each of the N subsystems is the positive, real half line, $\mathcal{R}_+ = [0, +\infty)$. Our model will be based on the probability densities,

$$p^{(a)}(x_1, x_2, \dots, x_N) = \begin{cases} \frac{1}{2^k} & \text{if } k-1 \leq x_i < k; \quad (i = 1, 2, \dots, N; k = 1, 2, 3, \dots) \\ 0 & \text{otherwise} \end{cases} \quad (2.52)$$

and

$$p^{(b)}(x_1, x_2, \dots, x_N) = p(x_1)p(x_2) \dots p(x_N), \quad (2.53)$$

where

$$p(x) = \frac{1}{2^k} \quad \text{if } k-1 \leq x < k; \quad k = 1, 2, 3, \dots \quad (2.54)$$

The probability densities $p^{(a)}(x, y)$ and $p^{(b)}(x, y)$ corresponding to the case of two subsystems ($N = 2$), along with the corresponding marginal probability $p(x)$, are represented in Figures 2.3 and 2.4. The marginal probability $p(x)$ is obtained by integrating over the y -coordinate:

$$p(x) = \int_0^\infty p^{(a,b)}(x, y) dy, \quad (2.55)$$

which is equivalent to summing the probability densities in each ‘‘column’’ of width $k-1 \leq x < k$. An important formula that is needed is the infinite geometric series for $|s| < 1$:

$$\sum_{n=0}^{\infty} s^n = \frac{1}{1-s}. \quad (2.56)$$

Once again, let $p^{(c)}$ be given by equation (2.17). The marginal probability distribution for both $p^{(a)}$ and $p^{(b)}$, and hence for $p^{(c)}$, is then given by (2.54). For the continuous case, the S_q entropic measure is defined as

$$S_q[p(x_1, x_2, \dots, x_N); N] = \frac{1}{q-1} \left[1 - \int_0^\infty \int_0^\infty \dots \int_0^\infty [p(x_1, x_2, \dots, x_N)]^q dx_1 dx_2 \dots dx_N \right]. \quad (2.57)$$

The entropy corresponding to (2.54) is

$$S_q[p] = \frac{1}{q-1} \left(\frac{2^q - 2}{2^q - 1} \right) \quad (2.58)$$

2.5 A continuous system

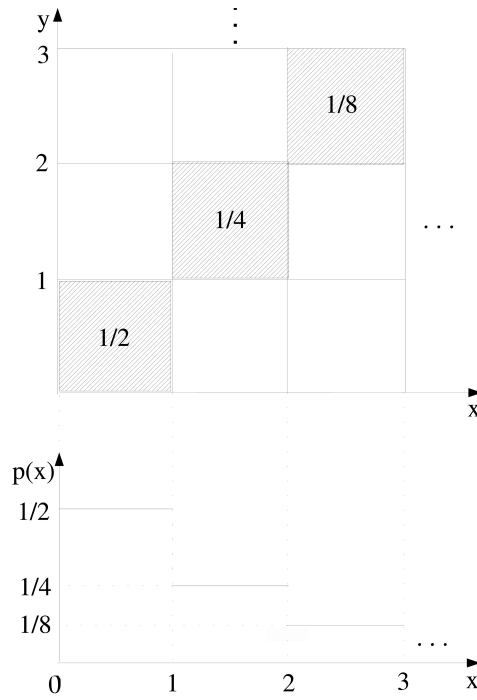


Figure 2.3: The upper part of the figure represents $p^{(a)}(x, y)$. The shaded regions have the uniform probability densities indicated in the figure. The probability density is zero elsewhere. The lower part corresponds to the marginal probability distribution $p(x)$.

and the entropy for $p^{(a)}$ is

$$S_q[p^{(a)}; N] = S_q[p], \quad (2.59)$$

since

$$\begin{aligned}
 & \int_0^\infty \int_0^\infty \cdots \int_0^\infty [p^{(a)}(x_1, x_2, \dots, x_N)]^q dx_1 dx_2 \dots dx_N \\
 &= \sum_{k=1}^\infty \int_{k-1}^k \int_{k-1}^k \cdots \int_{k-1}^k \left(\frac{1}{2^{kq}}\right) dx_1 dx_2 \dots dx_N \\
 &= \sum_{k=1}^\infty \left(\frac{1}{2^q}\right)^k \quad q \neq 1.
 \end{aligned} \quad (2.60)$$

2.5 A continuous system

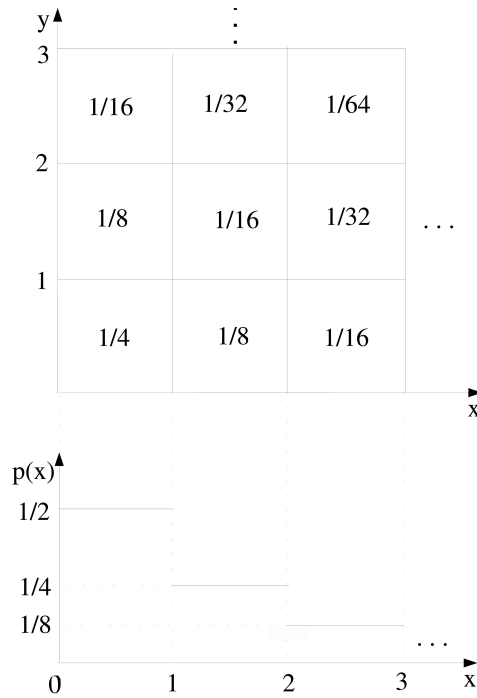


Figure 2.4: The upper part of the figure represents $p^{(b)}(x, y)$, the square regions have the uniform probability densities indicated in the figure. In the lower part the marginal probability distribution $p(x)$ is depicted.

To obtain the entropy for $p^{(b)}$, one follows exactly the same procedure as for the discrete case, since $p^{(b)}$ is factorizable.

Thus

$$S_q[p^{(b)}; N] = \frac{1}{q-1} \{1 - [1 + (1-q)S_q[p]]^N\}, \quad N \geq 2. \quad (2.61)$$

To obtain $S_q[p^{(c)}; N]$, one uses

$$S_q[p^{(c)}; N] = \frac{1}{q-1} \left[1 - \int_0^\infty \int_0^\infty \cdots \int_0^\infty [p^{(c)}(x_1, x_2, \dots, x_N)]^q dx_1 dx_2 \dots dx_N \right] \quad (2.62)$$

where

2.5 A continuous system

$$\begin{aligned}
& \int_0^\infty \int_0^\infty \cdots \int_0^\infty [\lambda p^{(a)} + (1-\lambda)p^{(b)}]^q dx_1 dx_2 \dots dx_N \\
&= (1-\lambda)^q \int_0^\infty \int_0^\infty \cdots \int_0^\infty [p^{(b)}]^q dx_1 dx_2 \dots dx_N \\
&\quad - (1-\lambda)^q \sum_{k=1}^\infty \int_{k-1}^k \int_{k-1}^k \cdots \int_{k-1}^k \left(\frac{1}{2^{kNq}} \right) dx_1 dx_2 \dots dx_N \\
&\quad + \sum_{k=1}^\infty \int_{k-1}^k \int_{k-1}^k \cdots \int_{k-1}^k \left(\lambda \frac{1}{2^k} + (1-\lambda) \frac{1}{2^{kN}} \right)^q dx_1 dx_2 \dots dx_N \quad (2.63)
\end{aligned}$$

and the volume of the hypercubes is one. This gives

$$S_q[p^{(c)}; N] = \frac{1}{q-1} \{1 - (1-\lambda)^q [1 + (1-q)S_q[p]]^N - C_1 + C_2\}, \quad (2.64)$$

where

$$\begin{aligned}
C_1 &= \sum_{k=1}^\infty \left[\lambda \left(\frac{1}{2^k} \right) + (1-\lambda) \left(\frac{1}{2^{kN}} \right) \right]^q < 8, \\
C_2 &= (1-\lambda)^q \left(\frac{1}{2^{qN} - 1} \right). \quad (2.65)
\end{aligned}$$

Now

$$\begin{aligned}
S_q[p^{(c)}; N](\lambda = 0) &= S_q[p^{(b)}; N] \\
S_q[p^{(c)}; N](\lambda = 1) &= S_q[p^{(a)}; N]. \quad (2.66)
\end{aligned}$$

Since $S_q[p^{(b)}; N]$ increases exponentially with N and $NS_q[p]$ only linearly, it means that there exists an N from which onward $S_q[p^{(b)}; N] > NS_q[p] > S_q[p] = S_q[p^{(a)}; N]$ and thus a λ exists for which

$$S_q[p^{(c)}; N](\lambda) = NS_q[p]. \quad (2.67)$$

For large N equation (2.67) will hold and so in this limit,

$$NS_q[p] \approx \frac{1}{1-q} (1-\lambda)^q [1 + (1-q)S_q[p]]^N. \quad (2.68)$$

2.6 Conclusions

Hence for large N ,

$$\lambda \approx 1 - \left\{ \frac{(1-q)NS_q[p]}{[1+(1-q)S_q[p]]^N} \right\}^{\frac{1}{q}}. \quad (2.69)$$

Thus in the thermodynamic limit, λ tends to one and hence $p^{(c)}$ tends to $p^{(a)}$ which is maximally correlated. This means that as N increases, the correlations have to become stronger until the system is completely correlated.

2.6 Conclusions

I have considered two models of phase space occupancy probabilities leading, for appropriate values of the relevant parameters, to an extensive behaviour of the power-law entropy S_q . Our models allow for an explicit analysis of the $N \rightarrow \infty$ (thermodynamic) limit. In that limit I obtained asymptotic analytic expressions for the values of the parameter λ that yield an extensive S_q . We also considered a quantum version of one of our models. I showed that for $p = \frac{1}{2}$ and for large enough values of N , the density matrix associated with an extensive q -entropy describes an entangled state.

Taking as a “reference point” the completely uncorrelated (that is, factorized) probability distribution I showed that (within our models) it is necessary to incorporate strong correlations among the subsystems in order to reach an additive regime for S_q . As a matter of fact, in the limit $N \rightarrow \infty$, the probability distribution that makes S_q additive tends towards a maximally correlated distribution.

Chapter 3

Two Particles in a Double Well: Illustrating the Connection Between Entanglement and the Speed of Quantum Evolution

The concept of entanglement is of fundamental importance and it is thus essential to thoroughly explore all the implications of entanglement. The problem of the “speed” of quantum evolution is very relevant as explained in the Introduction (Section 1.0.3), because basic computational steps involve moving from one quantum state to an orthogonal one. This implies that lower bounds on the time needed to reach an orthogonal state can provide estimations on how fast one can perform elementary computation operations [14]. The connection between entanglement and the speed of quantum evolution (as measured by the time needed to reach an orthogonal state) will presently be discussed in the case of two quantum particles moving in a one-dimensional double well [74].

3.1 Overview

The aim of the present chapter is to illustrate some aspects of the relationship between quantum entanglement and the speed of quantum evolution, in connection

3.2 Two particles in a double well: separable vs entangled states

with the problem of the tunneling time in a double well potential [75; 76]: quantum entanglement enhances the “speed” of evolution of certain quantum states, as measured by the time needed to reach an orthogonal state. The purpose of this discussion is two-fold: on the one hand, to introduce the basic idea of the connection between entanglement and “quantum speed” using a simple example. On the other hand, to show that this simple illustration also has considerable didactic value and can be incorporated into a university course in quantum physics. That is, due to its great importance both from the fundamental and from the practical points of view it is imperative that the concept of entanglement is incorporated into the teaching of quantum mechanics. With regards to this educational aspect, it is worth mentioning that, despite being at the heart of quantum physics, quantum entanglement is still not included in most standard quantum mechanics textbooks. In most of these cases the word “entanglement” is not even mentioned in the subject index. It is important to develop didactic examples of quantum problems that integrate the concept of entanglement with other fundamental aspects of quantum physics (see [77]).

The chapter is organized as follows: in Section 3.2 I compare separable and entangled states, Section 3.3 focuses on the role of entanglement in the speed of quantum evolution and finally I draw some conclusions in Section 3.4.

3.2 Two particles in a double well: separable vs entangled states

I am going to consider a system consisting of two distinguishable particles of mass m (with coordinates x_1 and x_2) moving in a one-dimensional double well potential $V(x)$ (see Figure 3.1). The considerations discussed here hold for general double well potentials. However, the pictures depicted in this chapter correspond to the particular, exactly soluble potential [78]

$$V(x) = \frac{\hbar^2 \kappa^2}{2m} \left[\frac{1}{8} \xi^2 \cosh 4\kappa x - 4\xi \cosh 2\kappa x - \frac{1}{8} \xi^2 \right], \quad (3.1)$$

3.2 Two particles in a double well: separable vs entangled states

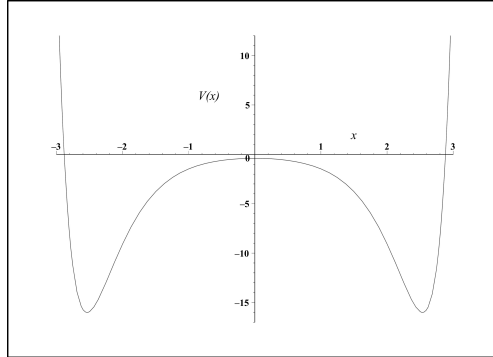


Figure 3.1: Double well potential function (3.1). The potential $V(x)$, and the coordinate x are depicted, respectively, in units of $\hbar^2\kappa^2/2m$ and $1/\kappa$.

with $\xi = 0.1$. The potential function (3.1) is plotted in Figure 3.1, using for $V(x)$ units of $\frac{\hbar^2\kappa^2}{2m}$ and for x units of $1/\kappa$. The eigenstates associated with the potential (3.1) can be used, for instance, as an approximate description of the low-lying states of a homonuclear diatomic molecule [78]. A pair of such molecules constitutes a possible physical realization of the bipartite composite quantum system that I am going to consider here.

Let $|\psi_0\rangle$ and $|\psi_1\rangle$ denote the (one particle) ground and first excited states corresponding to the potential $V(x)$, with eigenenergies E_0 and E_1 , respectively. The ground state $|\psi_0\rangle$ is described by an even wave function, while the state $|\psi_1\rangle$ is described by an odd wave function (see Figure 3.2). The explicit expressions for the ground and first excited states wave eigenfunctions of the potential (3.1) (here we are measuring the spatial coordinate x in units of $1/\kappa$ which, of course, is tantamount to adopting $\kappa = 1$) are given by [78]

$$\psi_0(x) = e^{-\frac{1}{4}\xi \cosh 2x} \left[3\xi \cosh x + \left(4 - \xi + 2\sqrt{4 - 2\xi + \xi^2} \right) \cosh 3x \right], \quad (3.2)$$

$$\psi_1(x) = e^{-\frac{1}{4}\xi \cosh 2x} \left[3\xi \sinh x + \left(4 + \xi + 2\sqrt{4 + 2\xi + \xi^2} \right) \sinh 3x \right]. \quad (3.3)$$

The corresponding energy eigenvalues are

$$E_{0,1} = \frac{\hbar^2\kappa^2}{2m} \epsilon_{0,1}, \quad (3.4)$$

with

3.2 Two particles in a double well: separable vs entangled states

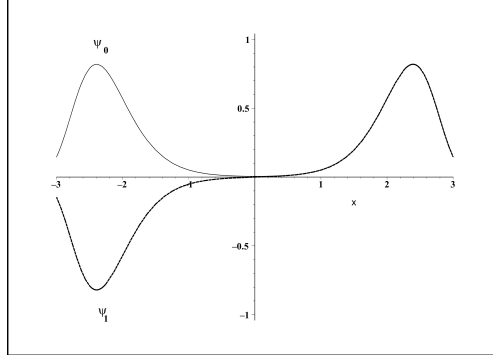


Figure 3.2: The ground state and first excited state wave functions of the double well potential (3.1). The wave functions and the spatial coordinate x are depicted, respectively, in units of $\sqrt{\kappa}$ and $1/\kappa$.

$$\epsilon_0 = -\xi - 5 - 2\sqrt{4 - 2\xi + \xi^2}, \quad (3.5)$$

$$\epsilon_1 = \xi - 5 - 2\sqrt{4 + 2\xi + \xi^2}. \quad (3.6)$$

The linear combinations

$$|\psi_R\rangle = \frac{1}{\sqrt{2}}\{|\psi_0\rangle + |\psi_1\rangle\}, \quad (3.7)$$

and

$$|\psi_L\rangle = \frac{1}{\sqrt{2}}\{|\psi_0\rangle - |\psi_1\rangle\}, \quad (3.8)$$

correspond to states of a particle localized, respectively, in the right hand side well and in the left hand side well of $V(x)$. If we consider only (single-particle) states that are linear combinations of $|\psi_0\rangle$ and $|\psi_1\rangle$, we have a system described by an effective two-dimensional Hilbert space or, in quantum information parlance, an effective one-qubit system.

Now we are going to focus our attention on states of two distinguishable quantum particles living in the potential $V(x)$. We are going to work only with states that are linear combinations of the four states $|\psi_0\rangle|\psi_0\rangle$, $|\psi_0\rangle|\psi_1\rangle$, $|\psi_1\rangle|\psi_0\rangle$ and $|\psi_1\rangle|\psi_1\rangle$. In other words, we are going to work with an effective two-qubit system. Pure states of this composite system can be classified into factorizable

3.2 Two particles in a double well: separable vs entangled states

pure states and entangled pure states. On the one hand we have factorizable states,

$$|\phi\rangle = |\phi\rangle_1 \otimes |\phi\rangle_2, \quad (3.9)$$

where $|\phi\rangle_k$ ($k = 1, 2$) are pure states of the k -particle. On the other hand we have entangled states, which are those that cannot be written in the form (3.9). In the case of factorizable states, each subsystem (in our case, each one of the two particles) is described by an individual pure state of its own (that is, the states $|\phi\rangle_k$ ($k = 1, 2$) in (3.9)). On the contrary, when we have an entangled state it is not possible to assign an individual pure state to each subsystem. In this case, the subsystems are in mixed states, which are described by density matrices. If our two particle system is in a (pure) entangled state $|\psi\rangle$, each particle's state is described by a (marginal) density matrix obtained by taking the trace of the projector $|\psi\rangle\langle\psi|$ over the coordinate of the other particle. That is, the particles are described by density matrices ρ_k given by

$$\begin{aligned} \rho_1 &= \text{Tr}_2(|\psi\rangle\langle\psi|), \\ \rho_2 &= \text{Tr}_1(|\psi\rangle\langle\psi|). \end{aligned} \quad (3.10)$$

More explicitly, the matrix elements of the density matrices ρ_k are given by

$$\begin{aligned} \langle x'_1 | \rho_1 | x_1 \rangle &= \int \langle x'_1, x_2 | \psi \rangle \langle \psi | x_1, x_2 \rangle dx_2, \\ \langle x'_2 | \rho_2 | x_2 \rangle &= \int \langle x_1, x'_2 | \psi \rangle \langle \psi | x_1, x_2 \rangle dx_1. \end{aligned} \quad (3.11)$$

Not all entangled states are endowed with the same amount of entanglement. A quantitative measure of the amount of entanglement of a pure state $|\psi\rangle$ is given by the von Neumann entropy of either of the matrices ρ_k ,

$$\mathcal{E}(|\psi\rangle) = -\text{Tr}(\rho_1 \log_2 \rho_1) = -\text{Tr}(\rho_2 \log_2 \rho_2). \quad (3.12)$$

It is clear that according to the measure $\mathcal{E}(|\psi\rangle)$ factorizable pure states have zero entanglement.

3.2 Two particles in a double well: separable vs entangled states

A fundamental property of the measure of entanglement (3.12) is that it does not change under the action of local unitary transformations. That is, it does not change under the action of transformations of the form

$$U = U_1 \otimes U_2, \quad (3.13)$$

where $U_{1,2}$ represent unitary transformations acting on each particle individually.

In the problem we are considering, we have two non-interacting quantum particles moving in the same potential $V(x)$. The Hamiltonian of our system is of the form

$$H = H_1 \otimes I_2 + I_1 \otimes H_2, \quad (3.14)$$

where I_k stands for the identity operator acting on the Hilbert space associated with the k -particle ($k = 1, 2$) and

$$H_k = -\frac{\hbar^2}{2m} \frac{\partial^2}{\partial x_k^2} + V(x_k) \quad (k = 1, 2). \quad (3.15)$$

It is clear that the time evolution operator of this system is local (that is, it has the form (3.13)) with

$$U_k = \exp \left[-\frac{itH_k}{\hbar} \right] \quad (k = 1, 2). \quad (3.16)$$

Consequently, the amount of entanglement of our two particles is not going to change in time. Notice that the amount of entanglement exhibited by a given state of our two particle system is an intrinsic property of that state. It does not depend on the form of the Hamiltonian. However, the Hamiltonian governs the evolution of the state and, consequently, also determines eventual changes in the amount of entanglement. In the case of the Hamiltonian (3.14-3.15) that we are going to consider, the amount of entanglement at any time is going to be the same as the amount of entanglement $\mathcal{E}(|\psi(t_0)\rangle\rangle)$ associated with the initial state $|\psi(t_0)\rangle$. Obviously, the initial entanglement $\mathcal{E}(|\psi(t_0)\rangle\rangle)$ is, in turn, determined by the particular way in which the initial state was prepared.

3.3 Entanglement and the speed of quantum evolution

3.3 Entanglement and the speed of quantum evolution

3.3.1 The speed of quantum evolution and its lower bound

As already mentioned in the Introduction, a natural measure for the “speed” of quantum evolution is provided by the time interval τ that a given initial state $|\psi(t_0)\rangle$ takes to evolve into an orthogonal state [53; 55; 79; 80],

$$\langle\psi(t_0)|\psi(t_0 + \tau)\rangle = 0. \quad (3.17)$$

In our present example involving two particles in a double well potential, τ can be regarded as the tunneling time of the two particle system. Let E denote the energy’s expectation value,

$$E = \langle H \rangle, \quad (3.18)$$

and ΔE the energy’s uncertainty,

$$\Delta E = \sqrt{\langle H^2 \rangle - \langle H \rangle^2}. \quad (3.19)$$

A lower limit for the evolution time τ to an orthogonal state is given by [55]

$$\tau_{min} = \frac{\pi\hbar}{2\Delta E}. \quad (3.20)$$

3.3.2 Comparing a separable state and a maximally entangled state

Let us first consider the factorizable, two particle state

$$|\psi_{RR}\rangle = |\psi_R\rangle \otimes |\psi_R\rangle, \quad (3.21)$$

corresponding to a situation where both particles are localized in the right hand side well (see Figure 3.3). The expansion of this state in the Hamiltonian’s eigenbasis is,

3.3 Entanglement and the speed of quantum evolution

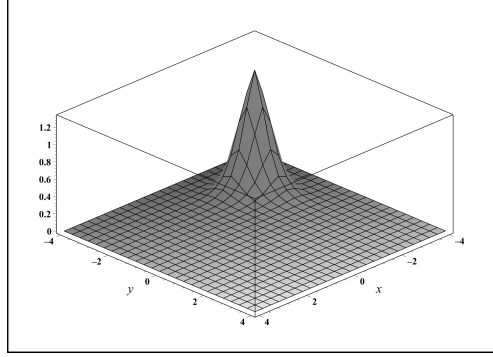


Figure 3.3: The wave function corresponding to the state $|\psi_{RR}\rangle$. The wave function and the spatial coordinates $x_{1,2}$ are depicted, respectively, in units of κ and $1/\kappa$.

$$|\psi_{RR}\rangle = \frac{1}{2} \{ |\psi_0\rangle|\psi_0\rangle + |\psi_0\rangle|\psi_1\rangle + |\psi_1\rangle|\psi_0\rangle + |\psi_1\rangle|\psi_1\rangle \}, \quad (3.22)$$

the energy expectation value is,

$$E_{RR} = E_0 + E_1, \quad (3.23)$$

and the energy uncertainty is

$$\Delta E_{RR} = \frac{1}{\sqrt{2}}(E_1 - E_0). \quad (3.24)$$

The concomitant lower bound for the time to reach an orthogonal state is then (see equation (3.20))

$$\tau_{min}(|\psi_{RR}\rangle) = \frac{\hbar\pi}{2\Delta E_{RR}} = \frac{\hbar\pi}{\sqrt{2}(E_1 - E_0)}. \quad (3.25)$$

On the other hand, the time actually needed by state $|\psi_{RR}\rangle$ to evolve into the orthogonal state $|\psi_{LL}\rangle = |\psi_L\rangle \otimes |\psi_L\rangle$ (whose wave function is depicted in Figure 3.4) is the same as the time needed by the one particle state $|\psi_R\rangle$ to evolve to $|\psi_L\rangle$,

$$\tau(|\psi_{RR}\rangle) = \tau(|\psi_R\rangle) = \frac{\hbar\pi}{(E_1 - E_0)}. \quad (3.26)$$

Consequently,

3.3 Entanglement and the speed of quantum evolution

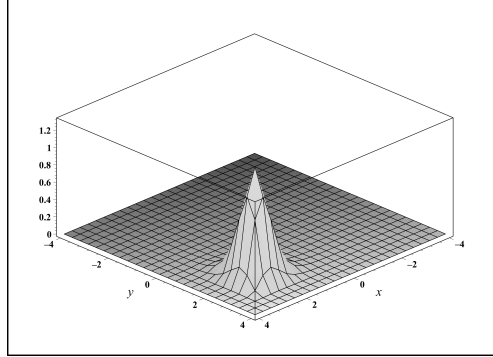


Figure 3.4: The wave function corresponding to the state $|\psi_{LL}\rangle$. The wave function and the spatial coordinates $x_{1,2}$ are depicted, respectively, in units of κ and $1/\kappa$.

$$\tau_{min}(|\psi_{RR}\rangle) = \frac{1}{\sqrt{2}}\tau(|\psi_{RR}\rangle) < \tau(|\psi_{RR}\rangle). \quad (3.27)$$

Therefore, we see that the state $|\psi_{RR}\rangle$ does not saturate the bound (3.20). Its evolution is not as fast as it is allowed by the bound (3.20). Let us now consider the entangled state

$$|\psi_{ent}\rangle = \frac{1}{\sqrt{2}}(|\psi_0\rangle|\psi_0\rangle + |\psi_1\rangle|\psi_1\rangle), \quad (3.28)$$

whose energy expectation value is

$$E_{ent} = E_0 + E_1, \quad (3.29)$$

and whose energy uncertainty is

$$\Delta E_{ent} = E_1 - E_0. \quad (3.30)$$

The state $|\psi_{ent}\rangle$ is (within our effective two-qubit system) maximally entangled. The amount of entanglement of this state is (see equation (3.12))

$$\mathcal{E}(|\psi_{ent}\rangle) = \log_2 2 = 1, \quad (3.31)$$

which is the maximum amount of entanglement in a two-qubit system.

3.3 Entanglement and the speed of quantum evolution

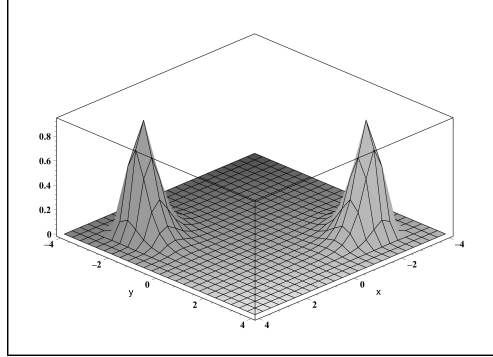


Figure 3.5: The wave function corresponding to the state $|\psi_{ent}\rangle$. The wave function and the spatial coordinates $x_{1,2}$ are depicted, respectively, in units of κ and $1/\kappa$.

The wave function of state $|\psi_{ent}\rangle$ is exhibited in Figure 3.5. After a time interval $\tau(|\psi_{ent}\rangle)$, this state evolves into the orthogonal state $|\psi_{ent}\rangle^\perp$, whose wave function is plotted in Figure 3.6. In this case, the actual time needed to reach an orthogonal state coincides with the bound given by (3.20),

$$\begin{aligned}
 \tau(|\psi_{ent}\rangle) &= \frac{\tau_{min}(|\psi_{ent}\rangle)}{\pi\hbar} \\
 &= \frac{1}{2(E_1 - E_0)}.
 \end{aligned}
 \tag{3.32}$$

In other words, the entangled state $|\psi_{ent}\rangle$ saturates the bound (3.20).

It is instructive to compare some general aspects of the time evolution of states $|\psi_{RR}\rangle$ and $|\psi_{ent}\rangle$. In the case of the separable state $|\psi_{RR}\rangle$, it is possible to associate the individual pure state $|\psi_R\rangle$ to each particle, and these single particle states evolve in such a way that the associated wave functions are localized alternately in each well. In other words, the expectation values $\langle x_{1,2} \rangle$ oscillate between the two wells. On the contrary, in the case of the entangled state $|\psi_{ent}\rangle$ each particle is described by the mixed state

$$\rho_{1,2} = \frac{1}{2} \left(|\psi_0\rangle\langle\psi_0| + |\psi_1\rangle\langle\psi_1| \right) = \frac{1}{2} \left(|\psi_L\rangle\langle\psi_L| + |\psi_R\rangle\langle\psi_R| \right).
 \tag{3.33}$$

The density matrices describing the single particle states do not evolve in time. The associated probability densities have two peaks, one in each well. The expectation values $\langle x_{1,2} \rangle$ are constant in time. In order to “detect” the time evolution

3.3 Entanglement and the speed of quantum evolution

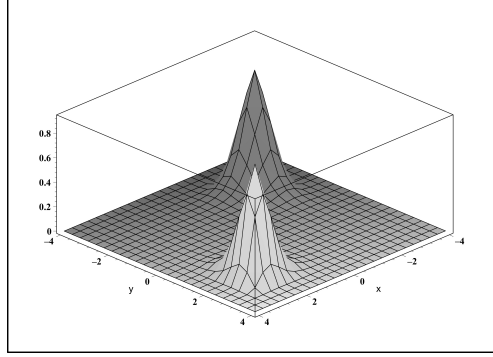


Figure 3.6: The wave function corresponding to the state $|\psi_{ent}\rangle^\perp$. The wave function and the spatial coordinates $x_{1,2}$ are depicted, respectively, in units of κ and $1/\kappa$.

of the two particle system one has to consider the behaviour of the expectation values of operators involving both particles. For instance, the expectation value

$$\langle (x_2 - x_1)^2 \rangle \quad (3.34)$$

exhibits a periodic time dependence. It adopts its maximum value for the wave function $|\psi_{ent}\rangle$ depicted in Figure 3.5, and its minimum value for the orthogonal wave function $|\psi_{ent}\rangle^\perp$ depicted in Figure 3.6.

3.3.3 More general states

The general state of our effective two qubit system is

$$|\psi\rangle = a_1|\psi_0\rangle|\psi_0\rangle + a_2|\psi_0\rangle|\psi_1\rangle + a_3|\psi_1\rangle|\psi_0\rangle + a_4|\psi_1\rangle|\psi_1\rangle, \quad (3.35)$$

where the a_i 's are complex coefficients satisfying the normalization requirement,

$$|a_1|^2 + |a_2|^2 + |a_3|^2 + |a_4|^2 = 1. \quad (3.36)$$

The time τ needed for this state to evolve into an orthogonal one is given by

$$\begin{aligned} \langle \psi(t_0) | \psi(t_0 + \tau) \rangle &= e^{-2iE_0\tau/\hbar} [|a_1|^2 + (|a_2|^2 + |a_3|^2) e^{-i(E_1 - E_0)\tau/\hbar} + |a_4|^2 e^{-2i(E_1 - E_0)\tau/\hbar}] \\ &= 0. \end{aligned} \quad (3.37)$$

3.3 Entanglement and the speed of quantum evolution

This equation for τ can be recast as

$$P(x) = |a_4|^2 x^2 + (|a_2|^2 + |a_3|^2) x + |a_1|^2 = 0, \quad (3.38)$$

with

$$x = e^{-i(E_1 - E_0)\tau/\hbar}. \quad (3.39)$$

The initial state (3.35) evolves to an orthogonal state if and only if the quadratic equation (3.38) admits at least one root with modulus equal to 1. Let me consider the family of states (which I denote the “ β -family”) leading to an equation (3.38) with two complex conjugate roots with modulus equal to one,

$$e^{\pm i\beta}, \quad \text{with } \beta = (E_1 - E_0)\tau/\hbar \in [\pi/2, \pi]. \quad (3.40)$$

If that is the case, we can rewrite the polynomial $P(x)$ under the guise

$$P(x) = |a_4|^2 (x - e^{i\beta}) (x - e^{-i\beta}). \quad (3.41)$$

Comparing now the expressions (3.38) and (3.41) for $P(x)$, and taking into account the normalization requirement (3.36), one obtains,

$$\begin{aligned} |a_1|^2 = |a_4|^2 &= \frac{1}{2(1 - \cos \beta)}, \\ |a_2|^2 + |a_3|^2 &= -\frac{\cos \beta}{1 - \cos \beta}. \end{aligned} \quad (3.42)$$

We thus see that the β -family of states evolving to an orthogonal state constitute a monoparametric family parameterized by the parameter β . Therefore, all the relevant quantities concerning these states can be written in terms of β . In particular,

$$\tau_{min} = \frac{\pi \hbar}{2\Delta E} = \frac{\pi \hbar}{2(E_1 - E_0)} \sqrt{1 - \cos \beta}, \quad (3.43)$$

and the quotient between the actual time τ of evolution to an orthogonal state (which is related to β through equation (3.40)) and the lower bound τ_{min} , is

3.3 Entanglement and the speed of quantum evolution

$$\frac{\tau}{\tau_{min}}(\beta) = \frac{2\beta}{\pi\sqrt{1 - \cos\beta}}. \quad (3.44)$$

It is plain from this last equation that the lower bound on τ is saturated (that is, $\tau/\tau_{min} = 1$) only in the case $\beta = \pi/2$, corresponding to the maximally entangled state $|\psi_{ent}\rangle$ given by equation (3.28).

On the other hand, let us consider a separable pure state

$$|\phi\rangle = |\phi_a\rangle \otimes |\phi_b\rangle, \quad (3.45)$$

that evolves to an orthogonal state. In order for this to happen, at least one of the states $|\phi_{a,b}\rangle$ has to evolve to an orthogonal state. Lets assume that

$$|\phi_a\rangle = c_0|\psi_0\rangle + c_1|\psi_1\rangle \quad (3.46)$$

evolves to an orthogonal state. In that case, we have

$$|c_0|^2 + e^{-\frac{i\tau(E_1-E_0)}{\hbar}}|c_1|^2 = 0. \quad (3.47)$$

Equation (3.47) clearly implies that

$$\begin{aligned} |c_0|^2 &= |c_1|^2, \\ e^{-\frac{i\tau(E_1-E_0)}{\hbar}} &= -1, \end{aligned} \quad (3.48)$$

and consequently, if the state belongs to the β -family, we have $\beta = \pi$. Therefore, it follows from equation (3.44) that separable states in the β -family have the highest possible value of τ/τ_{min} ,

$$\left(\frac{\tau}{\tau_{min}}\right)_{\text{separable}} = \sqrt{2}. \quad (3.49)$$

The separable state given by equations (3.21-3.22), which we have previously considered in connection with the two-particle system in a double well, is an example of a state corresponding to the case $\beta = \pi$. This state illustrates an important feature of separable states: separable states that are energetically symmetric

3.4 Conclusions

(that is, the energy and the energy's uncertainty are shared evenly between the subsystems) do not saturate the bound (3.20). In fact, all energetically symmetric separable states that evolve to an orthogonal state correspond to the case $\beta = \pi$. It must be emphasized that the two particles that we are considering do not interact with each other, and that the entanglement of the system (which is conserved in time) is given by its initial state.

3.4 Conclusions

I have used a system of two non-interacting quantum particles in a double well potential to illustrate the connection between the speed of quantum evolution and quantum entanglement. The entanglement is conserved in time and is given by the initial state of the system. The time required by separable (energetically symmetric) initial states to reach an orthogonal state does not saturate the bound (3.20). On the contrary, there exist (energetically symmetric) maximally entangled states (within an effective two-qubit description) that do saturate the bound. That is, they evolve as fast as it is permitted by the value of their energy dispersion ΔE . States of intermediate entanglement were also considered, and I proved that within the β -family all the states that saturate the bound require maximum quantum entanglement (however, not all states with maximum entanglement do saturate the bound).

The connection between speed of evolution and entanglement in a system of two particles in a double well potential offers interesting opportunities to illustrate the concept of entanglement in university courses on quantum mechanics. On the one hand, this illustration is based upon a set of well-known ingredients (i.e. quantum double well potential, tunneling time, etc.) that are usually covered in courses on quantum mechanics. On the other hand, this example provides a clear instance of what we might call a “positive” feature of quantum entanglement, as contrasted with the “negative” way in which entanglement is usually defined. Entangled states are normally defined in terms of what they are not: an entangled pure state is a state that cannot be factorized. Most of the “positive” aspects of entanglement involve its role as a resource to implement novel, non-classical types of computation and communication processes. Unfortunately, a discussion

3.4 Conclusions

of these processes in a quantum mechanics course would require the introduction of various new concepts in information theory and computer science. On the contrary, the role played by entanglement in “speeding up” the evolution of two particles in a double well requires mostly ideas that are already part of standard courses in quantum mechanics.

Chapter 4

Entanglement and the Speed of Evolution of Multi-Partite Quantum Systems

Due to its great importance, both from the fundamental and from the practical points of view, it is imperative to investigate and survey in detail all the implications of the concept of entanglement. The aim of this chapter is to explore some aspects of the relationship between quantum entanglement and the speed of quantum evolution.

4.1 Overview

As already illustrated in the previous chapter, there exists an interesting relationship between entanglement and the time evolution of composite quantum systems: quantum entanglement enhances the “speed” of evolution of certain quantum states, as measured by the time needed to reach an orthogonal state. Previous research done on this subject has been focused upon comparing extreme cases (highly entangled states versus separable states) or upon bi-partite systems. In the present chapter I explore the aforementioned connection between entanglement and time evolution in the case of two-qubits (independent and interacting), three-qubits and N -qubits systems, taking into account states of intermediate entanglement. In the case of three qubits I perform a numerical survey of the

4.2 Independent bi-partite systems

system's Hilbert space, finding a clear correlation between entanglement and the time of evolution to an orthogonal state which is seen to hold also for states of intermediate entanglement. In addition to numerical results, some analytical results are also reported. In the case of two qubits I pay special attention to states of low entanglement saturating the quantum speed limit. Some of the results obtained for two non-interacting qubits are extended to the case of N -qubits. In particular, I introduce and investigate a family of energetically symmetric states of low entanglement that saturate the quantum speed bound [50]. I show that, as the number of qubits increases, very little entanglement is needed to reach the quantum speed limit.

The chapter is organized as follows. The connection between entanglement and speed of evolution for independent two-qubit systems is revisited in Section 4.2 and explored for interacting two-qubit systems in Section 4.3. In both instances I pay special attention to states of low entanglement saturating the quantum speed limit. The three-qubit system is treated in Section 4.4. Some of the results obtained for two qubits are extended to the case of N -qubits in Section 4.5. The role of entanglement in time-optimal quantum evolution of two qubits and symmetric, orthogonal initial and final states is analyzed in Section 4.6. Finally, some conclusions are drawn in Section 4.7.

4.2 Independent bi-partite systems

First I am going to consider a composite system consisting of two qubits. That is, two identical (but distinguishable) subsystems each one described by a two-dimensional Hilbert space. The Hamiltonian governing the evolution of our system is of the form

$$H = H_1 + H_2, \tag{4.1}$$

where H_i is a Hamiltonian acting only on the i -qubit. The time evolution operator associated with the Hamiltonian (4.1) is local and, consequently, the amount of entanglement of the system does not change in time. The two single qubit

4.2 Independent bi-partite systems

Hamiltonians H_i have the same structure, with eigenstates, $\{|0\rangle, |1\rangle\}$, and corresponding eigenenergies $E_0 = 0$, $E_1 = \epsilon$. Hamiltonians such as (4.1) are relevant for the study of some fundamental aspects of quantum entanglement (see for instance [81]) and, particularly, in connection with the problem of the speed of quantum evolution of entangled states (see [53]). Besides, there are interacting systems that, by recourse to an appropriate transformation, can be recast under the guise of two or more non-interacting components described by a separable Hamiltonian like (4.1) (see for example [82]).

Our composite system can be described in terms of the basis $\{|00\rangle, |01\rangle, |10\rangle, |11\rangle\}$, which can be rewritten as $\{|0\rangle, |1\rangle, |2\rangle, |3\rangle\}$. The general state of our two qubit system is then

$$|\psi(t_0)\rangle = \sum_{j=0}^3 a_j |j\rangle \quad (4.2)$$

where the a_j 's are complex coefficients satisfying the normalization requirement,

$$\sum_{j=0}^3 |a_j|^2 = 1. \quad (4.3)$$

The degree of mixedness of the marginal density matrix associated with one of the subsystems,

$$\rho_1 = \text{Tr}_2(|\psi\rangle\langle\psi|), \quad (4.4)$$

provides a quantitative characterization of the amount of entanglement of a pure state $|\psi\rangle$ of a bipartite system. This degree of mixedness can be measured in several ways. One possibility is to use the von Neumann entropy $S = -\text{Tr}(\rho_1 \log_2 \rho_1)$, leading to an entanglement measure called entropy of entanglement. Another possibility, frequently used in the literature because of its advantages for numerical and analytical computations, is given by the linear entropy, $1 - \text{Tr}(\rho_1^2)$ [83]. It is important to notice that this entropic measure coincides (up to a constant multiplicative factor) with the power-law entropy S_q with Tsallis' parameter $q = 2$.

4.2 Independent bi-partite systems

This choice leads to the entanglement measure

$$\mathcal{E}(|\psi\rangle) = 2 [1 - \text{Tr}(\rho_1^2)], \quad (4.5)$$

which is the one I am going to use in the present work. In terms of the measure $\mathcal{E}(|\psi\rangle)$, factorizable pure states (which have zero entanglement) are characterized by $\mathcal{E}(|\phi_1\rangle|\phi_2\rangle) = 0$. On the other hand, states of maximum entanglement, such as

$$|\psi_{EPR}\rangle = \frac{1}{\sqrt{2}}(|00\rangle + |11\rangle), \quad (4.6)$$

have $\mathcal{E}(|\psi_{EPR}\rangle) = 1$. Intermediate degrees of entanglement correspond to values $0 < \mathcal{E}(|\psi\rangle) < 1$. It must be mentioned that the main results that are going to be reported here do not depend on the particular measure (4.5) adopted. Similar results would be obtained if other measures (such as the concurrence or the entropy of entanglement) were used.

In order to characterize those initial states $|\psi(t_0)\rangle$ that evolve into orthogonal ones, one has to consider the equation

$$P(x) = \langle\psi(t_0)|\psi(t_0 + \tau)\rangle = |a_3|^2 x^2 + (|a_1|^2 + |a_2|^2)x + |a_0|^2 = 0, \quad (4.7)$$

where

$$x = e^{-i\epsilon\tau/\hbar}. \quad (4.8)$$

The initial state (4.2) evolves to an orthogonal state if and only if the quadratic equation (4.7) admits at least one root with modulus equal to one. This may happen in two different ways: equation (4.7) may have two complex conjugate roots of modulus one, or it may have two real roots, of which one must have modulus equal to one. Due to the notation that we are going to introduce shortly, these two cases are going to be designated, respectively, the β -case and the s -case.

4.2 Independent bi-partite systems

4.2.1 β -case

This is the case where equation (4.7) has two complex conjugate roots

$$x = e^{\pm i\beta}, \quad (4.9)$$

with

$$\beta = \frac{\epsilon\tau}{\hbar}. \quad (4.10)$$

The coefficients appearing in (4.7) can be written in terms of β ,

$$\begin{aligned} |a_0|^2 = |a_3|^2 &= \frac{1}{2(1 - \cos \beta)}, \\ |a_1|^2 + |a_2|^2 &= -\frac{\cos \beta}{1 - \cos \beta} = C. \end{aligned} \quad (4.11)$$

Expressing the energy's expectation value E and uncertainty ΔE in terms of β (where $\pi/2 \leq \beta \leq \pi$) it can be verified that

$$\Delta E \leq E, \quad (4.12)$$

and consequently,

$$\frac{\tau}{\tau_{min}}(\beta) = \frac{\pi\hbar}{2\Delta E} = \frac{2\beta}{\pi\sqrt{1 - \cos \beta}}. \quad (4.13)$$

In order to get expressions for $|a_1|^2$ and $|a_2|^2$, one has to introduce a parameter $0 \leq \delta \leq 1$, such that

$$\begin{aligned} |a_1|^2 &= \delta C, \\ |a_2|^2 &= (1 - \delta)C. \end{aligned} \quad (4.14)$$

Since a global phase factor doesn't affect the physical properties of a state, one can choose the global phase factor such that a_0 is real. Introducing three phase parameters

4.2 Independent bi-partite systems

$$0 \leq \gamma_1, \gamma_2, \gamma_3 < 2\pi, \quad (4.15)$$

the coefficients a_0, a_1, a_2 and a_3 can be parameterized as follows

$$\begin{aligned} a_0 &= \frac{1}{\sqrt{2(1 - \cos \beta)}}, \\ a_1 &= e^{i\gamma_1} \sqrt{\delta \frac{(-\cos \beta)}{1 - \cos \beta}}, \\ a_2 &= e^{i\gamma_2} \sqrt{(1 - \delta) \frac{(-\cos \beta)}{1 - \cos \beta}}, \\ a_3 &= e^{i\gamma_3} \frac{1}{\sqrt{2(1 - \cos \beta)}}. \end{aligned} \quad (4.16)$$

Consequently, the entanglement $\mathcal{E}(|\psi(t_0)\rangle)$ is a function of β and of four independent parameters, whereas τ/τ_{min} is only a function of β (remember that the entanglement of the system does not change in time). Since we are interested in the relation between entanglement and the speed of time evolution, we have to obtain an analytic expression for the boundary curve of this relation, that is, one has to find the set of parameters yielding the minimum possible entanglement for a given value of τ/τ_{min} . This means finding the set of parameters minimizing the value of $\mathcal{E} = 2[1 - \text{Tr}(\rho_1^2)]$ for each value of β in the interval $\pi/2 \leq \beta \leq \pi$. For a quantum state characterized by the coefficients (4.16) we have,

$$\mathcal{E} = \frac{1}{(1 - \cos \beta)^2} \left\{ 1 + 4\sqrt{\delta(1 - \delta)} \cos(\gamma_3 - \gamma_1 - \gamma_2) \cos \beta + 4\delta(1 - \delta) \cos^2 \beta \right\}. \quad (4.17)$$

We see that, for any given value of δ the minimum value of the expression (4.17) is obtained when

$$\cos(\gamma_3 - \gamma_1 - \gamma_2) = 1. \quad (4.18)$$

In particular, by setting $\gamma_1 = \gamma_2 = \gamma_3 = 0$, hence by making all the coefficients real, the measure \mathcal{E} is minimized. Taking the partial derivative of $\mathcal{E}(\beta, \delta)$ with respect to δ and then choosing $\delta = 1/2$ gives zero for all β in the domain and

4.2 Independent bi-partite systems

hence $\delta = 1/2$ corresponds to a critical point. The second derivative test shows that $\mathcal{E}(\beta, \delta)$ is a convex function of δ for all allowed β and thus the critical point is indeed the global minimum.

From this point on we shall assume the above values for the four parameters. The concomitant expression for the entanglement measure is then given by

$$\mathcal{E}(\beta) = 2 - \frac{1 - 6 \cos \beta + \cos^2 \beta}{(-1 + \cos \beta)^2}. \quad (4.19)$$

The parametric plot of $\tau/\tau_{min}(\beta)$ versus $\mathcal{E}(\beta, \delta = 1/2)$, with $\beta \in [\pi/2, \pi]$, yields the curve bounding region R_1 from below in Figure 4.1.

Summing up, the β -case corresponds to the shaded region R_1 in the $(\mathcal{E}, \tau/\tau_{min})$ -plane. All the points in this region are physically realizable.

4.2.2 s -case

In this case equation (4.7) has two real roots. One of these roots must have modulus equal to one, meaning it must be ± 1 and thus either $\tau = 0$ which is impossible since a state can never be orthogonal to itself or

$$\tau = \frac{\pi \hbar}{\epsilon}. \quad (4.20)$$

Therefore, one root must be -1 . Denoting the other root s , the polynomial appearing in equation (4.7) can be written under the guise

$$P(x) = |a_3|^2 (x^2 + (1 - s)x - s). \quad (4.21)$$

Notice that the particular instance of the β -case corresponding to $\beta = \pi$ coincides with the s -case for $s = -1$. The coefficients of $P(x)$ have to be positive, resulting in the restriction $s \leq 0$. Comparing the expressions (4.7) and (4.21) for $P(x)$, and taking into account the normalization requirement (4.3), results in

$$\begin{aligned} |a_3|^2 &= \frac{1}{2(1 - s)}, \\ |a_0|^2 &= -s|a_3|^2 = \frac{-s}{2(1 - s)}, \end{aligned}$$

4.2 Independent bi-partite systems

$$|a_1|^2 + |a_2|^2 = \frac{1-s}{2(1-s)} = \frac{1}{2}. \quad (4.22)$$

Introducing four parameters as in the β -case, we get

$$\begin{aligned} a_0 &= \sqrt{\frac{-s}{2(1-s)}}, \\ a_1 &= e^{i\mu_1} \sqrt{\frac{\lambda}{2}}, \\ a_2 &= e^{i\mu_2} \sqrt{\frac{1-\lambda}{2}}, \\ a_3 &= e^{i\mu_3} \frac{1}{\sqrt{2(1-s)}}. \end{aligned} \quad (4.23)$$

Since τ has the constant value (4.20), all the states in the s -family take the same amount of time (actually maximum possible time) to evolve to an orthogonal state, but what can be different among the states is the dispersion of the energy and hence τ_{min} . Thus

$$\frac{\tau}{\tau_{min}}(s) = \sqrt{\frac{1-6s+s^2}{(-1+s)^2}} \quad (4.24)$$

changes from state to state.

Once again, we are interested in the boundary curve of the entanglement and speed of time evolution relation. In this case we are looking for the curve in the $(\mathcal{E}, \tau/\tau_{min})$ -plane corresponding to the maximum value of \mathcal{E} (maximum entanglement) for any given value of τ/τ_{min} . The \mathcal{E} -measure associated with a state given by (4.23) is

$$\mathcal{E} = \frac{\lambda(1-\lambda)(1-s)^2 - s}{(1-s)^2} - \frac{2}{1-s} \sqrt{-s\lambda(1-\lambda)} \cos(\mu_3 - \mu_2 - \mu_1). \quad (4.25)$$

For given values of s and λ , the maximum of \mathcal{E} is achieved when

$$\cos(\mu_3 - \mu_2 - \mu_1) = -1. \quad (4.26)$$

4.2 Independent bi-partite systems

In particular, one can choose $\mu_1 = \mu_2 = 0$, $\mu_3 = \pi$, and thus make all the coefficients real. Assuming that relation (4.26) holds, \mathcal{E} becomes a function solely of s and λ and, for any given value of s , the maximum of \mathcal{E} corresponds to $\lambda = 1/2$. On the other hand, for given values of s and λ , the minimum of (4.25) corresponds to $\cos(\mu_3 - \mu_2 - \mu_1) = 1$, and letting $\lambda(1 - \lambda) = -s/(1 - s)^2$ yields $\mathcal{E} = 0$ (that is, a separable state). In other words, the minimum entanglement compatible with a given value of s (or a given value of τ/τ_{min}) is zero.

Both \mathcal{E} and τ/τ_{min} (assuming (4.26)) have the property that for any $u < 0$

$$\begin{aligned}\mathcal{E}(s = u, \lambda) &= \mathcal{E}(s = \frac{1}{u}, \lambda), \\ \frac{\tau}{\tau_{min}}(s = u) &= \frac{\tau}{\tau_{min}}(s = \frac{1}{u}).\end{aligned}\tag{4.27}$$

Thus the case $-1 \leq s \leq 0$ is equivalent to the case $s \leq -1$, and so we are only going to consider $-1 \leq s \leq 0$. Another property of \mathcal{E} is that for any $0 \leq c \leq 1$

$$\mathcal{E}(s, \lambda = c) = \mathcal{E}(s, \lambda = 1 - c).\tag{4.28}$$

In order to obtain the family of states that saturate the speed bound, we set $\tau/\tau_{min} = 1$ in equation (4.24). The only solutions are $s = 0$ and $s \rightarrow -\infty$. The parameter λ may adopt any value in the range $[0, 1]$, with $\lambda = 1/2$ and $\lambda = 0, 1$ corresponding, respectively, to the maximum and minimum value of \mathcal{E} , namely $1/4$ and 0 . In the latter instance the two qubits are not entangled (the state is factorizable). One of the two qubits is in an eigenstate of its Hamiltonian and thus does not evolve in time, nor does it contribute to the dispersion of the energy. The other qubit has maximal dispersion and hence evolves to an orthogonal state at the speed limit. On the other hand, all the states

$$\begin{aligned}|\psi(s = 0, \lambda)\rangle &= \sqrt{\frac{\lambda}{2}}|01\rangle + \sqrt{\frac{1 - \lambda}{2}}|10\rangle - \frac{1}{\sqrt{2}}|11\rangle \\ |\psi(s \rightarrow -\infty, \lambda)\rangle &= \frac{1}{\sqrt{2}}|00\rangle + \sqrt{\frac{\lambda}{2}}|01\rangle + \sqrt{\frac{1 - \lambda}{2}}|10\rangle\end{aligned}\tag{4.29}$$

with $0 < \lambda < 1$, thus with $0 < \mathcal{E} \leq 1/4$, are entangled. We see that, unlike the β -case (see equation (4.13)) where only $\beta = \pi/2$, hence only maximally entangled

4.2 Independent bi-partite systems

states saturate the bound, there is now a continuous family of partially entangled states (parameterized by the parameter λ) that saturate the speed bound and evolve as fast as possible. On the opposite side of the quantum speed range, the slowest evolution occurs when $\tau/\tau_{min} = \sqrt{2}$, thus when $s = -1$. In that case $\lambda = 1/2$ (together with condition (4.26)) corresponds to the state

$$\frac{1}{2} \left[|0\rangle \otimes (|0\rangle + |1\rangle) + |1\rangle \otimes (|0\rangle - |1\rangle) \right], \quad (4.30)$$

which is clearly maximally entangled (and, consequently, has $\mathcal{E} = 1$). The set of parameter values $s = -1$, $\lambda = 1/2$, together with $\mu_3 = \mu_2 = \mu_1 = 0$, corresponds to the state

$$\frac{1}{2} \left[|0\rangle|0\rangle + |0\rangle|1\rangle + |1\rangle|0\rangle + |1\rangle|1\rangle \right], \quad (4.31)$$

which also evolves in the slowest way, but has zero entanglement. We thus see that the states of the s -family with $\tau/\tau_{min} = \sqrt{2}$ cover the complete range of entanglement values: from separability to maximum entanglement.

A summary of the above results is provided in Figure 4.1. The parametric plot $\{\mathcal{E}(s, \lambda = 1/2), \tau/\tau_{min}(s)\}$ (taking into account (4.26)) corresponds to the boundary of the region R_2 . This curve is given (in terms of the parameter s) by the equations

$$\begin{aligned} \mathcal{E}(s, \lambda = 1/2) &= 2 - \frac{1}{4} \left[-4 \frac{\sqrt{-s}}{1-s} + \frac{7 + s(-10 + 7s)}{(-1 + s)^2} \right], \\ \frac{\tau}{\tau_{min}}(s) &= \sqrt{\frac{1 - 6s + s^2}{(-1 + s)^2}}. \end{aligned} \quad (4.32)$$

Therefore, the s -case corresponds to the shaded region R_2 in the $(\mathcal{E}, \frac{\tau}{\tau_{min}})$ -plane. All the points within this region are associated with physically realizable states.

We see that, in a sense, the β -family (Region R_1) and the s -family (Region R_2) behave in opposite ways. In region R_1 states evolving faster (that is, with smaller values of τ/τ_{min}) tend to exhibit increasing entanglement. On the contrary, in region R_2 states with decreasing values of τ/τ_{min} tend to have lower entanglement. However, it must be kept in mind that regions R_1 and R_2 also differ in connection with the absolute time τ needed to reach an orthogonal state. In region R_2 all

4.2 Independent bi-partite systems

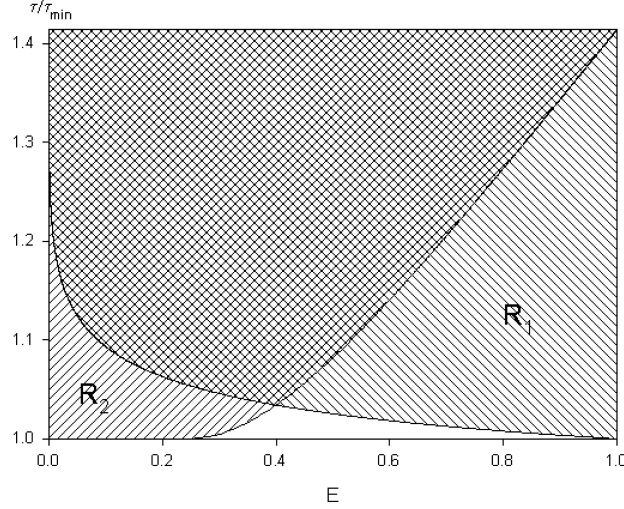


Figure 4.1: \mathcal{E} vs τ/τ_{min} for the independent two-qubit case: the curves bounding regions R_1 and R_2 correspond to $\{\mathcal{E}(\beta, \delta = 1/2), \tau/\tau_{min}(\beta)\}$ and $\{\mathcal{E}(s, \lambda = 1/2), \tau/\tau_{min}(s)\}$ respectively.

states take the same time τ to evolve into an orthogonal state. In region R_1 , the absolute evolution time to an orthogonal state is minimized by states of maximum entanglement.

The lower boundaries of region R_1 and region R_2 intersect at a point corresponding to the parameter values $\beta = 1.79841$ and $s = -0.0179989$. Thus the blank region, which corresponds to points in the $(\mathcal{E}, \frac{\tau}{\tau_{min}})$ -plane that are not physically allowed, is bounded by $\{\mathcal{E}(s, \lambda = 1/2), \tau/\tau_{min}(s)\}$ for $-0.0179989 \leq s \leq 0$ and $\{\mathcal{E}(\beta, \delta = 1/2), \tau/\tau_{min}(\beta)\}$ for $\pi/2 \leq \beta \leq 1.79841$. These results are consistent with previous research, in the sense that either entanglement or the asymmetry of the state can enhance time evolution.

The states evolving to an orthogonal state at the highest possible speed (in the sense of the speed bound) have either maximum entanglement ($\mathcal{E} = 1$) or (relatively) low entanglement ($0 \leq \mathcal{E} \leq 1/4$). Consequently, there is an entanglement gap, given by

$$\frac{1}{4} < \mathcal{E} < 1, \quad (4.33)$$

4.3 Interacting bi-partite systems

corresponding to entanglement values that are not physically permitted for states evolving at the quantum speed limit. Those states saturating the speed bound and having the particular amount of entanglement given by

$$\mathcal{E}_{ESSLE} = \frac{1}{4} \quad (4.34)$$

are especially interesting because they define a family of *energetically symmetric states with low entanglement* (ESSLE) that saturate the speed bound. By “energetically symmetric” states we mean states where the energy’s expectation value E , and the energy’s variance $(\Delta E)^2$ are evenly shared among all the subsystems (in this case, the two qubits involved).

4.3 Interacting bi-partite systems

For two interacting qubits the Hamiltonian is of the form

$$H = H_1 + H_2 + H_{int} \quad (4.35)$$

where H_1, H_2 are the free Hamiltonians of the two qubits and H_{int} is a non-trivial interaction Hamiltonian between them. Unlike the case of two non-interacting qubits, the time evolution is not a local unitary operation but only a global unitary evolution. This means time evolution changes entanglement. As was shown in [53], H_{int} can build up entanglement so that the system may reach the bound even though no entanglement was present initially. They used the following interaction capable of speeding up the dynamics:

$$H = \hbar\omega_0 [2 I^{(1)} \otimes I^{(2)} - \sigma_x^{(1)} \otimes I^{(2)} - I^{(1)} \otimes \sigma_x^{(2)}] + \hbar\omega [I^{(1)} \otimes I^{(2)} - \sigma_x^{(1)} \otimes \sigma_x^{(2)}], \quad (4.36)$$

where I is the identity matrix and σ_x is the x -Pauli operator. The free Hamiltonian which rotates each of the qubits independently at frequency ω_0 is given by the first term of eq. (4.36), while the second term is a global interaction which couples the two qubits together by collectively rotating them at frequency ω . Expressing H in the σ_z -basis $\{|0\rangle, |1\rangle\}$,

4.3 Interacting bi-partite systems

$$H = \hbar \begin{pmatrix} 2\omega_0 + \omega & -\omega_0 & -\omega_0 & -\omega \\ -\omega_0 & 2\omega_0 + \omega & -\omega & -\omega_0 \\ -\omega_0 & -\omega & 2\omega_0 + \omega & -\omega_0 \\ -\omega & -\omega_0 & -\omega_0 & 2\omega_0 + \omega \end{pmatrix}, \quad (4.37)$$

we obtain the eigenvalues $\{0, 4\hbar\omega_0, 2\hbar(\omega + \omega_0), 2\hbar(\omega + \omega_0)\}$ and the eigenvectors

$$|u_0\rangle = \frac{1}{2}\{|00\rangle + |01\rangle + |10\rangle + |11\rangle\} \quad (4.38)$$

$$|u_1\rangle = \frac{1}{2}\{|00\rangle - |01\rangle - |10\rangle + |11\rangle\} \quad (4.39)$$

$$|u_2\rangle = \frac{1}{\sqrt{2}}\{-|00\rangle + |11\rangle\} \quad (4.40)$$

$$|u_3\rangle = \frac{1}{\sqrt{2}}\{-|01\rangle + |10\rangle\}. \quad (4.41)$$

The above Hamiltonian is of technological importance as it can increase the communication rate [84]. Giovannetti *et al* considered a separable initial state and then analyzed the effect of varying ω and ω_0 . The procedure used here is similar to the one used in the case of two independent qubits in the sense that we shall consider a general state and restrict ourselves to three specific cases of ω and ω_0 .

The initial state at time t_0 is given by

$$\begin{aligned} |\psi(t_0)\rangle &= a_0|u_0\rangle + a_1|u_1\rangle + a_2|u_2\rangle + a_3|u_3\rangle \\ &= \left[\frac{1}{2}a_0 + \frac{1}{2}a_1 - \frac{1}{\sqrt{2}}a_2\right]|00\rangle + \left[\frac{1}{2}a_0 - \frac{1}{2}a_1 - \frac{1}{\sqrt{2}}a_2\right]|01\rangle \\ &\quad + \left[\frac{1}{2}a_0 - \frac{1}{2}a_1 + \frac{1}{\sqrt{2}}a_2\right]|10\rangle + \left[\frac{1}{2}a_0 + \frac{1}{2}a_1 + \frac{1}{\sqrt{2}}a_2\right]|11\rangle, \end{aligned} \quad (4.42)$$

with

$$|a_0|^2 + |a_1|^2 + |a_2|^2 + |a_3|^2 = 1. \quad (4.43)$$

In order to calculate the linear entanglement $\mathcal{E} = 2(1 - \text{Tr}(\rho_1^2))$ of this state one has to express $\rho = |\psi(t_0)\rangle\langle\psi(t_0)|$ in terms of the basis $\{|00\rangle, |01\rangle, |10\rangle, |11\rangle\}$. This

4.3 Interacting bi-partite systems

enables one to take the partial trace over the second qubit, thereby obtaining $\rho_1 = \text{Tr}_2 \rho$.

At time τ the state will have evolved to

$$|\psi(t_0 + \tau)\rangle = a_0|u_0\rangle + a_1e^{-4i\omega_0\tau}|u_1\rangle + a_2e^{-2i(\omega_0+\omega)\tau}|u_2\rangle + a_3e^{-2i(\omega_0+\omega)\tau}|u_3\rangle. \quad (4.44)$$

To obtain all possible states evolving to an orthogonal state we find the coefficients satisfying

$$\langle\psi(t_0)|\psi(t_0 + \tau)\rangle = |a_0|^2 + e^{-4i\omega_0\tau}|a_1|^2 + e^{-2i(\omega_0+\omega)\tau} [|a_2|^2 + |a_3|^2] = 0. \quad (4.45)$$

This is a transcendental equation which cannot be solved analytically, so we shall concentrate on the three cases

1. $\omega = \omega_0$
2. $\omega_0 = 0$
3. $\omega = 3\omega_0$.

4.3.1 $\omega = \omega_0$

In this case the eigenenergies become $\{0, 4\hbar\omega_0, 4\hbar\omega_0, 4\hbar\omega_0\}$ and from eq. (4.45) we obtain

$$\begin{aligned} |a_0|^2 &= |a_1|^2 + |a_2|^2 + |a_3|^2, \\ \tau &= \frac{\pi}{4\omega_0} \end{aligned} \quad (4.46)$$

which, together with the normalization condition, gives

$$\begin{aligned} a_0 &= |a_0| = \frac{1}{\sqrt{2}} \\ a_1 &= e^{i\gamma_1} \sqrt{\frac{\delta_1}{2}} \end{aligned}$$

4.3 Interacting bi-partite systems

$$\begin{aligned} a_2 &= e^{i\gamma_2} \sqrt{\frac{\delta_2(1-\delta_1)}{2}} \\ a_3 &= e^{i\gamma_3} \sqrt{\frac{(1-\delta_1)(1-\delta_2)}{2}}. \end{aligned} \quad (4.47)$$

As before, $0 \leq \delta_1, \delta_2 \leq 1$ and $0 \leq \gamma_1, \gamma_2, \gamma_3 < 2\pi$. The mean energy E and the dispersion ΔE are then both equal to $2\hbar\omega_0$, thus giving rise to

$$\tau_{min} = \frac{\pi}{4\omega_0} = \tau. \quad (4.48)$$

Hence all the states evolving to an orthogonal state evolve at the speed limit. Setting $\gamma_1, \gamma_2, \gamma_3 = 0$, the expression for the linear entanglement becomes

$$\mathcal{E}(\delta_1, \delta_2) = \frac{1}{4} (1 + 2\sqrt{\delta_1} - 2\delta_2 + \delta_1(-1 + 2\delta_2))^2. \quad (4.49)$$

A plot of this equation shows that \mathcal{E} can adopt any value between zero and one. Thus any degree of initial entanglement will allow the initial state to evolve at maximum speed to an orthogonal state.

4.3.2 $\omega_0 = 0$

This case is similar to the former case, with the eigenenergies now being $\{0, 0, 2\hbar\omega, 2\hbar\omega\}$ and

$$\begin{aligned} |a_0|^2 + |a_1|^2 &= |a_2|^2 + |a_3|^2, \\ \tau &= \frac{\pi}{2\omega}. \end{aligned} \quad (4.50)$$

This gives

$$\begin{aligned} a_0 &= |a_0| = \sqrt{\frac{\delta_1}{2}} \\ a_1 &= e^{i\gamma_1} \sqrt{\frac{1-\delta_1}{2}} \\ a_2 &= e^{i\gamma_2} \sqrt{\frac{\delta_2}{2}} \\ a_3 &= e^{i\gamma_3} \sqrt{\frac{1-\delta_2}{2}}. \end{aligned} \quad (4.51)$$

4.3 Interacting bi-partite systems

Once again

$$\frac{\tau}{\tau_{min}} = 1, \quad (4.52)$$

since $E = \Delta E = \hbar\omega$ gives $\tau_{min} = \frac{\pi}{2\omega}$. The entanglement for $\gamma_1, \gamma_2, \gamma_3 = 0$ is

$$\mathcal{E}(\delta_1, \delta_2) = \frac{1}{4} (1 - 4(-1 + \delta_1)\delta_1 + 4(-1 + \delta_2)\delta_2 - 4\sqrt{(1 - \delta_1)\delta_1}(-1 + 2\delta_2)). \quad (4.53)$$

Thus the entanglement is continuous between zero and one.

4.3.3 $\omega = 3\omega_0$

The eigenenergies are $\{0, 4\hbar\omega_0, 8\hbar\omega_0, 8\hbar\omega_0\}$ and thus eq. (4.45) becomes

$$\begin{aligned} P(x) &= |a_0|^2 + |a_1|^2 x + [|a_2|^2 + |a_3|^2] x^2 = 0, \\ x &= e^{-4i\omega_0\tau}. \end{aligned} \quad (4.54)$$

Now, either we have two complex conjugate roots (β -case) or we have two real roots (s -case) of which one root must be -1 in order for the state to evolve to an orthogonal state.

4.3.3.1 β -case

Assume that $e^{i\beta}, e^{-i\beta}$ are the complex roots, so that

$$P(x) = [|a_2|^2 + |a_3|^2] \left\{ x^2 + \frac{|a_1|^2}{|a_2|^2 + |a_3|^2} x + \frac{|a_0|^2}{|a_2|^2 + |a_3|^2} \right\} \quad (4.55)$$

$$= [|a_2|^2 + |a_3|^2] \{x - e^{i\beta}\} \{x - e^{-i\beta}\} \quad (4.56)$$

$$= [|a_2|^2 + |a_3|^2] \{x^2 - 2 \cos \beta x + 1\}. \quad (4.57)$$

Comparing eqs. (4.55) and (4.57) yields

$$\frac{|a_1|^2}{|a_2|^2 + |a_3|^2} = -2 \cos \beta, \quad \frac{|a_0|^2}{|a_2|^2 + |a_3|^2} = 1. \quad (4.58)$$

4.3 Interacting bi-partite systems

This, together with the normalization condition, gives

$$\begin{aligned}
 |a_0|^2 &= \frac{1}{2(1 - \cos \beta)} \\
 |a_1|^2 &= \frac{-\cos \beta}{1 - \cos \beta} \\
 |a_2|^2 &= \frac{\delta}{2(1 - \cos \beta)} \\
 |a_3|^2 &= \frac{1 - \delta}{2(1 - \cos \beta)}.
 \end{aligned} \tag{4.59}$$

Since the squares of the absolute values of the coefficients have to be positive, β is restricted to the interval $[\frac{\pi}{2}, \pi]$ and $\delta \in [0, 1]$. Introducing the phases $0 \leq \phi_1, \phi_2, \phi_3 < 2\pi$, we have

$$\begin{aligned}
 a_0 &= \frac{1}{\sqrt{2(1 - \cos \beta)}} \\
 a_1 &= e^{i\phi_1} \sqrt{\frac{-\cos \beta}{1 - \cos \beta}} \\
 a_2 &= e^{i\phi_2} \sqrt{\frac{\delta}{2(1 - \cos \beta)}} \\
 a_3 &= e^{i\phi_3} \sqrt{\frac{1 - \delta}{2(1 - \cos \beta)}}.
 \end{aligned} \tag{4.60}$$

The expression for the linear entanglement in terms of the above parameters is

$$\begin{aligned}
 \mathcal{E}(\beta, \delta, \phi_1, \phi_2, \phi_3) &= \frac{1}{4(-1 + \cos \beta)^2} \{1 - 8 \cos \beta - 4\sqrt{2}\sqrt{-\cos \beta} [\delta \cos(\phi_1 - 2\phi_2) \\
 &\quad + (-1 + \delta) \cos(\phi_1 - 2\phi_3)] + 4(-1 + \delta) \delta \cos^2(\phi_2 - \phi_3)\}.
 \end{aligned} \tag{4.61}$$

The time needed to reach an orthogonal state is

$$\tau(\beta) = \frac{\beta}{4\omega_0}, \tag{4.62}$$

the mean energy is $E = 4\hbar\omega_0$ and the dispersion is $\Delta E = \frac{4\hbar\omega_0}{\sqrt{1 - \cos \beta}}$. Since we are dealing with two qubits, the dispersion of the energy is always less than the mean energy and thus we have for the minimum possible time

4.3 Interacting bi-partite systems

$$\tau_{min}(\beta) = \frac{\pi\sqrt{1 - \cos\beta}}{8\omega_0}. \quad (4.63)$$

The quantities we are interested in are

$$\frac{\tau}{\tau_{min}}(\beta) = \frac{2\beta}{\pi\sqrt{1 - \cos\beta}} \quad (4.64)$$

and the entanglement for $\phi_1, \phi_2, \phi_3 = 0$. We set the phases equal to zero since we want to determine the boundary curves in the $\{\mathcal{E}, \tau/\tau_{min}\}$ -plane. The expression for the linear entanglement then becomes

$$\mathcal{E}(\beta, \delta) = \frac{(1 - 2\delta)(1 - 2\delta + 4\sqrt{2}\sqrt{-\cos\beta}) + 8\cos\beta}{4(-1 + \cos\beta)^2}. \quad (4.65)$$

The boundary curves, starting at the top and moving counterclockwise, are given by

$$\begin{aligned} & \left\{ \frac{1}{16}(9 - 4\sqrt{2}) \leq \mathcal{E}(\beta = \pi, \delta) \leq \frac{1}{16}(9 + 4\sqrt{2}), \tau/\tau_{min}(\beta = \pi) = \sqrt{2} \right\}, \quad \delta \in [0, 1] \\ & \left\{ \mathcal{E}(\beta, \delta = 1), \tau/\tau_{min}(\beta) \right\}, \quad \beta \in [1.696, \pi] \\ & \left\{ \mathcal{E}(\beta, \delta, \phi_1, \phi_2, \phi_3) = 0, 1 \leq \tau/\tau_{min}(\beta) \leq 1.018 \right\}, \quad \beta \in \left[\frac{\pi}{2}, 1.696 \right] \\ & \left\{ 0 \leq \mathcal{E}(\beta = \frac{\pi}{2}, \delta) \leq \frac{1}{4}, \tau/\tau_{min}(\beta = \frac{\pi}{2}) = 1 \right\}, \quad \delta \in [0, 1] \\ & \left\{ \mathcal{E}(\beta, \delta = 0), \tau/\tau_{min}(\beta) \right\}, \quad \beta \in \left[\frac{\pi}{2}, \pi \right]. \end{aligned} \quad (4.66)$$

Figure 4.2 shows a random plot of the $\{\mathcal{E}(\beta, \delta, \phi_1, \phi_2, \phi_3), \tau/\tau_{min}(\beta)\}$ -plane. Only the states within the bounded region evolve to an orthogonal state.

The states having $\beta = \frac{\pi}{2}$ evolve at the speed limit and their possible entanglement values range from 0 to $\frac{1}{4}$.

Once again of interest are the energetically symmetric states:

$$\begin{aligned} a_0 &= \frac{1}{\sqrt{2(1 - \cos\beta)}} \\ a_1 &= a_2 = e^{i\phi_1} \sqrt{\frac{-\cos\beta}{1 - \cos\beta}} \end{aligned}$$

4.3 Interacting bi-partite systems

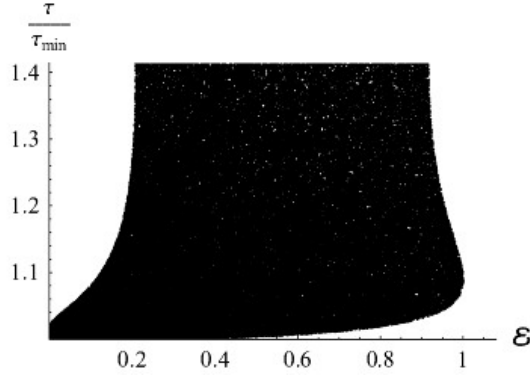


Figure 4.2: \mathcal{E} vs τ/τ_{min} for the β -case.

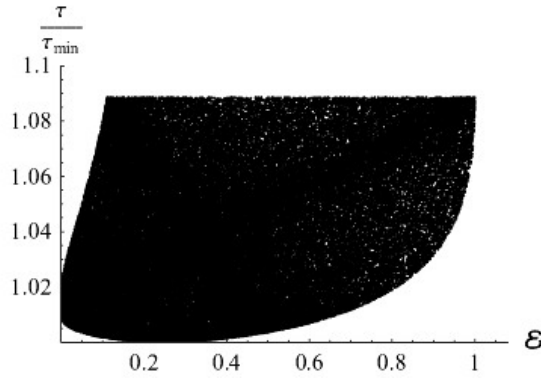


Figure 4.3: \mathcal{E} vs τ/τ_{min} for the symmetric β -case ($\phi_1 = \phi_2$, $\delta = -2 \cos \beta$ and $\frac{\pi}{2} \leq \beta \leq \frac{2\pi}{3}$).

$$a_3 = e^{i\phi_3} \sqrt{\frac{1 + 2 \cos \beta}{2(1 - \cos \beta)}}, \quad (4.67)$$

with $\beta \in [\frac{\pi}{2}, \frac{2\pi}{3}]$. Figure 4.3 shows the region in the $\{\mathcal{E}, \tau/\tau_{min}\}$ -plane which the symmetric states occupy. The states saturating the speed bound have entanglement $\frac{1}{4}$. As in the non-interacting two-qubit case these states are especially interesting because they define a family of energetically symmetric states with low entanglement (ESSLE) that saturate the speed bound.

4.3.3.2 s -case

One of the real roots has to be -1 and let the other one be s . Then we have

4.3 Interacting bi-partite systems

$$P(x) = [|a_2|^2 + |a_3|^2] \left\{ x^2 + \frac{|a_1|^2}{|a_2|^2 + |a_3|^2} x + \frac{|a_0|^2}{|a_2|^2 + |a_3|^2} \right\} \quad (4.68)$$

$$= [|a_2|^2 + |a_3|^2] \{ x^2 + (1-s)x - s \}. \quad (4.69)$$

Comparing eqs. (4.68) and (4.69) gives

$$\frac{|a_1|^2}{|a_2|^2 + |a_3|^2} = 1 - s, \quad \frac{|a_0|^2}{|a_2|^2 + |a_3|^2} = -s. \quad (4.70)$$

This, together with the normalization condition, gives

$$\begin{aligned} |a_0|^2 &= \frac{-s}{2(1-s)} \\ |a_1|^2 &= \frac{1-s}{2(1-s)} = \frac{1}{2} \\ |a_2|^2 &= \frac{\lambda}{2(1-s)} \\ |a_3|^2 &= \frac{1-\lambda}{2(1-s)}, \end{aligned} \quad (4.71)$$

with $\lambda \in [0, 1]$. From the positivity condition we see that $s \leq 0$. Again introducing three phases $\mu_1, \mu_2, \mu_3 \in [0, 2\pi)$ we have

$$\begin{aligned} a_0 &= \sqrt{\frac{-s}{2(1-s)}} \\ a_1 &= e^{i\mu_1} \frac{1}{\sqrt{2}} \\ a_2 &= e^{i\mu_2} \sqrt{\frac{\lambda}{2(1-s)}} \\ a_3 &= e^{i\mu_3} \sqrt{\frac{1-\lambda}{2(1-s)}}. \end{aligned} \quad (4.72)$$

The linear entanglement is hence

$$\begin{aligned} \mathcal{E}(s, \lambda, \mu_1, \mu_2, \mu_3) &= \frac{1}{4(1-s)^{5/2}} \{ 4(-1+s) \sqrt{-s} [\lambda \cos(\mu_1 - 2\mu_2) \\ &\quad + (-1+\lambda) \cos(\mu_1 - 2\mu_3)] + \sqrt{1-s} [1 + 4(-1+s)s] \} \end{aligned}$$

4.3 Interacting bi-partite systems

$$+ 2(-1 + \lambda) \lambda + 2(-1 + \lambda) \lambda \cos(2(\mu_2 - \mu_3))] \}. \quad (4.73)$$

Since the one root is -1, the time needed to reach an orthogonal state is constant, implying that all the states that do evolve to an orthogonal state take the same amount of time, namely

$$\tau = \frac{\pi}{4\omega_0}. \quad (4.74)$$

What differs among the states are the energy resources:

$$E = \frac{2\omega_0 \hbar (3 - s)}{1 - s}, \quad \Delta E = \frac{2\omega_0 \hbar \sqrt{1 - 6s + s^2}}{1 - s}. \quad (4.75)$$

This results in

$$\frac{\tau}{\tau_{min}}(s) = \frac{\sqrt{1 - 6s + s^2}}{1 - s}. \quad (4.76)$$

For the same reason as in the β -case, we set the phases equal to zero. The linear entanglement then becomes

$$\mathcal{E}(s, \lambda) = \frac{4(-1 + s)\sqrt{-s}(-1 + 2\lambda) + \sqrt{1 - s}(1 + 4(-1 + s)s + 4(-1 + \lambda)\lambda)}{4(1 - s)^{5/2}}. \quad (4.77)$$

What we are interested in is the region in the $\{\mathcal{E}(s, \lambda, \mu_1, \mu_2, \mu_3), \tau/\tau_{min}(s)\}$ -plane where states evolve to orthogonal states. The boundary curves of this region are given in the same order as before:

$$\begin{aligned} & \left\{ \frac{1}{16}(9 - 4\sqrt{2}) \leq \mathcal{E}(s = -1, \lambda) \leq \frac{1}{16}(9 + 4\sqrt{2}), \tau/\tau_{min}(s = -1) = \sqrt{2} \right\}, \quad \lambda \in [0, 1] \\ & \left\{ \mathcal{E}(s, \lambda = 1), \tau/\tau_{min}(s) \right\}, \quad s \in [-1, -0.207] \\ & \left\{ \mathcal{E}(s, \lambda, \mu_1, \mu_2, \mu_3) = 0, 1 \leq \tau/\tau_{min}(s) \leq 1.252 \right\}, \quad s \in [-0.207, 0] \\ & \left\{ 0 \leq \mathcal{E}(s = 0, \lambda) \leq \frac{1}{4}, \tau/\tau_{min}(s = 0) = 1 \right\}, \quad \lambda \in [0, 1] \\ & \left\{ \mathcal{E}(s, \lambda = 0), \tau/\tau_{min}(s) \right\}, \quad s \in [-0.203777, 0] \\ & \left\{ \mathcal{E}(s, \lambda = 1), \tau/\tau_{min}(s) \right\}, \quad s \leq -4.907334 \\ & \left\{ \mathcal{E}(s, \lambda = 0), \tau/\tau_{min}(s) \right\}, \quad s \leq -1. \end{aligned} \quad (4.78)$$

4.3 Interacting bi-partite systems

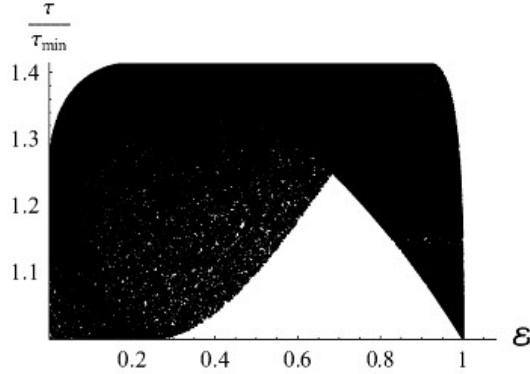


Figure 4.4: \mathcal{E} vs τ/τ_{min} for the s -case.

Figure 4.4 is a random plot of the $\{\mathcal{E}(s, \lambda, \mu_1, \mu_2, \mu_3), \tau/\tau_{min}(s)\}$ -plane. To find the states evolving at the speed limit, we set $\tau/\tau_{min}(s) = 1$. This means either $s = 0$ or $s \rightarrow -\infty$. The former instance yields $0 \leq \mathcal{E} \leq \frac{1}{4}$, whereas the latter gives $\mathcal{E} = 1$. The symmetric states correspond to $\lambda = 1$ and thus have $\mathcal{E} = \frac{1}{4}$.

Figure 4.5 is a combined plot of the s - and β -cases, thus showing all the allowed states for the case $\omega = 3\omega_0$. The point of intersection which is the tip of the blank triangular region is $\{\mathcal{E}(s = -41.9633, \lambda = 1) = \mathcal{E}(\beta = 1.85986, \delta = 0), \tau/\tau_{min}(s = -41.9633) = \tau/\tau_{min}(\beta = 1.85986)\}$. The allowed region looks similar to the one for two non-interacting qubits (Figure 4.1): in both cases the states evolving to an orthogonal state at the highest possible speed have either maximum entanglement ($\mathcal{E} = 1$) or (relatively) low entanglement ($0 \leq \mathcal{E} \leq 1/4$). Consequently, there is an entanglement gap, given by

$$\frac{1}{4} < \mathcal{E} < 1, \quad (4.79)$$

corresponding to entanglement values that are not physically permitted for states evolving at the quantum speed limit [50]. The difference between Figures 4.1 and 4.5 is, that in the latter figure there are states outside the triangular region that are also not allowed: there are no states evolving at the slowest possible speed with either very low entanglement or entanglement close to one.

4.4 Entanglement and the speed of quantum evolution of three-partite systems

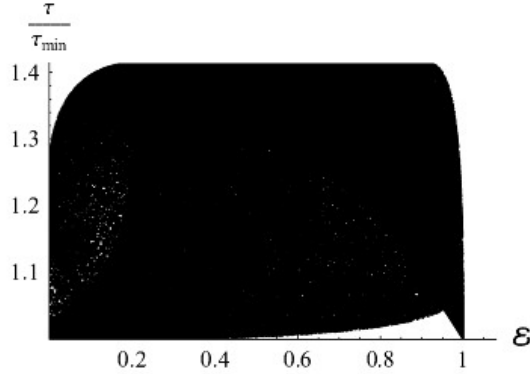


Figure 4.5: \mathcal{E} vs τ/τ_{min} for the interacting two-qubit case with $\omega = 3\omega_0$.

4.4 Entanglement and the speed of quantum evolution of three-partite systems

In this section I extend from a bi-partite to a three-partite system in order to see if for three qubits there is a similar correlation for states of intermediate entanglement. This section also illustrates that the equations get complicated very quickly in going just from two to three qubits.

We are going to consider a composite system consisting of three identical (but distinguishable) subsystems each one having two possible states, $\{|0\rangle, |1\rangle\}$, with eigenenergies $E_0 = 0$, $E_1 = \epsilon$ respectively. Our composite system can be described in terms of the basis $\{|000\rangle, |001\rangle, \dots, |111\rangle\}$, which can be rewritten as $\{|0\rangle, |1\rangle, \dots, |7\rangle\}$.

The general state of our three qubit system is

$$|\psi(t_0)\rangle = \sum_{j=0}^7 c_j |j\rangle \quad (4.80)$$

where the c_j 's are complex coefficients satisfying the normalization requirement,

$$\sum_{j=0}^7 |c_j|^2 = 1. \quad (4.81)$$

4.4 Entanglement and the speed of quantum evolution of three-partite systems

A quantitative measure of the amount of entanglement of a three-partite pure state $|\psi\rangle$ is given by the sum of the linear entanglement (1.37) of the three unique bi-partitions:

$$\mathcal{E}(|\psi\rangle) = \text{Tr}(\rho_1^2) + \text{Tr}(\rho_2^2) + \text{Tr}(\rho_3^2), \quad (4.82)$$

where

$$\begin{aligned} \rho_1 &= \text{Tr}_{23}(|\psi\rangle\langle\psi|), \\ \rho_2 &= \text{Tr}_{13}(|\psi\rangle\langle\psi|), \\ \rho_3 &= \text{Tr}_{12}(|\psi\rangle\langle\psi|). \end{aligned} \quad (4.83)$$

According to the measure $\mathcal{E}(|\psi\rangle)$, factorizable pure states have zero entanglement, that is, $\mathcal{E}(|\phi_1\rangle|\phi_2\rangle|\phi_3\rangle) = 0$. The GHZ state

$$|\psi_{GHZ}\rangle = \frac{1}{\sqrt{2}}(|000\rangle + |111\rangle) \quad (4.84)$$

has $\mathcal{E}(|\psi_{GHZ}\rangle) = 3/2$, which corresponds to maximum entanglement.

A fundamental property of the measure of entanglement (4.82) is that it does not change under the action of local unitary transformations. That is, it does not change under the action of transformations of the form

$$U = U_1 \otimes U_2 \otimes U_3, \quad (4.85)$$

where $U_{1,2,3}$ represent unitary transformations acting on each particle individually.

In the problem we are considering, we have three non-interacting quantum particles, thus the Hamiltonian of our system is of the form

$$H = H_1 \otimes I_2 \otimes I_3 + I_1 \otimes H_2 \otimes I_3 + I_1 \otimes I_2 \otimes H_3, \quad (4.86)$$

where I_k stands for the identity operator acting on the Hilbert space associated with the k -particle ($k = 1, 2, 3$). It is clear that the time evolution operator of this system is local, that is, it has the form

$$U_k = \exp\left[-\frac{itH_k}{\hbar}\right] \quad (k = 1, 2, 3). \quad (4.87)$$

4.4 Entanglement and the speed of quantum evolution of three-partite systems

Consequently, the amount of entanglement of our three particles is not going to change in time. Notice that the amount of entanglement exhibited by a given state of our three particle system is an intrinsic property of that state. It does not depend on the form of the Hamiltonian. However, the Hamiltonian governs the evolution of the state and, consequently, also determines eventual changes in the amount of entanglement. In the case of the Hamiltonian (4.86) that we are going to consider, the amount of entanglement at any time is going to be the same as the amount of entanglement $\mathcal{E}(|\psi(t_0)\rangle)$ associated with the initial state $|\psi(t_0)\rangle$. Obviously, the initial entanglement $\mathcal{E}(|\psi(t_0)\rangle)$ is, in turn, determined by the particular way in which the initial state was prepared.

The time τ needed for this state to evolve into an orthogonal one is given by eq. (1.48)

$$\begin{aligned} \langle \psi(t_0) | \psi(t_0 + \tau) \rangle &= \sum_{j=0}^7 |c_j| \exp \left[-\frac{i\tau E_j}{\hbar} \right] & (4.88) \\ &= |c_0|^2 + \{|c_1|^2 + |c_2|^2 + |c_4|^2\} e^{-i\epsilon\tau/\hbar} \\ &\quad + \{|c_3|^2 + |c_5|^2 + |c_6|^2\} e^{-i2\epsilon\tau/\hbar} + |c_7|^2 e^{-i3\epsilon\tau/\hbar}. & (4.89) \end{aligned}$$

This equation for τ can be recast as

$$\begin{aligned} P(x) &= |c_0|^2 + \{|c_1|^2 + |c_2|^2 + |c_4|^2\}x \\ &\quad + \{|c_3|^2 + |c_5|^2 + |c_6|^2\}x^2 + |c_7|^2x^3 = 0, & (4.90) \end{aligned}$$

with

$$x = e^{-i\epsilon\tau/\hbar}. \quad (4.91)$$

Since the coefficients of $P(x)$ are real, the initial state (4.80) evolves to an orthogonal state if and only if the cubic equation (4.90) admits two complex conjugate roots with modulus equal to one and one real root or three real roots of which one must have modulus equal to one. That is, in the first case

$$e^{\pm i\alpha}, \quad \text{with } \alpha = \epsilon\tau/\hbar \in [0, \pi] \quad \text{and } r \in \mathfrak{R}. \quad (4.92)$$

4.4 Entanglement and the speed of quantum evolution of three-partite systems

In the second case, one of the three real numbers has to be ± 1 . Now, $+1$ implies that $\alpha = 0$ and thus $\tau = 0$ which is impossible, since a state can't be orthogonal to itself. This means that only -1 is possible, so $\alpha = \pi$ and thus $\tau = \pi\hbar/\epsilon$ is the only solution. This is the maximum possible time, but because we are interested in τ/τ_{min} which changes since τ_{min} can differ from state to state due to the varying dispersion of the energy, we also have to consider this case.

4.4.1 $\{\alpha, r\}$ -case

If (4.92) is the case, we can rewrite the polynomial $P(x)$ under the guise

$$P(x) = |c_7|^2 (x - e^{i\alpha}) (x - e^{-i\alpha}) (x - r). \quad (4.93)$$

$P(x)$ can be expanded as follows

$$P(x) = |c_7|^2 \{x^3 + (-2 \cos \alpha - r)x^2 + (1 + 2r \cos \alpha)x - r\}. \quad (4.94)$$

Using the normalization condition (4.81), one obtains an expression for $|c_7|^2$,

$$|c_7|^2 = \frac{1}{2(1 - \cos \alpha)(1 - r)}. \quad (4.95)$$

The coefficients of $P(x)$ have to be positive, resulting in the following three restrictions on α and r

- $-2 \cos \alpha - r \geq 0$,
- $1 + 2r \cos \alpha \geq 0$,
- $-r \geq 0$.

These lead to the following conditions on α and r

1. For $-1 \leq r \leq 0 \Rightarrow \arccos(\frac{-r}{2}) \leq \alpha \leq \pi$
2. For $r \leq -1 \Rightarrow \arccos(\frac{-1}{2r}) \leq \alpha \leq \pi$.

4.4 Entanglement and the speed of quantum evolution of three-partite systems

Comparing now the expressions (4.90) and (4.94) for $P(x)$, one obtains

$$\begin{aligned} |c_1|^2 + |c_2|^2 + |c_4|^2 &= \frac{1 + 2r \cos \alpha}{2(1 - \cos \alpha)(1 - r)} = A, \\ |c_3|^2 + |c_5|^2 + |c_6|^2 &= \frac{-2 \cos \alpha - r}{2(1 - \cos \alpha)(1 - r)} = B. \end{aligned} \quad (4.96)$$

In order to get expressions for $|c_1|^2, |c_2|^2, \dots, |c_6|^2$, one has to introduce four parameters,

$$0 \leq \delta_1, \delta_2, \delta_3, \delta_4 \leq 1 \quad (4.97)$$

such that

$$\begin{aligned} |c_1|^2 &= \delta_1 A, \\ |c_2|^2 &= \delta_2(1 - \delta_1)A, \\ |c_4|^2 &= (1 - \delta_2)(1 - \delta_1)A, \\ |c_3|^2 &= \delta_3 B, \\ |c_5|^2 &= \delta_4(1 - \delta_3)B, \\ |c_6|^2 &= (1 - \delta_4)(1 - \delta_3)B. \end{aligned} \quad (4.98)$$

Since a global phase factor doesn't affect the physical properties of a state, one can choose the global phase factor such that c_0 is real. Introducing seven phase parameters

$$0 \leq \beta_1, \beta_2, \dots, \beta_7 < 2\pi \quad (4.99)$$

the expressions for c_0, c_1, \dots, c_7 are as follows

$$\begin{aligned} c_0 &= \sqrt{\frac{-r}{2(1 - \cos \alpha)(1 - r)}}, \\ c_1 &= e^{i\beta_1} \sqrt{\delta_1 \frac{1 + 2r \cos \alpha}{2(1 - \cos \alpha)(1 - r)}}, \\ c_2 &= e^{i\beta_2} \sqrt{\delta_2(1 - \delta_1) \frac{1 + 2r \cos \alpha}{2(1 - \cos \alpha)(1 - r)}}, \end{aligned}$$

4.4 Entanglement and the speed of quantum evolution of three-partite systems

$$\begin{aligned}
c_3 &= e^{i\beta_3} \sqrt{\delta_3 \frac{-2 \cos \alpha - r}{2(1 - \cos \alpha)(1 - r)}}, \\
c_4 &= e^{i\beta_4} \sqrt{(1 - \delta_2)(1 - \delta_1) \frac{1 + 2r \cos \alpha}{2(1 - \cos \alpha)(1 - r)}}, \\
c_5 &= e^{i\beta_5} \sqrt{\delta_4(1 - \delta_3) \frac{-2 \cos \alpha - r}{2(1 - \cos \alpha)(1 - r)}}, \\
c_6 &= e^{i\beta_6} \sqrt{(1 - \delta_4)(1 - \delta_3) \frac{-2 \cos \alpha - r}{2(1 - \cos \alpha)(1 - r)}}, \\
c_7 &= e^{i\beta_7} \frac{1}{\sqrt{2(1 - \cos \alpha)(1 - r)}}.
\end{aligned} \tag{4.100}$$

Consequently, the entanglement $\mathcal{E}(|\psi(t_0)\rangle)$ is a function of α and r and also of the eleven independent parameters, whereas the quotient between the actual time τ of evolution to an orthogonal state (which is related to α through equation (4.92)) and the lower bound τ_{min} , is only a function of α and r ,

$$\frac{\tau}{\tau_{min}} = \min \left(\frac{2\alpha E}{\epsilon \pi}, \frac{2\alpha \Delta E}{\epsilon \pi} \right), \tag{4.101}$$

where ΔE is given by

$$\Delta E = \epsilon \sqrt{(A + 4B + 9|c_7|^2) - (A + 2B + 3|c_7|^2)^2}. \tag{4.102}$$

Clearly, neither τ/τ_{min} nor \mathcal{E} depend on ϵ .

Now, in order to determine whether ΔE is less than or equal to E in the allowed domain for α and r (conditions 1 and 2), we considered the difference

$$D(\alpha, r) = E - \Delta E. \tag{4.103}$$

Since both E and ΔE are positive, $E \geq \Delta E \iff E^2 \geq (\Delta E)^2$. Thus we can work with

$$D^*(\alpha, r) = E^2 - (\Delta E)^2 \tag{4.104}$$

instead of $D(\alpha, r)$. The first partial derivative of $D^*(\alpha, r)$ with respect to α is strictly greater than zero for all $\alpha \in [\pi/3, \pi)$ and zero for $\alpha = \pi$. The second

4.4 Entanglement and the speed of quantum evolution of three-partite systems

partial derivative with respect to α is strictly negative for all $\alpha \in [\pi/3, \pi]$. Hence $D^*(\alpha, r)$ is a concave function of α for any fixed $r \leq 0$, having its absolute maximum at $\alpha = \pi$ and its absolute minimum at the lower bound for α . Now, if this minimum is greater than or equal to zero for any $r \leq 0$, then $D^*(\alpha, r) \geq 0$ for all α and r in the domain. Substituting the expressions for the lower bound of α into $D^*(\alpha, r)$, one sees that $D^*_{min}(r) \geq 0$ for $r \leq 0$, equality being reached only for $r = -1$. The conclusion is that $D(\alpha, r) \geq 0$ and hence $E \geq \Delta E$ for all α and r in the domain, which means

$$\frac{\tau}{\tau_{min}}(\alpha, r) = \frac{2\alpha \Delta E}{\epsilon \pi} = \frac{\alpha}{\pi} \sqrt{-\frac{4r}{(-1+r)^2} + 2 \csc^2\left(\frac{\alpha}{2}\right)}. \quad (4.105)$$

Now, τ/τ_{min} is a monotonically increasing function of α , for any fixed $r \leq 0$. The same holds for the extreme case $r \rightarrow -\infty$. Thus, the maximum of τ/τ_{min} (for any r) is at the upper boundary, namely when $\alpha = \pi$. Likewise, the minimum occurs at the smallest allowed value for α , depending on the particular r chosen (conditions 1 and 2).

Keeping α fixed at any value in the domain and varying r , one finds that τ/τ_{min} (for any allowed α) has its maximum at $r = -1$, so for that value of r the function has its greatest range, $\tau/\tau_{min}(\alpha = \pi/3, r = -1) = 1$ and $\tau/\tau_{min}(\alpha = \pi, r = -1) = \sqrt{3}$.

Investigating the behaviour of τ/τ_{min} for $\alpha = \pi$, one sees that $(\tau/\tau_{min})_{max}$ decreases monotonically from $\sqrt{3}$ to $\sqrt{2}$ as r goes from -1 to 0 or to $-\infty$.

The behaviour at the lower bound for α is more complicated, since the bound itself decreases monotonically from $\pi/3$ to $\pi/2$ as r goes from -1 to 0 or to $-\infty$ (conditions 1 and 2). For $r \leq -1$, $(\tau/\tau_{min})_{min}$ increases from 1 at $r = -1$ to 1.05235 when $r = -0.332247$ or the inverse thereof and then starts to decrease slowly to 1 again as r goes to 0 or $-\infty$.

To show that the relation between entanglement and the ‘‘speed’’ of time evolution also holds for three qubits, we performed a numerical survey of the system’s Hilbert space. That is, using random choices of the eleven parameters and fixed values of r , we plotted $\tau/\tau_{min}(\alpha)$ versus $\mathcal{E}(\alpha)$. From Figures 4.6 and 4.7, which illustrate the cases $r = -1$ and $r = 0$ respectively, one can clearly see

4.4 Entanglement and the speed of quantum evolution of three-partite systems

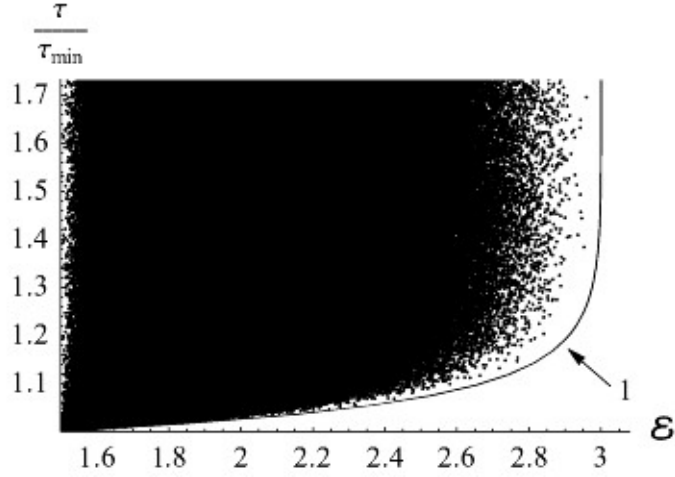


Figure 4.6: $\{\alpha, r\}$ -case for $r = -1$: numerical survey of $\{\mathcal{E}, \tau/\tau_{min}\}$ using random values for the δ_i 's, β_i 's and α .

a correlation between entanglement and the time of evolution to an orthogonal state.

To obtain an analytic expression for the global boundary curve of this relation, one has to find the set of parameters that maximize the entanglement measure for all values of α and r in the domain. In order to achieve that we first have to try and find the maximum boundary for any fixed r and all the allowed α -values.

Setting $\beta_1 = \beta_2 = \dots = \beta_7 = 0$, hence making all the coefficients real, maximizes the entanglement measure.

Both τ/τ_{min} and \mathcal{E} then have the property that for any $a < 0$

$$\begin{aligned}
 \frac{\tau}{\tau_{min}}(\alpha, r = a) &= \frac{\tau}{\tau_{min}}(\alpha, r = \frac{1}{a}), \\
 \mathcal{E}(\alpha, r = a, \delta_1, \delta_2, \delta_3, \delta_4) &= \mathcal{E}(\alpha, r = \frac{1}{a}, \delta_3, \delta_4, \delta_1, \delta_2). \quad (4.106)
 \end{aligned}$$

Since we can always interchange $\delta_1 \leftrightarrow \delta_3$ and $\delta_2 \leftrightarrow \delta_4$, it means the two cases $-1 \leq r \leq 0$ and $r \leq -1$ are equivalent and so we only need to consider the case $-1 \leq r \leq 0$.

4.4 Entanglement and the speed of quantum evolution of three-partite systems

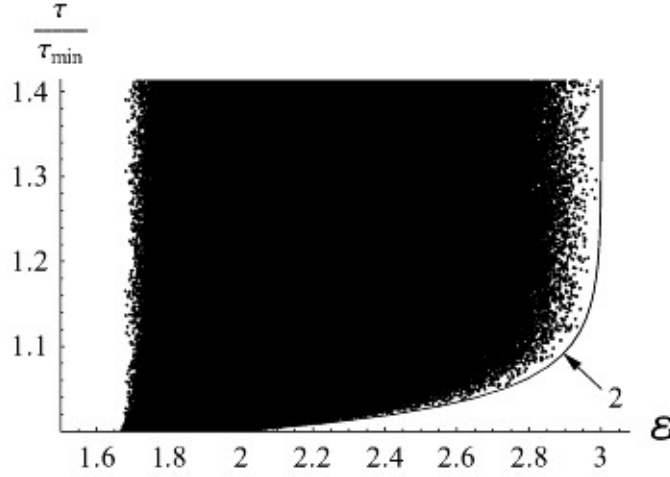


Figure 4.7: $\{\alpha, r\}$ -case for $r = 0$: numerical survey of $\{\mathcal{E}, \tau/\tau_{min}\}$ using random values for the δ_i 's, β_i 's and α .

The greatest range for τ/τ_{min} occurs at $r = -1$, so we shall first focus on that value for r . The following δ_i 's maximize the entanglement measure:

$$\delta_1 = \delta_3 = \frac{1}{3}, \delta_2 = \delta_4 = \frac{1}{2}. \quad (4.107)$$

This choice of parameters implies that $c_1 = c_2 = c_4$ and $c_3 = c_5 = c_6$.

To prove that this set of values does indeed maximize the entanglement measure, one first has to show that they correspond to a critical point, that is, the partial derivatives of \mathcal{E} with respect to all four parameters must be zero at the critical point. Since that is the case for all α and r in the domain, it means that the critical point is either a local/global maximum, local minimum or saddle point. It can't be global minimum since we know there are other sets of values yielding smaller values for the entanglement. In order to determine the nature of the critical point, one has to construct the Hessian matrix and show whether it is negative/positive definite or semi-definite. For all values of $r \neq -1$, the critical point is either a saddle point or a local maximum/minimum.

For $r = -1$, all four eigenvalues of the matrix are negative for $\pi/3 < \alpha < \pi$ and although some are zero at $\alpha = \pi/3, \pi$ this doesn't influence the negative definiteness of the matrix since for $\alpha = \pi/3$ only one value ($\mathcal{E} = 3/2$) is possible

4.4 Entanglement and the speed of quantum evolution of three-partite systems

for any choice of the δ_i 's, and for $\alpha = \pi$ the entanglement value is 3 and thus definitely maximal. Thus for $r = -1$ the above choice of parameters corresponds to the global maximum of the concave entanglement function (for all α). In that case we have the following expressions for $\tau/\tau_{min}(\alpha)$ and $\mathcal{E}(\alpha)$,

$$\frac{\tau}{\tau_{min}}(\alpha) = \frac{\alpha}{\pi} \sqrt{\frac{-5 + \cos \alpha}{-1 + \cos \alpha}}, \quad (4.108)$$

$$\mathcal{E}(\alpha) = \frac{1}{12(-1 + \cos \alpha)^2} \{39 + 4g + \cos 2\alpha (13 + 2g) - 2 \cos \alpha (28 + 3g)\} \quad (4.109)$$

where

$$g = \frac{2\sqrt{3}}{1 - \cos \alpha} \sqrt{1 - 2 \cos \alpha}. \quad (4.110)$$

Plotting $\tau/\tau_{min}(\alpha)$ versus $\mathcal{E}(\alpha)$ results in curve 1 depicted in Figures 4.6 and 4.8. The extreme cases ($\alpha = \pi/3, \pi$) correspond to maximum entanglement ($\mathcal{E} = 3/2$) and thus fastest evolution and zero entanglement ($\mathcal{E} = 3$) and thus slowest evolution respectively, consistent with previous research. The correlation between entanglement and time evolution is seen to hold also for states of intermediate entanglement.

The minimum range for τ/τ_{min} , namely $[1, \sqrt{2}]$, occurs at $r = 0$ and so we shall consider that case now.

The expression for τ/τ_{min} is then

$$\frac{\tau}{\tau_{min}}(\alpha) = \frac{2\alpha}{\pi \sqrt{1 - \cos \alpha}}. \quad (4.111)$$

The following choice of parameters maximizes the entanglement measure for all $\alpha \in [\pi/2, \pi]$:

$$\delta_1 = \delta_2 = \delta_3 = 0, \delta_4 = \frac{1}{2}. \quad (4.112)$$

This set of parameters is actually equivalent to three other sets

- $\delta_1 = 1, \delta_2 = 1, \delta_3 = \frac{1}{2}, \delta_4 = 1,$

4.4 Entanglement and the speed of quantum evolution of three-partite systems

- $\delta_1 = 0, \delta_2 = 1, \delta_3 = \frac{1}{2}, \delta_4 = 0,$
- $\delta_1 = 1, \delta_2 = 0, \delta_3 = \frac{1}{2}, \delta_4 = 1,$

since they all have exactly the same expressions for the entanglement measure, namely

$$\mathcal{E}(\alpha) = \frac{3 - 8 \cos \alpha + \cos 2\alpha}{(-1 + \cos \alpha)^2}. \quad (4.113)$$

To show that the choice given in (4.112) does maximize the entanglement measure for $r = 0$, one has to take the partial derivatives of \mathcal{E} with respect to the δ_i 's and evaluate them at the point in question. For the δ_4 partial derivative this gives zero for all α in the domain, whereas for the other partial derivatives we either obtain that they are indeterminate or non-zero for all allowed α . Evaluating the δ_1, δ_2 and δ_3 partial derivatives for any selection of δ_i 's, we see that no critical point exists for δ_1, δ_2 and δ_3 and thus the global maximum must occur at the boundary values, since \mathcal{E} is a smooth function of the δ_i 's. Taking the second partial derivative of \mathcal{E} with respect to δ_4 and substituting the values given in (4.112), results in a negative function of α for $\alpha \in (\pi/2, \pi)$. For $\alpha = \pi/2, \pi$ the result is zero, since \mathcal{E} is equal to 2 in the first instance and a very flat function of δ_4 (but still a maximum) in the latter case. Thus, when the first three δ_i 's are equal to zero, then $\delta_4 = 1/2$ does correspond to a global maximum for the δ_4 -direction.

Plotting $\tau/\tau_{min}(\alpha)$ versus $\mathcal{E}(\alpha)$ results in curve 2 depicted in Figures 4.7 and 4.8. The extreme cases ($\alpha = \pi/2, \pi$) correspond to $\mathcal{E} = 2$ and thus fastest evolution and zero entanglement ($\mathcal{E} = 3$) and thus slowest evolution respectively, consistent with previous research. The correlation between entanglement and time evolution is seen to hold also for states of intermediate entanglement.

The state corresponding to the δ_i 's in equation (4.112) is given below

$$|\psi(\alpha)\rangle = y|100\rangle + z|101\rangle + z|110\rangle + y|111\rangle, \quad (4.114)$$

where

4.4 Entanglement and the speed of quantum evolution of three-partite systems

$$\begin{aligned} y &= \frac{1}{2} \csc\left(\frac{\alpha}{2}\right), \\ z &= \frac{1}{2} \csc\left(\frac{\alpha}{2}\right) \sqrt{-\cos \alpha}. \end{aligned} \quad (4.115)$$

Clearly, the state is separable in the first qubit for all α in the domain. This means that, although the first qubit contributes to the mean energy of the state, it does not contribute to the dispersion of the energy and hence not to τ/τ_{min} . Thus the first qubit cannot enhance the speed of time evolution and so this case is essentially a two-qubit case.

The general state for the parameter choice (4.112) is not separable for $-1 \leq r < 0$ and all α in the domain. Only in the limit $r \rightarrow 0$ does the state become separable, which means we can have fully 3-qubit entangled states arbitrarily close to state (4.114).

From a graphical analysis, for $-1 < r \lesssim -0.041$ the maximum boundary is a combination of the $r = -1$ and $r = 0$ boundaries, that is, for a certain range of α the $r = -1$ boundary holds and for the other values of α the $r = 0$ boundary maximizes the entanglement measure. By plotting graphs for $-0.041 \lesssim r \leq 0$, it seems that the choice of parameters given by eq. (4.112) does indeed maximize the entanglement measure for those values of r .

From the graphical approach one can then conclude that for $\tau/\tau_{min}(\alpha, r)$ between 1 and $\sqrt{2}$, the global boundary for the entanglement measure is $\{\mathcal{E}(\alpha, r = 0, \delta_1 = \delta_2 = \delta_3 = 0, \delta_4 = 1/2), \tau/\tau_{min}(\alpha, r = 0)\}$. For $\tau/\tau_{min}(\alpha, r) \in [\sqrt{2}, \sqrt{3}]$, the global boundary is $\mathcal{E} = 3$.

To obtain the family of states that saturate the bound, we set $\tau/\tau_{min} = 1$. The only solutions are $(\alpha = \pi/3, r = -1)$, $(\alpha = \pi/2, r \rightarrow -\infty)$ and $(\alpha = \pi/2, r = 0)$. As mentioned before, the first solution adopts only one value for the entanglement ($\mathcal{E} = 3/2$) irrespective of the choice of parameters. The corresponding state is

4.4 Entanglement and the speed of quantum evolution of three-partite systems

the $|GHZ\rangle$ state:

$$|\psi(\alpha = \frac{\pi}{3}, r = -1)\rangle = |GHZ\rangle = \frac{1}{\sqrt{2}}\{|000\rangle + |111\rangle\}. \quad (4.116)$$

For the latter solution \mathcal{E} is independent of δ_3 and δ_4 . Varying both δ_1 and δ_2 gives a continuous range for \mathcal{E} between $5/3 \approx 1.66667$ and 2 , where $\mathcal{E} = 5/3, 2$ corresponds to δ_1 and δ_2 as in equations (4.107) and (4.112) respectively. The corresponding spectrum of states and their entanglement are

$$|\psi(\delta_1, \delta_2)\rangle = \sqrt{\frac{\delta_1}{2}}|001\rangle + \sqrt{\frac{\delta_2(1-\delta_1)}{2}}|010\rangle + \sqrt{\frac{(-1+\delta_1)(-1+\delta_2)}{2}}|100\rangle + \frac{1}{\sqrt{2}}|111\rangle, \\ \mathcal{E}(\delta_1, \delta_2) = 2 - \delta_2 + \delta_2^2 + \delta_1(-1 + 2\delta_2 - 2\delta_2^2) + \delta_1^2(1 - \delta_2 + \delta_2^2). \quad (4.117)$$

From the expression for $|\psi(\delta_1, \delta_2)\rangle$ one can determine whether these states are fully 3-qubit entangled. For $(\delta_1 = \delta_2 = 0)$, $(\delta_1 = 0, \delta_2 = 1)$ and $(\delta_1 = 1, \delta_2 \in [0, 1])$ the respective states are separable in one qubit and the entanglement in each case is $\mathcal{E} = 2$. Any other combinations of δ_1 and δ_2 lead to states that are not separable in any of the three qubits. Thus all states with $5/3 \leq \mathcal{E} < 2$ are 3-qubit entangled. This means that there exists a spectrum of states that do not have maximum entanglement ($\mathcal{E} = 3/2$) and that nevertheless reach the lower limit for the evolution time. The solution $\alpha = \pi/2, r \rightarrow -\infty$ yields the same results for the entanglement, but the corresponding spectrum of states is a unitary transformation of $|\psi(\delta_1, \delta_2)\rangle$:

$$|\psi(\delta_3, \delta_4)\rangle = \frac{1}{\sqrt{2}}|000\rangle + \sqrt{\frac{\delta_3}{2}}|011\rangle + \sqrt{\frac{\delta_4(1-\delta_3)}{2}}|101\rangle + \sqrt{\frac{(-1+\delta_3)(-1+\delta_4)}{2}}|110\rangle. \quad (4.118)$$

The state

$$|W\rangle = \frac{1}{\sqrt{3}}(|001\rangle + |010\rangle + |100\rangle) \quad (4.119)$$

has the same entanglement as the state in eq. (4.117) for $\delta_1 = 1/3, \delta_2 = 1/2$, namely $\mathcal{E} = 5/3$, but it does not evolve to an orthogonal state.

4.4 Entanglement and the speed of quantum evolution of three-partite systems

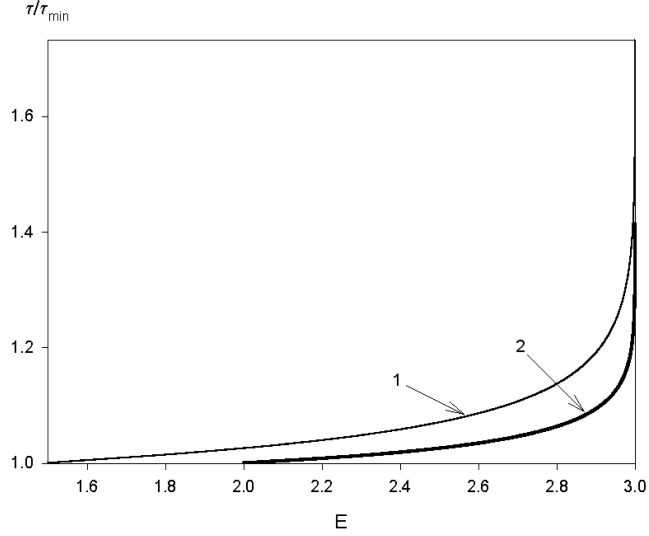


Figure 4.8: Three-qubit case: curves 1 and 2 correspond to $\{\mathcal{E}(\alpha, r = -1, \delta_1 = 1/3, \delta_2 = 1/2, \delta_3 = 1/3, \delta_4 = 1/2), \tau/\tau_{min}(\alpha, r = -1)\}$ and $\{\mathcal{E}(\alpha, r = 0, \delta_1 = \delta_2 = \delta_3 = 0, \delta_4 = 1/2), \tau/\tau_{min}(\alpha, r = 0)\}$ respectively.

4.4.2 $\{r_1, r_2\}$ -case

If we let r_1 and r_2 be the two real roots, the polynomial $P(x)$ can be rewritten under the guise

$$P(x) = |c_7|^2 (x - r_1)(x - r_2)(x + 1). \quad (4.120)$$

$P(x)$ can be expanded as follows

$$P(x) = |c_7|^2 \{x^3 + (-r_2 - r_1 + 1)x^2 + (r_1 r_2 - r_2 - r_1)x + r_1 r_2\}. \quad (4.121)$$

Using the normalization condition (4.81), one obtains an expression for $|c_7|^2$,

$$|c_7|^2 = \frac{1}{2(r_1 - 1)(r_2 - 1)}. \quad (4.122)$$

The coefficients of $P(x)$ have to be positive, resulting in the following three restrictions on r_1 and r_2

4.4 Entanglement and the speed of quantum evolution of three-partite systems

- $-r_2 - r_1 + 1 \geq 0$,
- $r_1 r_2 - r_2 - r_1 \geq 0$,
- $r_1 r_2 \geq 0$.

These lead to the following conditions on r_1 and r_2

$$r_1 \leq 0 \text{ and } r_2 \leq 0. \quad (4.123)$$

Comparing the expressions (4.90) and (4.121) for $P(x)$, one obtains,

$$\begin{aligned} |c_1|^2 + |c_2|^2 + |c_4|^2 &= \frac{r_1 r_2 - r_2 - r_1}{2(r_1 - 1)(r_2 - 1)} = E, \\ |c_3|^2 + |c_5|^2 + |c_6|^2 &= \frac{-r_2 - r_1 + 1}{2(r_1 - 1)(r_2 - 1)} = F. \end{aligned} \quad (4.124)$$

In order to get expressions for $|c_1|^2, |c_2|^2, \dots, |c_6|^2$, one again has to introduce four parameters,

$$0 \leq \lambda_1, \lambda_2, \lambda_3, \lambda_4 \leq 1 \quad (4.125)$$

and seven phase parameters

$$0 \leq \eta_1, \eta_2, \dots, \eta_7 < 2\pi, \quad (4.126)$$

so that the expressions for c_0, c_1, \dots, c_7 are as follows

$$\begin{aligned} c_0 &= \sqrt{\frac{r_1 r_2}{2(r_1 - 1)(r_2 - 1)}}, \\ c_1 &= e^{i\eta_1} \sqrt{\lambda_1 \frac{r_1 r_2 - r_2 - r_1}{2(r_1 - 1)(r_2 - 1)}}, \\ c_2 &= e^{i\eta_2} \sqrt{\lambda_2 (1 - \delta_1) \frac{r_1 r_2 - r_2 - r_1}{2(r_1 - 1)(r_2 - 1)}}, \\ c_3 &= e^{i\eta_3} \sqrt{\lambda_3 \frac{-r_2 - r_1 + 1}{2(r_1 - 1)(r_2 - 1)}}, \\ c_4 &= e^{i\eta_4} \sqrt{(1 - \lambda_2)(1 - \lambda_1) \frac{r_1 r_2 - r_2 - r_1}{2(r_1 - 1)(r_2 - 1)}}, \end{aligned}$$

4.4 Entanglement and the speed of quantum evolution of three-partite systems

$$\begin{aligned}
c_5 &= e^{i\eta_5} \sqrt{\lambda_4(1-\lambda_3) \frac{-r_2-r_1+1}{2(r_1-1)(r_2-1)}}, \\
c_6 &= e^{i\eta_6} \sqrt{(1-\lambda_4)(1-\lambda_3) \frac{-r_2-r_1+1}{2(r_1-1)(r_2-1)}}, \\
c_7 &= e^{i\eta_7} \frac{1}{\sqrt{2(r_1-1)(r_2-1)}}.
\end{aligned} \tag{4.127}$$

The entanglement $\mathcal{E}(|\psi(t_0)\rangle)$ is a function of r_1 and r_2 and also of the eleven independent parameters, whereas τ/τ_{min} is only a function of r_1 and r_2 . The expression for τ/τ_{min} is given by

$$\frac{\tau}{\tau_{min}}(r_1, r_2) = \frac{2\Delta E}{\epsilon} = \sqrt{\frac{1+(-6+r_1)r_1}{(-1+r_1)^2} - \frac{4}{(-1+r_2)^2} - \frac{4}{-1+r_2}}, \tag{4.128}$$

where ΔE is given by equation (4.102) with A and B replaced by E and F respectively.

Equation (4.128) holds since $E \geq \Delta E$ for all r_1 and r_2 . This was established using a similar approach as in the $\{\alpha, r\}$ -case.

Figure 4.9 was generated by choosing random values for the λ_i 's and η_i 's and for $-1000 \leq r_1, r_2 \leq 0$. From the figure one can see that either there are no physically forbidden states and hence there would be no clear correlation between entanglement and the speed of evolution or there is a minimum boundary which would correlate highly entangled states and the speed of evolution.

Since it is not easily established whether a minimum boundary for the entanglement measure exists, we just analyze what happens for the maximum and minimum evolution speed. For that purpose we set $\eta_1 = \eta_2 = \dots = \eta_7 = 0$. Then both τ/τ_{min} and \mathcal{E} have the properties that they are symmetric in r_1 and r_2 and that for any $v, w < 0$

$$\begin{aligned}
\frac{\tau}{\tau_{min}}(r_1 = v, r_2 = w) &= \frac{\tau}{\tau_{min}}(r_1 = \frac{1}{v}, r_2 = \frac{1}{w}), \\
\mathcal{E}(r_1 = v, r_2 = w, \lambda_1, \lambda_2, \lambda_3, \lambda_4) &= \mathcal{E}(r_1 = \frac{1}{v}, r_2 = \frac{1}{w}, \lambda_3, \lambda_4, \lambda_1, \lambda_2).
\end{aligned} \tag{4.129}$$

4.4 Entanglement and the speed of quantum evolution of three-partite systems

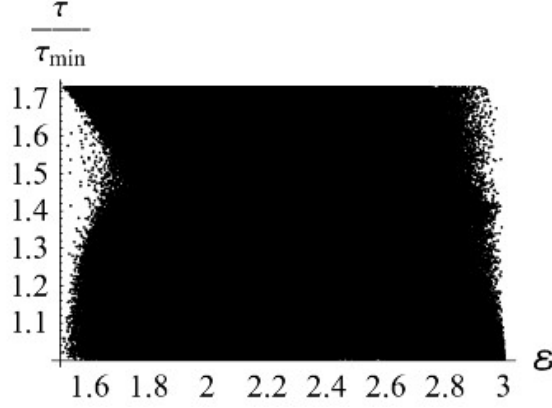


Figure 4.9: $\{r_1, r_2\}$ -case: numerical survey of $\{\mathcal{E}, \tau/\tau_{min}\}$ using random values for the λ_i 's, η_i 's and for $-1000 \leq r_1, r_2 \leq 0$.

Since we can always interchange $\lambda_1 \leftrightarrow \lambda_3$ and $\lambda_2 \leftrightarrow \lambda_4$, it means we only need to consider the two cases $-1 \leq r_1 \leq 0, -1 \leq r_2 \leq 0$ and $r_1 \leq -1, -1 \leq r_2 \leq 0$.

The slowest evolution occurs when $\tau/\tau_{min} = \sqrt{3}$, thus when $r_1 = r_2 = -1$. In that case $3/2 \leq \mathcal{E} \leq 3$.

To obtain the family of states that saturate the bound, we set $\tau/\tau_{min} = 1$. The only solutions are $(r_1 = r_2 = 0)$, $(r_1, r_2 \rightarrow -\infty)$ and $(r_1 \rightarrow -\infty, r_2 = 0)$, $(r_1 = 0, r_2 \rightarrow -\infty)$. The spectrum of states corresponding to the first pair of solutions are unitary transformations of each other:

$$\begin{aligned}
 |\psi\rangle_{r_1,2=0} &= \sqrt{\frac{\lambda_3}{2}}|011\rangle + \sqrt{\frac{\lambda_4(1-\lambda_3)}{2}}|101\rangle + \sqrt{\frac{(-1+\lambda_3)(-1+\lambda_4)}{2}}|110\rangle + \frac{1}{\sqrt{2}}|111\rangle, \\
 |\psi\rangle_{r_1,2 \rightarrow -\infty} &= \frac{1}{\sqrt{2}}|000\rangle + \sqrt{\frac{\lambda_1}{2}}|001\rangle + \sqrt{\frac{\lambda_2(1-\lambda_1)}{2}}|010\rangle \\
 &\quad + \sqrt{\frac{(-1+\lambda_1)(-1+\lambda_2)}{2}}|100\rangle.
 \end{aligned} \tag{4.130}$$

The second pair gives rise to the same spectrum of states:

$$\begin{aligned}
 &|\psi(r_1 = 0, r_2 \rightarrow -\infty)\rangle = |\psi(r_1 \rightarrow -\infty, r_2 = 0)\rangle \\
 &= \sqrt{\frac{\lambda_1}{2}}|001\rangle + \sqrt{\frac{\lambda_2(1-\lambda_1)}{2}}|010\rangle + \sqrt{\frac{\lambda_3}{2}}|011\rangle + \sqrt{\frac{(-1+\lambda_1)(-1+\lambda_2)}{2}}|100\rangle
 \end{aligned}$$

4.5 N -qubits ESSLE states saturating the quantum speed limit

$$+\sqrt{\frac{\lambda_4(1-\lambda_3)}{2}}|101\rangle+\sqrt{\frac{(-1+\lambda_3)(-1+\lambda_4)}{2}}|110\rangle. \quad (4.131)$$

Assuming the latter solution and choosing $\lambda_1 = 1$, $\lambda_2 = \lambda_3 = 0$ and varying λ_4 from zero to one gives a continuous range for \mathcal{E} from $3/2$ to 3 . The corresponding state is

$$|\psi(\lambda_4)\rangle = \frac{1}{\sqrt{2}}|001\rangle + \sqrt{\frac{\lambda_4}{2}}|101\rangle + \sqrt{\frac{1-\lambda_4}{2}}|110\rangle. \quad (4.132)$$

In order to determine if these states are fully 3-qubit entangled, one has to see whether the three marginal density matrices ρ_1, ρ_2 and ρ_3 are all mixed, which means that they are not equal to their squares. For $\lambda_4 = 1$ all three marginal density matrices are pure which means the state is completely separable. Any other $\lambda_4 \in [0, 1)$ corresponds to a state that is not separable in any of the three qubits. Thus all states with $3/2 \leq \mathcal{E} < 3$ are 3-qubit entangled. This means that there exists a spectrum of states that do not have maximum entanglement and that nevertheless reach the lower limit for the evolution time.

4.5 N -qubits ESSLE states saturating the quantum speed limit

Now we are going to consider a system consisting of N qubits evolving according to the Hamiltonian

$$H = \sum_{i=1}^N H_i, \quad (4.133)$$

where each of the single qubit Hamiltonians H_i have eigenstates $|0\rangle, |1\rangle$ with eigenvalues $0, \epsilon$ respectively.

When considering entangled N -qubit states, we can take as a reference the GHZ state,

$$|GHZ\rangle = \frac{1}{\sqrt{2}}\{|0\dots 0\rangle + |1\dots 1\rangle\}. \quad (4.134)$$

4.5 N -qubits ESSLE states saturating the quantum speed limit

This is an entangled, energetically symmetric state that evolves into an orthogonal state and saturates the quantum speed bound. The time needed for the GHZ state to reach an orthogonal state is

$$\tau_{GHZ} = \frac{\pi\hbar}{N\epsilon}. \quad (4.135)$$

Although there is no rigorous criteria for defining a maximally entangled multipartite state, there are various reasons for describing the N -partite $|GHZ\rangle$ states as maximally entangled. For instance, the N -qubit $|GHZ\rangle$ states exhibit the maximum violations of multiparty inequalities imposed by local realistic theories [85]. To have an idea of how much entanglement the GHZ state contains, notice that the marginal density matrix ρ_1 associated with any of the N qubits corresponds to the totally mixed qubit state $\frac{1}{2}I_2$, which has the maximum possible von Neumann entropy, namely $\log_2 2 = 1$ (and also the maximum possible value of the $\mathcal{E} = 2(1 - \text{Tr}(\rho_1^2))$ measure, namely $\mathcal{E} = 1$). This means that, when considering the N -qubit system as partitioned into a single-qubit subsystem and an $(N - 1)$ -qubit subsystem, the GHZ state exhibits maximum entanglement.

Let us now consider the (energetically symmetric) N -qubit state [50]

$$|ESSLE\rangle = \frac{1}{\sqrt{2}}|00\dots 0\rangle + \frac{1}{\sqrt{2N}}\left\{|100\dots 0\rangle + |010\dots 0\rangle + \dots + |00\dots 01\rangle\right\}. \quad (4.136)$$

This state corresponds, for $N = 2$, to the s -case (see equations (4.23)) with $s \rightarrow -\infty$ and $\lambda = 1/2$ (which, as far as the values of \mathcal{E} and τ/τ_{min} are concerned, is equivalent to the state (4.29) with $s = 0$ and $\lambda = 1/2$). The state (4.136) takes a time

$$\tau = \frac{\pi\hbar}{\epsilon} \quad (4.137)$$

to evolve into the orthogonal state

$$|ESSLE\rangle^\perp = \frac{1}{\sqrt{2}}|00\dots 0\rangle - \frac{1}{\sqrt{2N}}\left\{|100\dots 0\rangle + |010\dots 0\rangle + \dots + |00\dots 01\rangle\right\}. \quad (4.138)$$

4.5 N -qubits ESSLE states saturating the quantum speed limit

The state $|ESSLE\rangle^\perp$, in turn, takes a time τ to evolve back to the state $|ESSLE\rangle$. The energy's expectation value and the energy's dispersion of the state $|ESSLE\rangle$ are given by

$$E = \Delta E = \frac{\epsilon}{2} \quad (4.139)$$

and from equation (1.53), it follows that this state saturates the speed limit,

$$\tau = \tau_{min}. \quad (4.140)$$

In order to compare the amount of entanglement exhibited by $|ESSLE\rangle$ with that associated with $|GHZ\rangle$ we need an appropriate measure of N -qubit entanglement. The study of the properties and applications of multi-partite entanglement measures has been the focus of intense research activity in recent years [14; 49; 50; 51; 86; 87; 88; 89; 90; 91; 92; 93; 94]. The GE measure (1.37) discussed in Section 1.0.2.5 is widely regarded as a legitimate, useful and practical N -qubit entanglement measure [88; 89; 90; 91; 92]. This measure is invariant under local unitary transformations and non-increasing on average under local quantum operations and classical communication. In other words, Q is an entanglement monotone. Another desirable property of this measure is that it can be observed without the need for full quantum state tomography [88]. This measure has been applied to the study of several problems involving multi-partite entanglement, such as entanglement generation by nearly random operators [89] and by operators exhibiting particular matrix element distributions [90], thermal entanglement in multi-qubit Heisenberg models [91], and multipartite entanglement in one-dimensional time-dependent Ising models [92]. The measures Q_m (generalized GE measures, also discussed in Section 1.0.2.5) have been applied to the study of quantum error correcting codes and to the analysis of the (multi-partite) entangling power of quantum evolutions [86].

Another way of characterizing the global amount of entanglement exhibited by an N -qubit state is provided by the sum of the (bi-partite) entanglement measures associated with all the possible bi-partitions of the N -qubits system

4.5 N -qubits ESSLE states saturating the quantum speed limit

[49]. That is, in order to compare the amount of entanglement exhibited by the N -qubit state

$$|ESSLE\rangle = \frac{1}{\sqrt{2}}|00\dots 0\rangle + \frac{1}{\sqrt{2N}}\{|100\dots 0\rangle + |010\dots 0\rangle + \dots + |000\dots 01\rangle\} \quad (4.141)$$

with that associated with $|GHZ\rangle$, we sum all the bi-partite entanglement measures obtained from the $(M$ -qubits): $((N - M)$ -qubits) bi-partitions with $M = 1, 2, \dots, [N/2]$. The ESSLE state is energetically symmetric, from which it follows that the $M : (N - M)$ bi-partitions are equivalent.

The marginal density matrix describing a subsystem consisting of the first M qubits is given by

$$\rho_M = \text{Tr}_{M+1, M+2, \dots, N} \{|ESSLE\rangle\langle ESSLE|\}. \quad (4.142)$$

Changing the order of the Hilbert space basis to $\{|00\dots 0\rangle, |100\dots 0\rangle, |010\dots 0\rangle, \dots, |00\dots 01\rangle, |110\dots 0\rangle, \dots, |11\dots 1\rangle\}$, the M -qubits marginal density matrix is of the form

$$\rho_M = \begin{pmatrix} \mathbf{B} & \mathbf{O} \\ \mathbf{O} & \mathbf{O} \end{pmatrix}, \quad (4.143)$$

where \mathbf{B} is an $(M + 1) \times (M + 1)$ matrix which can be cast as

$$\mathbf{B} = \begin{pmatrix} \frac{1}{2} + \frac{N-M}{2N} & \frac{1}{2\sqrt{N}} & \frac{1}{2\sqrt{N}} & \cdots & \frac{1}{2\sqrt{N}} \\ \frac{1}{2\sqrt{N}} & \frac{1}{2N} & \frac{1}{2N} & \cdots & \frac{1}{2N} \\ \frac{1}{2\sqrt{N}} & \frac{1}{2N} & \frac{1}{2N} & \cdots & \frac{1}{2N} \\ \vdots & \vdots & \vdots & \ddots & \vdots \\ \frac{1}{2\sqrt{N}} & \frac{1}{2N} & \frac{1}{2N} & \cdots & \frac{1}{2N} \end{pmatrix}. \quad (4.144)$$

The rest of the $2^M \times 2^M$ matrix consists of zeros, thus $\text{Tr}(\rho_M^2) = \text{Tr}(\mathbf{B}^2)$. Hence

$$\mathcal{E}_M = 2(1 - \text{Tr}(\rho_M^2)) = \frac{M(N - M)}{N^2}, \quad (4.145)$$

which is well defined for all $0 \leq M \leq N$, since it has the property that $\mathcal{E}_M = \mathcal{E}_{N-M}$ (this property is needed since the $M : (N - M)$ and $(N - M) : M$ bi-partitions have to give rise to the same linear entanglement).

4.5 N -qubits ESSLE states saturating the quantum speed limit

To obtain the average total entanglement, we need to multiply \mathcal{E}_M by the number of possible $M : (N - M)$ bi-partitions, then sum from $M = 1$ to $N/2$ (even N) or $(N - 1)/2$ (odd N) and divide the resultant sum by the total number of unique bi-partitions:

$$N \text{ even} : \mathcal{E}_{av}(|ESSLE\rangle) = \frac{\sum_{M=1}^{N/2} \binom{N}{M} \frac{M(N-M)}{N^2} - \frac{1}{2} \binom{N}{N/2} \mathcal{E}_{M=N/2}}{2^{N-1} - 1} \quad (4.146)$$

$$N \text{ odd} : \mathcal{E}_{av}(|ESSLE\rangle) = \frac{\sum_{M=1}^{(N-1)/2} \binom{N}{M} \frac{M(N-M)}{N^2}}{2^{N-1} - 1}, \quad (4.147)$$

where in the even case we need to subtract the part which gets counted twice in the sum due to the binomial coefficient for $M = N/2$. The total number of possible bi-partitions is $2^{N-1} - 1$. Using the abovementioned property $\mathcal{E}_M = \mathcal{E}_{N-M}$, both the sums become

$$\mathcal{E}_{av}(|ESSLE\rangle) = \frac{1}{2} \frac{\frac{1}{N} \sum_{M=0}^N \binom{N}{M} M - \frac{1}{N^2} \sum_{M=0}^N \binom{N}{M} M^2}{2^{N-1} - 1}. \quad (4.148)$$

Now,

$$\sum_{M=0}^N \binom{N}{M} M = N 2^{N-1} \quad (4.149)$$

$$\sum_{M=0}^N \binom{N}{M} M^2 = (N^2 + N) 2^{N-2}. \quad (4.150)$$

Consequently,

$$\mathcal{E}_{av}(|ESSLE\rangle) = \frac{2^{N-3} \left(1 - \frac{1}{N}\right)}{2^{N-1} - 1}, \quad N \geq 2. \quad (4.151)$$

The entanglement initially decreases (for $N = 2$ to 5) and then slowly increases from $N = 6$ onwards. For large N , $\mathcal{E}_{av}(|ESSLE\rangle) \rightarrow 1/4$, whereas for any $N \geq 2$, $\mathcal{E}_{av}(|GHZ\rangle) = 1$ (for the GHZ state all possible bi-partitions are equivalent). This implies that the ESSLE state is always less entangled than the GHZ state.

4.5 N -qubits ESSLE states saturating the quantum speed limit

For the particular families of (symmetric) states that we are considering here, the main conclusions obtained from the (1-qubit):($(N - 1)$ -qubits) bi-partitions are the same as those obtained when taking into account all the possible bi-partitions.

We are now going to use the N -qubit measures of entanglement Q (1.37) and Q_m (1.38) to compare the amount of entanglement exhibited by the $|ESSLE\rangle$ and the $|GHZ\rangle$ states. Because of the symmetry of these states, the average of all the single-qubit linear entropies is equal to the linear entropy of the marginal density matrix associated with just one qubit,

$$\rho_1 = \text{Tr}_{2\dots N} \left\{ |ESSLE\rangle\langle ESSLE| \right\}, \quad (4.152)$$

which is given by

$$\rho_1 = \left(\frac{1}{2} + \frac{N-1}{2N} \right) |0\rangle\langle 0| + \frac{1}{2\sqrt{N}} \left\{ |0\rangle\langle 1| + |1\rangle\langle 0| \right\} + \frac{1}{2N} |1\rangle\langle 1|. \quad (4.153)$$

The eigenvalues of ρ_1 are

$$\lambda = \frac{1}{2} \left\{ 1 \pm \sqrt{1 - \frac{N-1}{N^2}} \right\}, \quad (4.154)$$

which, in the limit of a large number of qubits, yields

$$\lim_{N \rightarrow \infty} \lambda = 0, 1. \quad (4.155)$$

The GE entanglement measure of the ESSLE state is given by the single-qubit linear entropy,

$$Q(|ESSLE\rangle) = 2 \left[1 - \text{Tr}(\rho_1^2) \right] = \frac{N-1}{N^2}. \quad (4.156)$$

It is important to emphasize that this single-qubit marginal entropy actually represents a global property of the complete N -qubit system: *the entropy $1 - \text{Tr}(\rho_1^2)$ measures the amount of entanglement between each of the N qubits and the remaining $(N - 1)$ qubits.* We see that $Q(|ESSLE\rangle)$ is a decreasing function of N and tends to 0 when $N \rightarrow \infty$. Consequently, the amount of entanglement between each qubit of the system and the remaining $(N - 1)$ qubits tends to zero as

4.5 N -qubits ESSLE states saturating the quantum speed limit

N increases. Therefore, as N increases, the amount of entanglement exhibited by $|ESSLE\rangle$, as measured by the N -qubit GE measure, becomes much smaller than the amount of entanglement associated with $|GHZ\rangle$ ($Q(|GHZ\rangle) = 1$). However, the state $|ESSLE\rangle$ does saturate the quantum speed limit. We thus see that, as the number of qubits of the system increases, only a small amount of entanglement (as compared with the entanglement exhibited by the $|GHZ\rangle$ state) is needed to obtain an energetically symmetric state that saturates the quantum speed limit.

It is also useful to evaluate upon the $|ESSLE\rangle$ and $|GHZ\rangle$ states the more general N -qubit entanglement measure Q_m (given by equation (1.38)),

$$\begin{aligned} Q_m(|ESSLE\rangle) &= \frac{2^m}{2^m - 1} \left[\frac{m(N - m)}{2N^2} \right], \\ Q_m(|GHZ\rangle) &= \frac{2^m}{2^m - 1} \cdot \frac{1}{2}. \end{aligned} \quad (4.157)$$

We see that, for any given finite m , the measure $Q_m(|ESSLE\rangle)$ goes to zero as $N \rightarrow \infty$. For even values of N , we can also consider the case $m = N/2$ (that is, considering the average entanglement associated with all partitions of the system into two subsystems with $N/2$ qubits each). In that case we obtain, for $N \rightarrow \infty$,

$$Q_{N/2}(|ESSLE\rangle) \rightarrow \frac{1}{8}, \quad (4.158)$$

which is again much smaller than the value $\frac{1}{2}$ associated with the $|GHZ\rangle$ state.

An energetically symmetric state such as

$$|\psi\rangle = \frac{1}{\sqrt{2N}} \{ |100 \dots 0\rangle + |010 \dots 0\rangle + \dots + |000 \dots 01\rangle \} + \frac{1}{\sqrt{2}} |11 \dots 1\rangle \quad (4.159)$$

does not evolve into an orthogonal state at the speed limit, except when $N = 2, 3$. For even N , the orthogonal state is

$$|\psi\rangle^\perp = -\frac{1}{\sqrt{2N}} \{ |100 \dots 0\rangle + |010 \dots 0\rangle + \dots + |000 \dots 01\rangle \} + \frac{1}{\sqrt{2}} |11 \dots 1\rangle, \quad (4.160)$$

4.5 N -qubits ESSLE states saturating the quantum speed limit

which gives $\tau = \frac{\pi\hbar}{\epsilon}$. For $N = 3 + 4n$, $n = 0, 1, 2, \dots$ the orthogonal state is

$$|\psi\rangle^\perp = -\frac{i}{\sqrt{2N}} \{|100\dots 0\rangle + |010\dots 0\rangle + \dots + |000\dots 01\rangle\} + \frac{i}{\sqrt{2}} |11\dots 1\rangle, \quad (4.161)$$

yielding $\tau = \frac{\pi\hbar}{2\epsilon}$. For all other odd values of N the state does not evolve into an orthogonal state at all. The mean energy and dispersion of the energy of the state $|\psi\rangle$ are $\frac{\epsilon}{2}(N+1)$ and $\frac{\epsilon}{2}(N-1)$ respectively, thus

$$\tau_{min} = \frac{\pi\hbar}{\epsilon(N-1)}. \quad (4.162)$$

This yields

$$\begin{aligned} \frac{\tau}{\tau_{min}} &= N-1 & N \text{ even} \\ \frac{\tau}{\tau_{min}} &= \frac{N-1}{2} & N = 3 + 4n, \quad n = 0, 1, 2, \dots, \end{aligned} \quad (4.163)$$

which clearly shows that the speed limit is reached only when $N = 2, 3$.

Consider now the states

$$|N; M\rangle = \frac{1}{\sqrt{2}} |00\dots 0\rangle + \sqrt{\frac{M!(N-M)!}{2N!}} \left\{ |1\dots 10\dots 0\rangle + \dots + |0\dots 01\dots 1\rangle \right\}, \quad (4.164)$$

where

$$1 \leq M \leq N. \quad (4.165)$$

The sum within curly brackets in (4.164) consists of all the $\binom{N}{M}$ factorizable N -qubit states with M qubits in state $|1\rangle$ and $(N-M)$ qubits in state $|0\rangle$. The case $M = 1$ corresponds to the previously defined $|ESSLE\rangle$ state, while in the case $M = N$ the $|GHZ\rangle$ state is recovered. All the states $|N; M\rangle$ are energetically symmetric, and all of them evolve to an orthogonal state in the shortest possible time (that is, all of them saturate the speed bound). The mean energy and

4.5 N -qubits ESSLE states saturating the quantum speed limit

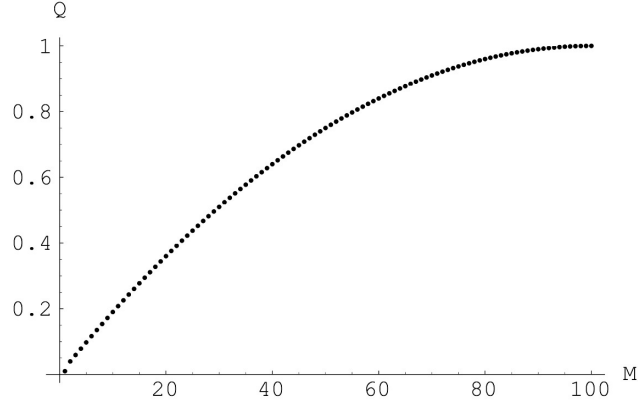


Figure 4.10: Entanglement versus M for $N = 100$.

dispersion of the energy are both equal to $\frac{M\epsilon}{2}$. The time required by $|N; M\rangle$ to reach an orthogonal state is

$$\tau(N; M) = \frac{\pi\hbar}{M\epsilon}. \quad (4.166)$$

To obtain the Q -entanglement for $|N; M\rangle$ we only need ρ_1 , since the symmetry of the states causes the average of all the single-qubit linear entropies to be equal to the linear entropy of the marginal density matrix associated with just one qubit. For $M = 2, 3, \dots, N - 1$

$$\rho_1 = \frac{1}{2} \left[1 + \frac{N - M}{N} \right] |0\rangle\langle 0| + \frac{M}{2N} |1\rangle\langle 1| \quad (4.167)$$

and thus

$$Q(|N; M\rangle) = \frac{2M}{N} - \frac{M^2}{N^2}, \quad M = 2, 3, \dots, N - 1. \quad (4.168)$$

For a given value of N , the amount of entanglement associated with $|N; M\rangle$ increases with M , adopting its maximum value for the $|GHZ\rangle$ state. Figure 4.10 shows the specific case $N = 100$.

We thus see that for the family of states $|N; M\rangle$ there is a correlation between the absolute time required to reach an orthogonal state and the amount of entanglement. Within this family of states, the states with higher entanglement reach an orthogonal state sooner.

4.6 Role of entanglement in time-optimal quantum evolution

4.6 Role of entanglement in time-optimal quantum evolution

Another approach to the investigation of the role of entanglement in quantum evolution is as follows: I explore the time-average of the entanglement of a designated state evolving to another quantum state (under a given set of constraints) in the shortest possible time τ . That is, I would like to quantify the amount of entanglement needed in order to implement the evolution of an initial state $|\psi_I\rangle$ to a final state $|\psi_F\rangle$ in the shortest possible time, under the constraint that the difference between the maximum and minimum eigenenergy of the Hamiltonian generating the unitary transformation $|\psi_I\rangle \rightarrow |\psi_F\rangle = e^{\frac{iH\tau}{\hbar}} |\psi_I\rangle$ is a constant. This constraint is imposed due to the following reason: if the differences between the eigenenergies of the Hamiltonian are large, then the value of τ can be made very small, since the magnitude of the velocity of the system in the projective Hilbert space is proportional to the energy uncertainty (the so-called Anandan-Aharonov relation [95]) [96]. That is, the “speed” of the unitary evolution increases proportionally when the differences between eigenvalues are made large, since that implies that the energy uncertainty can also be made large.

In the case of the quantum states $|\psi_I\rangle$ and $|\psi_F\rangle$ being orthogonal, we can compare the actual time τ with the minimum possible time τ_{min} given by eq. (1.53).

The expression for the time-average of the entanglement during the time evolution from $|\psi_I\rangle \rightarrow |\psi_F\rangle$, that is, during the timespan τ , is

$$\langle \mathcal{E} \rangle = \frac{1}{\tau} \int_0^\tau \mathcal{E}(t) dt. \quad (4.169)$$

Now, irrespective of the specific entanglement measure used, one has to obtain an expression for

$$\rho(t) = |\psi(t)\rangle\langle\psi(t)|, \quad (4.170)$$

where [96]

4.6 Role of entanglement in time-optimal quantum evolution

$$\begin{aligned}
 |\psi(t)\rangle &= \left[\cos\left(\frac{\omega t}{\hbar} \sin \frac{1}{2}\theta\right) - \frac{\cos \frac{1}{2}\theta}{\sin \frac{1}{2}\theta} \sin\left(\frac{\omega t}{\hbar} \sin \frac{1}{2}\theta\right) \right] |\psi_I\rangle \\
 &+ \frac{1}{\sin \frac{1}{2}\theta} \sin\left(\frac{\omega t}{\hbar} \sin \frac{1}{2}\theta\right) |\psi_F\rangle.
 \end{aligned} \tag{4.171}$$

This expression satisfies $|\psi(0)\rangle = |\psi_I\rangle$ and $|\psi(\tau)\rangle = |\psi_F\rangle$, where [96]

$$\tau = \frac{\hbar\theta}{2\omega \sin \frac{1}{2}\theta}. \tag{4.172}$$

The parameter ω is determined by the constraint that the difference between the largest and the smallest eigenvalue is 2ω , that is,

$$\Delta H = \omega \sin \frac{1}{2}\theta. \tag{4.173}$$

To obtain the parameter θ , the final state $|\psi_F\rangle$ has to be written in the form [96]

$$|\psi_F\rangle = \cos \frac{1}{2}\theta |\psi_I\rangle + e^{i(\phi+\pi/2)} \sin \frac{1}{2}\theta |\bar{\psi}_I\rangle, \tag{4.174}$$

where $|\bar{\psi}_I\rangle$ is the state orthogonal to the initial state $|\psi_I\rangle$ and which is contained in the two-dimensional span of the initial and final states in the full Hilbert space. Since both $|\psi_I\rangle$ and $|\psi_F\rangle$ are specified, the values of ϕ and θ are known, the latter being the angle of separation of the two states.

It is important to emphasize that the Hamiltonian H describes the evolution of states within the subspace spanned by $|\psi_I\rangle$ and $|\psi_F\rangle$, and that it can be extended to the full Hilbert space. Thus the full Hamiltonian can hold for either interacting or independent subsystems, depending on the specific initial and final states.

To facilitate the computations we use the linear entropy as entanglement measure. However, even when considering only two qubits and restricting $|\psi_I\rangle$ and $|\psi_F\rangle$ to be symmetric and orthogonal, the expression for $\langle \mathcal{E} \rangle$ becomes very long, thus making an analytic approach difficult. Future work would be to find the absolute minimum (lower bound \mathcal{E}_{min}) of the time-averaged entanglement ($\langle \mathcal{E} \rangle$) of all such possible states,

$$\langle \mathcal{E} \rangle \geq \mathcal{E}_{min} \quad \forall \text{ symmetric, orthogonal states} \tag{4.175}$$

4.6 Role of entanglement in time-optimal quantum evolution

in other words, the minimum amount of entanglement necessary to enable the transformation from $|\psi_I\rangle$ to $|\psi_F\rangle$ in the shortest possible time. Presently, we are going to consider two specific cases:

1. $|00\rangle \rightarrow \frac{\cos \alpha}{\sqrt{2}}\{|01\rangle + |10\rangle\} + \sin \alpha|11\rangle$
2. $\frac{1}{\sqrt{2}}\{|01\rangle + |10\rangle\} \rightarrow \frac{1}{\sqrt{2}}\{|00\rangle + |11\rangle\}$.

Since in both cases the initial and final states are orthogonal it means that $\theta = \pi$. Thus

$$\begin{aligned} \tau &= \frac{\pi \hbar}{2\omega} \\ |\psi(t)\rangle &= \cos\left(\frac{\omega t}{\hbar}\right) |\psi_I\rangle + \sin\left(\frac{\omega t}{\hbar}\right) |\psi_F\rangle. \end{aligned} \quad (4.176)$$

1. Evolution of a separable state into either another separable state ($\alpha = \frac{\pi}{2}$), an intermediately entangled state ($\alpha \in (0, \frac{\pi}{2})$) or a maximally entangled state ($\alpha = 0$): let $\xi = \frac{\omega t}{\hbar}$, then

$$\begin{aligned} |\psi(\xi, \alpha)\rangle &= \cos \xi |00\rangle + \frac{\sin \xi \cos \alpha}{\sqrt{2}} [|01\rangle + |10\rangle] + \sin \xi \sin \alpha |11\rangle \quad (4.177) \\ \mathcal{E}(\xi, \alpha) &= 2[1 - \cos^4 \xi - 2 \cos^2 \xi \sin^2 \xi \cos^2 \alpha \\ &\quad - \sin^4 \xi \left(\frac{\cos^4 \alpha}{2} + 2 \cos^2 \alpha \sin^2 \alpha + \sin^4 \alpha \right) - 2 \cos \xi \sin^3 \xi \cos^2 \alpha \sin \alpha] \\ \langle \mathcal{E}(\alpha) \rangle &= \frac{5}{4} - \frac{1}{2} \cos^2 \alpha - \frac{3}{4} \left(\frac{\cos^4 \alpha}{2} + 2 \cos^2 \alpha \sin^2 \alpha + \sin^4 \alpha \right) - \frac{2}{\pi} \cos^2 \alpha \sin \alpha. \end{aligned}$$

Figure 4.11 is a plot of the function $\langle \mathcal{E}(\alpha) \rangle$. For $|00\rangle \rightarrow |11\rangle$ ($\alpha = \frac{\pi}{2}$) we have that $\langle \mathcal{E} \rangle = \frac{1}{2}$, which is the maximum time-average entanglement in this case. For $|00\rangle \rightarrow \frac{1}{\sqrt{2}}[|01\rangle + |10\rangle]$ ($\alpha = 0$) we have that $\langle \mathcal{E} \rangle = \frac{3}{8}$. Of particular interest is the minimum of the time-average entanglement, which happens when $|00\rangle \rightarrow \frac{1}{\sqrt{3}}[|01\rangle + |10\rangle + |11\rangle]$ ($\alpha = \arcsin\left(\frac{1}{\sqrt{3}}\right)$) and gives $\langle \mathcal{E} \rangle = 0.088298$.

2. Transformation of a maximally entangled state to another maximally entangled state

4.6 Role of entanglement in time-optimal quantum evolution

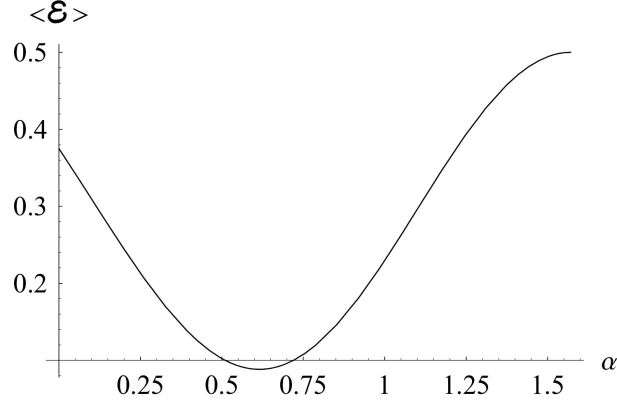


Figure 4.11: Plot of $\langle \mathcal{E}(\alpha) \rangle$ as a function of α , $\alpha \in [0, \frac{\pi}{2}]$.

$$\begin{aligned} \mathcal{E}(t) &= 2 \left[1 - \frac{1}{2} \cos^4 \left(\frac{\omega t}{\hbar} \right) - 3 \cos^2 \left(\frac{\omega t}{\hbar} \right) \sin^2 \left(\frac{\omega t}{\hbar} \right) - \frac{1}{2} \sin^4 \left(\frac{\omega t}{\hbar} \right) \right] \\ \langle \mathcal{E} \rangle &= \frac{1}{2}. \end{aligned} \quad (4.178)$$

From this one can deduce that for the cases considered the same amount of time-averaged entanglement is needed to transform a maximally entangled state into another maximally entangled state as is needed to transform a separable state into another separable state.

In general, for two qubits and symmetric, orthogonal initial and final states, the time-averaged entanglement $\langle \mathcal{E} \rangle$ is independent of ω and since $\tau = \frac{\pi \hbar}{2\omega}$, it means $\langle \mathcal{E} \rangle$ is also independent of the absolute time taken. For two qubits, the minimum possible time is

$$\tau_{min} = \frac{\pi \hbar}{2\Delta E} = \frac{\pi \hbar}{2\omega} = \tau. \quad (4.179)$$

Thus all the symmetric, orthogonal initial and final states evolve at the speed limit from $|\psi_I\rangle \rightarrow |\psi_F\rangle$.

4.7 Conclusions

I have investigated some aspects of the relationship between entanglement and the speed of quantum evolution in multi-qubit systems. As was pointed out by Giovannetti, Lloyd and Maccone, both entanglement, on the one hand, and the uniformity of the distribution of energy resources among the subsystems, on the other hand, play an important role in connection with the speed of quantum evolution of multi-partite systems. Energetically symmetric, separable pure states do not saturate the speed bound. On the contrary, the speed limit can be reached for energetically symmetric, entangled states. However, how much entanglement is needed to reach the aforementioned bound? In the case of two-qubits (independent and interacting), I found that maximally entangled states are not needed for that purpose. There are energetically symmetric states of (relatively) low entanglement that saturate the bound. In the present effort I have provided a systematic study of the connection between speed of evolution and entanglement for two-qubits pure states (summarized in Figures 4.1 and 4.5) paying special attention to the role played by the distribution of the energy resources among the qubits. In particular, I showed that there is triangular-shaped, physically forbidden region in the $(\mathcal{E}, \tau/\tau_{min})$ -plane involving states of low entanglement saturating the speed limit. On the line $\tau_{min} = \tau$, corresponding to the maximum quantum speed, this region gives the entanglement gap $1/4 < \mathcal{E} < 1$, corresponding to entanglement values that cannot be realized by states saturating the quantum speed limit.

The three-qubit analysis illustrated that the equations for the entanglement become complicated very quickly, thus making an analytic approach difficult. The numerical survey showed that there definitely exists a connection between entanglement and the speed of quantum evolution. In particular, I demonstrated by analytic means that there exists a spectrum of states that do not have maximum entanglement and that nevertheless reach the lower limit for the evolution time.

I have also constructed energetically symmetric states of low entanglement (ESSLE) for non-interacting N -qubits that evolve at the speed limit. The ESSLE states become less and less entangled (in comparison with the GHZ state) as N

4.7 Conclusions

increases. Thus, we can conclude that for large N very little entanglement is needed for an energetically symmetric state to reach the quantum speed limit. In the present effort I have only discussed pure states. It would be important to extend some of the present considerations to mixed states of multi-qubit systems. In that case, it would be interesting to systematically explore the correlations existing between entanglement and the time needed to reach a state with a given fidelity distance with respect to the initial state, in connection with the role played here by the evenness of the distribution of energy resources among the subsystems. The case of mixed states, however, is considerably more complicated than the case of pure states [97] and, consequently, it seems that the only way to conduct such a study is by recourse to a systematic numerical survey of the state-space.

The role of entanglement in time-optimal quantum evolution of two qubits and for specific cases of symmetric, orthogonal initial and final states has been analyzed. Depending on the initial and final states, the time-averaged entanglement varies between 0.088298 and 0.5 in the particular instances I considered. Hence entanglement is definitely needed to enable time-optimal evolution. I also showed that all the symmetric, orthogonal initial and final states evolve at the speed limit from $|\psi_I\rangle \rightarrow |\psi_F\rangle$.

Chapter 5

Conclusions

The subject of the present work was to use various information-entropic measures to characterize some entanglement-related features of composite quantum systems, paying special attention to the connections between entanglement and quantum evolution. In particular, I investigated the relationship between entanglement and the “speed” of quantum evolution (as measured by the time needed to reach an orthogonal state) of systems consisting of N -qubits. I also considered the quantum evolution of multi-qubit systems in the presence of CTC’s, in connection with the problem of quantum cloning. An exploration of classical and quantum systems exhibiting an extensive behaviour of the S_q entropies was also conducted.

All these investigations resulted in the following publications and in one conference proceeding:

- (A) C. Zander and A.R. Plastino, “Composite systems with extensive S_q (power-law) entropies”, *Physica A* **364**, (2006) pp. 145-156
- (B) S. Curilef, C. Zander and A.R. Plastino, “Two particles in a double well: illustrating the connection between entanglement and the speed of quantum evolution”, *Eur. J. Phys.* **27**, (2006) pp. 1193-1203
- (C) C. Zander, A.R. Plastino, A. Plastino and M. Casas, “Entanglement and the speed of evolution of multi-partite quantum systems”, *J. Phys. A: Math. Theor.* **40** (11), (2007) pp. 2861-2872

-
- (D) A.R. Plastino and C. Zander, “Would Closed Timelike Curves Help to Do Quantum Cloning?”, *AIP Conference Proceedings: A century of relativity physics*, *ERE* **841**, (2005) pp. 570-573.

In Chapter 2 I considered models of phase space occupancy probabilities leading, for appropriate values of the relevant parameters, to an extensive behaviour of the power-law entropy S_q . Our models allow for an explicit analysis of the thermodynamic limit. Taking as a “reference point” the completely uncorrelated probability distribution we showed that (within our models) it is necessary to incorporate strong correlations among the subsystems in order to reach an additive regime for S_q . In particular, in the limit $N \rightarrow \infty$, the probability distribution that makes S_q additive tends towards a maximally correlated distribution. We also considered a quantum version of one of our models. We showed that for $p = 1/2$ and for large enough values of N , the density matrix associated with an extensive q -entropy describes an entangled state.

In Chapter 3 I used a system of two quantum particles in a double well potential to illustrate the connection between the speed of quantum evolution and quantum entanglement. The time required by separable initial states to reach an orthogonal state does not saturate the speed bound, whereas there exist maximally entangled states that do saturate the bound. I proved that all the symmetric states that saturate the bound require quantum entanglement. This example offers interesting opportunities to illustrate the concept of entanglement in university courses on quantum mechanics. It provides a clear instance of what one might call a “positive” feature of quantum entanglement, as contrasted with the “negative” way in which entanglement is usually defined, that is, entangled states are normally defined in terms of what they are not. Most of the “positive” aspects of entanglement involve its role as a resource to implement novel, non-classical types of computation and communication processes. The role played by entanglement in “speeding up” the evolution of this particular system (two particles in a double well) requires mostly ideas that are already part of the traditional quantum physics “toolkit”.

In Chapter 4 I investigated some aspects of the relationship between entanglement and the speed of quantum evolution in multi-qubit systems: both entanglement and the uniformity of the distribution of energy resources among the subsystems play an important role. Energetically symmetric, separable pure states do not saturate the speed bound. Symmetric states that reach the quantum “speed” limit have to be entangled. However, in the case of two and three qubits I found that maximally entangled states are not needed to saturate the bound. There are energetically symmetric states of (relatively) low entanglement that saturate the bound. In general we paid special attention to the role played by the distribution of the energy resources among the qubits.

I also constructed energetically symmetric states of low entanglement (ESSLE) for N -qubits that evolve at the speed limit. The ESSLE states become less and less entangled (in comparison with the GHZ state) as N increases. Thus, we can conclude that for large N very little entanglement is needed for an energetically symmetric state to reach the quantum speed limit.

The role of entanglement in time-optimal quantum evolution of two qubits and specific cases of symmetric, orthogonal initial and final states has been analyzed. The time-averaged entanglement depends on the initial and final states and in the particular instances I considered it is always non-zero. Hence entanglement is definitely needed to enable time-optimal evolution. I also showed that all the symmetric, orthogonal initial and final states evolve at the speed limit from $|\psi_I\rangle \rightarrow |\psi_F\rangle$.

I explored the possibility of quantum cloning in the presence of closed timelike curves, that is, I considered a cloning process where a subsystem of the copy machine is allowed to travel in a closed timelike curve. For this kind of cloning process we proved that

- Contrary to what occurs in standard linear quantum evolution, it is possible to clone non-orthogonal states.
- The maximum number of non orthogonal states that can be cloned is limited by the dimension of the Hilbert space associated with the part of the copy machine travelling on a closed timelike curve.

One has to emphasize that the cloning process based upon closed timelike curves cannot be used to implement faster than light signalling.

Appendix A

Numerical Search for Highly Entangled Multi-Qubit States

Highly entangled multi-qubit states are very important, both from the theoretical and practical points of view. That is, highly and maximally entangled states have become a key concept in quantum mechanics and have numerous applications in quantum information as well [98]. For two and three qubits, maximally and highly entangled quantum states such as the Bell states and GHZ states have been discovered. It is thus of great importance to find highly entangled states for four and more qubits. I used different entanglement measures in a searching procedure for highly entangled multi-qubit states of three up to seven qubits. Our results are compared with those reported by Brown *et al* [49].

A.1 Overview

A considerable amount of research has recently been devoted to the study of multi-qubit entanglement measures defined as the sum of bi-partite entanglement measures over all (or an appropriate family of) the possible bi-partitions of the full system [49; 86; 99]. In particular, Brown *et al* [49] have performed a numerical search of multi-qubit states exhibiting a high value of an entanglement

A.2 Pure state multi-partite entanglement measures based on the degree of mixedness of subsystems

measure defined in the aforementioned way, based upon the negativity of the system's bi-partitions. I am going to focus on the results of running numerical searches of multi-qubit states (up to seven qubits) exhibiting high entanglement according to the von Neumann entropy, linear entropy and negativity. The results obtained using each of these three measures are compared to each other, and also compared to those reported by Brown *et al* [49].

The chapter is organized as follows. Some basic properties of the entanglement measures used here are reviewed in Section A.2. Our algorithms for the search of states of high entanglement are presented in Section A.3 and the main results obtained are discussed and compared with those reported by Brown *et al*. Finally, some conclusions are drawn in Section A.4 and the searching algorithm written in MATHEMATICA is provided in Section A.5.

A.2 Pure state multi-partite entanglement measures based on the degree of mixedness of subsystems

As was discussed in Section 1.0.2.5, one can evaluate the degree of mixedness of the marginal density matrices associated with each bi-partition in several ways. In what follows I am going to consider the following ways of computing the degrees of mixedness of the marginal density matrices ρ_i ,

- The linear entropy $S_L = 1 - \text{Tr}[\rho_i^2]$.
- The von Neumann entropy $S_{VN} = -\text{Tr}[\rho_i \log_2 \rho_i]$.
- The “negativity”: $\text{Neg.} = \sum |\alpha_i|$, where α_i are the negative eigenvalues of the partial transpose matrix associated with a given bi-partition. That is, I am going to consider the “negativity” as a measure of the amount of entanglement associated with a given bi-partition.

A.3 Search for multi-qubit states of high entanglement

The global, multipartite entanglement measures associated with the sum (over all bi-partitions) of each of these three quantities are here going to be denoted, respectively, by E_L , E_{VN} and E_N .

A.3 Search for multi-qubit states of high entanglement

A.3.1 Searching algorithm

In the present contribution we are going to restrict our search of multi-qubit states of high entanglement to *pure states*. In this respect our approach is a little different from that of Brown *et al* [49], who considered a search process within the complete space of possible states (that is, with any degree of mixedness). The kind of search studied by Brown *et al* is certainly of interest and may shed some light on the structure of the “entanglement landscape” of the full state space. However, it is reasonable to expect the states of maximum entanglement to be pure. Consequently, as far as the search of states of maximum entanglement is concerned, it seems that limiting the search to pure states is not going to reduce its efficiency. The results reported here fully confirm this expectation.

I am going to consider two different procedures for the search algorithm. The first program was written in the computer language MATHEMATICA and is given in Section A.5. The first procedure I am going to use is similar to the one employed by Brown *et al*, just adapted to pure states.

A general pure state of an N -qubit system can be represented as

$$|\Psi\rangle = \sum_{k=1}^{2^N} (a_k + ib_k)|k\rangle, \quad (\text{A.1})$$

where $|k\rangle$, ($k = 1, \dots, 2^N$) represents the states of the computational basis (that is, the 2^N states $|00\dots 0\rangle$, $|10\dots 0\rangle$, \dots , $|11\dots 1\rangle$). I initialize with a random state and calculate its entanglement. All random quantities are generated by a

A.3 Search for multi-qubit states of high entanglement

built-in function. At each step of the search process, a tentative state is generated according to the following procedure. One of the complex coefficients of $|\psi\rangle$ is randomly chosen and the real and imaginary parts are multiplied by random values δ_{re} and δ_{im} respectively. These random values are chosen from the interval $\{1 - \alpha, 1 + \alpha\}$ with α between 0.1 and 0.5. The new state is then renormalized and the entanglement is calculated. If this new entanglement is greater than the previous one, we keep the new state and set the counters to zero. If the new entanglement is less than the previous one, we reject the new state and randomly chose another coefficient of the previous state and slightly modify it as described. If after 100 steps we do not get a higher entanglement value, we chose a new random pair of numbers δ_{re} and δ_{im} from the interval $\{1 - \alpha, 1 + \alpha\}$ (α is an input parameter, we experiment with different values for α during individual runs of the program) and again choose a coefficient at random. If after 40 000 times of having chosen new random values for δ_{re} and δ_{im} and at each step having chosen random coefficients, we do not get a higher entanglement value than that of the previous state, the program halts. Some optimization is also included: if the magnitude of the real or imaginary part of a coefficient of a normalized state drops below 10^{-2} , that part is set to zero. At the end of a search the resulting state is hand-tweaked and remaining coefficients are set to zero.

The second program was written by a colleague in the computer language FORTRAN. The searching procedure is different to the first one and is as follows. We start our search process with the initial state $|000\dots 0\rangle$. In other words, the initial parameters characterizing the state (A.1) are $a_1 = 1$ and all the rest of the a_i 's and b_i 's are equal to zero. This initial state is fully factorizable and can thus be regarded as being “very distant” from states of high entanglement. Starting with an arbitrary, random initial pure state does not alter the results of the search process. Now, at each step of the search process a new, tentative state is generated according to the following procedure. A random quantity Δ (uniformly chosen from an interval $(-\Delta_{max}, \Delta_{max})$) is added to each a_i and b_i (a different, independent Δ is generated for each parameter). The new state generated in this way is then normalized to 1 and its entanglement measure is computed. If the entanglement of the new state is larger than the entanglement of

A.3 Search for multi-qubit states of high entanglement

the previous state the new state is kept, replacing the previous one. Otherwise, the new state is rejected and a new, tentative state is generated. In order to ensure the convergence of this algorithm to a state of high entanglement, the following two rules are also implemented:

- If 500 consecutive tentative new states are rejected, the interval for the random quantity Δ is changed according to $\Delta_{max} \rightarrow \frac{\Delta_{max}}{2}$ (as the initial value for Δ_{max} we take $\Delta_{max}^{init} = 0.1$).
- When a value $\Delta_{max} \leq 1 \cdot 10^{-8}$ is reached the search program halts.

The difference between the two programs is that for the first one we multiply the components of the coefficients by random numbers in the interval $\{1-\alpha, 1+\alpha\}$ (α is an input parameter and so the interval remains constant), hence by positive numbers. This means that the signs of the real and imaginary parts of the coefficients remain the same. Also, only one coefficient is chosen at each step and modified slightly, whereas the second program changes all the coefficients slightly by adding a small random number to the real and imaginary parts, thus enabling a change of their sign, and after 500 rejected states it halves the interval $(-\Delta_{max}, \Delta_{max})$, thereby narrowing the search.

A.3.2 Results yielded by the searching algorithm

The maximum entanglement values obtained from the searching algorithms are listed in Table A.1. It must be emphasized that the maximum values associated with different measures do not necessarily correspond to the same state. The states obtained when maximizing one particular measure do not exhibit, in general, a maximum value of the other measures. The results obtained by us after running the search algorithms several times (considering the entanglement measures E_L , E_{VN} and E_N) can be summarized as follows,

- Among the three measures considered here, E_L is computationally the easiest and quickest to evaluate. The algorithms run faster when maximizing this measure than when maximizing any of the other two. However, in the

A.3 Search for multi-qubit states of high entanglement

case of four-qubits most states that maximize E_L do not maximize the other measures.

- The measure E_{VN} is computationally more expensive than E_L . The states obtained when maximizing E_{VN} also maximize E_L and E_N .
- E_N is, by far, computationally the most expensive of the measures considered here. The states maximizing this measure also maximize E_L and E_{VN} .

	3 qubits	4 qubits	5 qubits	6 qubits	7 qubits
E_L	1.500000	4.00000	10.000000	23.000000	49.573765
E_{VN}	3.000000	9.37734	25.000000	66.000000	152.620140
E_N	1.500000	6.09807	17.500000	60.500000	155.812856

Table A.1: Maximum entanglement values obtained from search algorithms.

A.3.2.1 Four qubits

In the case of four-qubit systems, the first extremization process based upon either of the measures E_{VN} or E_N mostly results in states having higher entanglement values than the *BSSB4* state (obtained by Brown *et al*)

$$|BSSB4\rangle = \frac{1}{2} \left[|0000\rangle + |1101\rangle + \frac{1}{\sqrt{2}} \left(|0011\rangle + |1011\rangle + |0110\rangle - |1110\rangle \right) \right], \quad (\text{A.2})$$

but slightly lower values than the *HS* state discovered by Higuchi and Sudbery [99], which is given by

$$|HS\rangle = \frac{1}{\sqrt{6}} \left[|1100\rangle + |0011\rangle + \omega \left(|1001\rangle + |0110\rangle \right) + \omega^2 \left(|1010\rangle + |0101\rangle \right) \right], \quad (\text{A.3})$$

A.3 Search for multi-qubit states of high entanglement

with $\omega = -\frac{1}{2} + \frac{\sqrt{3}}{2}i$. Occasionally the program converged to the *HS* state and very few times to the *BSSB4* state.

The second extremization process (based upon either of the measures E_{VN} or E_N) always leads to states having the same entanglement values as those exhibited by the *HS* state. We repeated the search process starting with different, random initial conditions and always found states with entanglement values corresponding to the *HS* state.

In order to establish which feature of the second program is responsible for the convergence to the *HS* state, I modified the first program as follows: instead of multiplying by a positive number in the interval $\{1 - \alpha, 1 + \alpha\}$, I added a small random number from the interval $\{-\alpha, \alpha\}$ to the parts of the randomly chosen coefficient, keeping the size of the interval fixed. The modified program then converged nearly all the time to states with the same entanglement values as the *HS* state. It thus seems to be that the possibility of a sign-change in the parts of the coefficients enables the program to result in unitary transformations of the *HS* state.

This constitutes convincing numerical evidence that the *HS* state is, at least, a local maximum of both the E_{VN} and the E_N measures. Higuchi and Sudbery [99] have provided analytical arguments supporting the conjecture that the *HS* state is indeed a global maximum for E_{VN} , but this conjecture has not been proved yet. These authors have also proved that there is no pure state of four qubits such that all its two-qubit marginal density matrices are completely mixed [99].

It is interesting that Brown *et al* [49], when performing a search process (using a program written in MATLAB) similar (but not identical) to the ones considered here, obtained instead of the *HS* state always a state (which we here call *BSSB4*) exhibiting values of E_{VN} and E_N smaller than those exhibited by *HS*. Besides some intrinsic differences in the algorithm itself, there is the fact that the main results reported here were computed starting the search process with a pure state, while Brown *et al* started their search with a mixed state. When

A.3 Search for multi-qubit states of high entanglement

running the search algorithms maximizing the E_L measure, we obtained several different final states, some of them exhibiting values of E_{VN} larger than the value corresponding to the state $BSSB4$. Both the HS and the $BSSB4$ state have $E_L = 4$, as well as some states whose values for E_{VN} are less than that of $BSSB4$. It seems to be that $E_L = 4$ is the highest possible linear entanglement value for four qubits.

All these findings suggest that, perhaps, the state $BSSB4$ has no special significance (although it certainly is a highly entangled four-qubit state). Its appearance when running the searching scheme developed by Brown *et al* may be just an accident due to some subtle feature of that algorithm (such as multiplying the parts of the coefficients with random positive numbers in the interval $\{1 - \alpha, 1 + \alpha\}$, thus always keeping their signs the same) or due to the fact that they performed the search using mixed states.

A.3.2.2 Five qubits

When running our search schemes for states of five qubits, we always obtain states exhibiting the same entanglement values as the state obtained by Brown *et al* [49],

$$|BSSB5\rangle = \frac{1}{2} \left[|000\rangle |\Phi_{-}\rangle + |010\rangle |\Psi_{-}\rangle + |100\rangle |\Phi_{+}\rangle + |111\rangle |\Psi_{+}\rangle \right] \quad (\text{A.4})$$

where $\Psi_{\pm} = |00\rangle \pm |11\rangle$ and $\Phi_{\pm} = |01\rangle \pm |10\rangle$. This state has all its marginal density matrices (for 1 and 2 qubits) completely mixed.

A.3.2.3 Six qubits

In the case of six qubits, our algorithms converge to highly entangled states exhibiting all the marginal density matrices for states of 1, 2 and 3 qubits completely mixed. In particular, we discovered the following new state of high entanglement,

$$\begin{aligned} \Psi_{6qb} = \frac{1}{\sqrt{32}} & \left[|000000\rangle + |111111\rangle + |000011\rangle + |111100\rangle + |000101\rangle + |111010\rangle \right. \\ & \left. + |000110\rangle + |111001\rangle + |001001\rangle + |110110\rangle + |001111\rangle + |110000\rangle \right] \end{aligned}$$

A.3 Search for multi-qubit states of high entanglement

$$\begin{aligned}
 & +|010001\rangle + |101110\rangle + |010010\rangle + |101101\rangle + |011000\rangle + |100111\rangle \\
 & +|011101\rangle + |100010\rangle - (|001010\rangle + |110101\rangle + |001100\rangle + |110011\rangle \\
 & +|010100\rangle + |101011\rangle + |010111\rangle + |101000\rangle + |01011\rangle + |100100\rangle \\
 & +|011110\rangle + |100001\rangle). \tag{A.5}
 \end{aligned}$$

This state has a rather simple structure, with all its coefficients (when expanded in the computational basis) equal to 0 or ± 1 (the same situation occurs for maximally entangled states of 2, 3 and 5 qubits).

A.3.2.4 Seven qubits

When we ran the search programs for seven-qubit states of high entanglement we found states with the following features: they all have completely mixed single-qubit marginal density matrices. However, these states do not exhibit completely mixed two-qubit and three-qubit marginal density matrices (in this sense, the present situation seems to have some similarities with the four-qubit case).

The high-entanglement states of seven qubits that we found are characterized by two-qubits marginal density matrices exhibiting the following entropic values:

$$1 - \text{Tr}(\rho_i^2) = 0.7445111988 \tag{A.6}$$

$$S_{VN}(\rho_i) = 1.9841042. \tag{A.7}$$

The three-qubit marginal density matrices of these seven-qubit states have

$$1 - \text{Tr}(\rho_i^2) = 0.86209018886 \tag{A.8}$$

$$S_{VN}(\rho_i) = 2.93739788. \tag{A.9}$$

When running our programs (maximizing either E_{VN} or E_N) for five-qubit or six-qubit states, *the search process always leads to a state whose marginal density matrices of 1,2, and (in the six-qubit case) 3 qubits are completely mixed.* On the contrary, this never happens when running our algorithms for seven-qubits states. The marginal density matrices of 1-qubit subsystems turn out to be maximally mixed, but not the marginal density matrices corresponding to subsystems consisting of 2 or 3 qubits. Moreover, all the runs of the algorithms for

A.4 Conclusions

seven-qubits states yielded states with the same entropic values for the marginal statistical operators. This suggests that the case of seven qubits may have some similarities with the case of four qubits. In other words, our results constitute numerical evidence supporting the

Conjecture: *There is no pure state of seven qubits whose marginal density matrices for subsystems of 1, 2 and 3 qubits are all completely mixed.*

A.3.2.5 The single-qubit reduced states conjecture

It was conjectured by Brown *et al* [49] that multi-qubit states of maximum entanglement always have all their single-qubit marginal density matrices completely mixed. The results obtained by us when running the search algorithms maximizing the E_{VN} and E_N measures are consistent with the aforementioned conjecture. All the states yielded by the searching algorithms (up to systems of seven qubits) have maximally mixed single qubit marginal density matrices. Moreover, in the case of 5 qubits all the states obtained also exhibited maximally mixed two-qubits marginal density matrices. In the case of 6 qubits, all the states obtained had completely mixed marginal density matrices of one, two and three qubits.

A.4 Conclusions

In this Appendix I investigated some aspects of the entanglement properties of multi-qubit systems. I considered global multi-qubit entanglement measures based upon the idea of considering all the possible bi-partitions of the system. For each bi-partition we computed a bi-partite entanglement measure (such as the von Neumann entropy of the marginal density matrix associated with the subsystem with a Hilbert space of lower dimensionality) and then summed the measures associated with all the bi-partitions. In order to evaluate the bi-partite contributions we considered three different quantities: the von Neumann and linear entropies, and the negativity.

A.4 Conclusions

We determined, for systems of four, five, six and seven qubits, states of high entanglement using search schemes akin, but not identical to, the one recently advanced by Brown *et al* [49]. These authors performed the search process using an entanglement measure based on the negativity. The results obtained by us when using the three different measures have some interesting features. First of all, we found that a search algorithm based on the von Neumann entropy is as successful as one based upon negativity. However, the von Neumann entropy is (in general) considerably less expensive to compute than the negativity. Consequently, when initializing the search process with a pure state, it is better to use the von Neumann entropy.

In the case of four-qubit states our one algorithm always converged to states exhibiting the same entanglement measures as those characterizing the HS state and the other algorithm (before having being modified) converged most of the time to states with slightly lower values than the HS state but higher values than the $BSSB4$ state, whereas Brown *et al* reported that their search algorithm always converged (up to local unitary transformations) to a state (here called the $BSSB4$ state) exhibiting less entanglement than the HS state. Our results thus provide further support to the conjecture advanced by Higuichi and Sudbery [99] that the HS state corresponds to a global entanglement maximum for four-qubits states. Another interesting discovery made using our search algorithms is a particular state of six qubits that has all its marginal density matrices of 1, 2 and 3 qubits completely mixed. It is worth noting that (in the computational basis) all the coefficients characterizing this state are (up to a global normalization constant) equal to 0 or ± 1 .

On the basis of the numerical evidence obtained by us when running our search algorithms for highly entangled states of seven qubits, we make the conjecture that there is no pure state of seven qubits whose marginal density matrices for subsystems of 1, 2 and 3 qubits are all completely mixed.

A.5 Search algorithm (MATHEMATICA)

A.5 Search algorithm (MATHEMATICA)

```

(* Function definitions *)

(* Determine the kth basis vector of dimension n, 0 ≤ k ≤ 2n-1 *)
BasisVector[k_, n_] := Module[{l, a, Q, n1},
  l = 1;
  a = Mod[k, 2];
  Q = Table[0, {n}];
  Q[[l]] = a;
  l++;
  n1 =  $\frac{k - a}{2}$ ;
  While[n1 > 0, a = Mod[n1, 2]; Q[[l]] = a; n1 =  $\frac{n1 - a}{2}$ ; l++];
  Q = Reverse[Q]

(* Convert binary representation to decimal value *)
BasisConvert[inp_, n_] := Module[{k, bin}, bin = 0; For[k = 1, k ≤ Length[inp], k++, bin = bin + inp[[k]] * 2n-k]; bin = bin + 1]

(* Normalize the given state *)
NormalizeState[coef_] := Module[{norm}, norm = Chop[Sum[coef[[i]] * Conjugate[coef[[i]], {i, 1, Length[coef]}]]];  $\frac{\text{coef}}{\sqrt{\text{norm}}}$ ]

(* Partial trace of a multi-qubit system *)
SwapParts[expr_, pos1_, pos2_] := ReplacePart[#, #, {pos1, pos2}, {pos2, pos1}] &[expr]
TraceSystem[D_, s_] := (
  Qubits = Reverse[Sort[s]];
  TrkM = D;
  z = (Dimensions[Qubits][[1]] + 1);
  For[q = 1, q < z, q++,
    nq = Log[2, (Dimensions[TrkM][[1]])];
    Mt = TrkM;
    k = Qubits[[q]];
    If[k == nq,
      TrkM = {};
      For[p = 1, p < 2nq + 1, p = p + 2,
        TrkM = Append[TrkM, Take[Mt[[p, All]], {1, 2nq, 2}] + Take[Mt[[p + 1, All]], {2, 2nq, 2}]];
      ],
  ];
  For[j = 0, j < (nq - k), j++,
    b = {0};
    For[i = 1, i < 2nq + 1, i++,
      If[(Mod[(IntegerDigits[i - 1, 2, nq][[nq]] + IntegerDigits[i - 1, 2, nq][[nq - j - 1]], 2]) == 1 && Count[b, i] == 0,
        Permut = {i, (FromDigits[SwapParts[(IntegerDigits[i - 1, 2, nq]), {nq}, {nq - j - 1}], 2] + 1)}];
        b = Append[b, (FromDigits[SwapParts[(IntegerDigits[i - 1, 2, nq]), {nq}, {nq - j - 1}], 2] + 1)];
        c = Range[2nq];

```


A.5 Search algorithm (MATHEMATICA)

```
(* Calculates the von Neumann entropy  $E_{VN}$  of densityMatrix with given partition list and n *)
vNEntanglement [n_, plist_, densityMatrixspecific_] := Module[{marginalDensityMatrix, Entang, sumt},
  sumt = 0;
  Do[
    marginalDensityMatrix = TraceSystem[densityMatrixspecific, plist[[k]]];
    evalues = Chop[Eigenvalues[marginalDensityMatrix]];
    eigvalue = evalues;
    Do[If[eigvalue[[t]] == 0, eigvalue[[t]] = 1, eigvalue[[t]] = eigvalue[[t]]], {t, 1, Length[eigvalue]};
    diagonalizedmatrix = DiagonalMatrix[evalues];
    diagmatrix = DiagonalMatrix[Log[2, eigvalue]];
    Entang = -Chop[Tr[diagonalizedmatrix . diagmatrix]];
    sumt = sumt + Entang,
    {k, 1, 2n-1 - 1}]; sumt
]

(* Calculates the negativity  $E_N$  of densityMatrix with given partition list and n *)
NPTEntanglement [n_, plist_, densityMatrixspecific_] :=
Module[{k, u, t, m, kp, newPartialTranspose, eigenvalueSum, tot, eig, inputList, nb1, nb2},
  newPartialTranspose = Table[Table[0, {2n}], {2n};
  eigenvalueSum = 0;
  For[k = 1, k ≤ Length[plist], k++,
    For[u = 1, u ≤ 2n, u++,
      For[t = 1, t ≤ 2n, t++,
        inputList = plist[[k]];
        l1 = BasisVector[u - 1, n];
        l2 = BasisVector[t - 1, n];
        Do[temp = l1[[inputList[[m]]]];
          l1[[inputList[[m]]]] = l2[[inputList[[m]]]];
          l2[[inputList[[m]]]] = temp, {m, 1, Length[inputList]};
        nb1 = BasisConvert[l1, n];
        nb2 = BasisConvert[l2, n];
        newPartialTranspose[[nb1, nb2]] = densityMatrixspecific[[u, t]];
      ]
    ];
  eig = Chop[Eigenvalues[newPartialTranspose]];
  tot = 0;
  Do[tot = tot + If[eig[[kp]] < 0, eig[[kp]], 0], {kp, 1, 2n};
  (*Print[eig];*)
  eigenvalueSum = eigenvalueSum - tot;
]
eigenvalueSum;
N[eigenvalueSum]

(* Main program *)

(* Initialization of state *)
Clear[a, b, z]

n = 4
α = 0.1;
δre = Random[Real, {1 - α, 1 + α}];
δim = Random[Real, {1 - α, 1 + α}];
NoPartitions = 2n-1 - 1;

plist = PartitionList[n]

a = Table[Random[Real, {-1, 1}], {2n};
d = Table[Random[Real, {-1, 1}], {2n};

cnew = Table[a[[i]] + i d[[i]], {i, 1, 2n};
cnew = NormalizeState[cnew];
densityMatrix = Outer[Times, cnew, Conjugate[cnew]];
Enew = vNEntanglement[n, plist, densityMatrix];
N[Enew]
```

A.5 Search algorithm (MATHEMATICA)

```

(* Search algorithm *)
t0 = 0;
t1 = 0;
datalist = {Enew};
Timing[While[t0 < 20000,
  While[t1 < 100,
    cold = cnew;
    Eold = Enew;
    R = Random[Integer, {1, 2^n}];
    atemp = a[[R]];
    dtemp = d[[R]];
    a[[R]] = a[[R]]  $\delta_{re}$ ;
    d[[R]] = d[[R]]  $\delta_{im}$ ;
    cnew = Tweak[a, d, n];
    cnew = NormalizeState[cnew];
    densityMatrix = Outer[Times, cnew, Conjugate[cnew]];
    Enew = vNEntanglement[n, plist, densityMatrix];

    If[Enew > Eold,
      t0 = 0; t1 = 0; datalist = Append[datalist, Enew];, (* True - new state accepted *)

      cnew = cold; (* False - new state rejected *)
      Enew = Eold;
      a[[R]] = atemp;
      d[[R]] = dtemp;
      t0++;
      t1++;
    ];
  ];

  t1 = 0;
   $\delta_{re}$  = Random[Real, {1 -  $\alpha$ , 1 +  $\alpha$ });
   $\delta_{im}$  = Random[Real, {1 -  $\alpha$ , 1 +  $\alpha$ });
];
N[Enew]
cnew // MatrixForm
ListPlot[datalist]
datalist

(* Final state of search algorithm *)
Print["n = ", n]
Do[Print[cnew[[k + 1]], " ~ ", BasisVector[k, n]], {k, 0, 2^n - 1}]
cnew;
densityMatrixspecific = Chop[Outer[Times, cnew, Conjugate[cnew]]];
Print["EVM = ", Enew]
Print["EL = ", Entanglement[n, plist, densityMatrixspecific]]
Print["EN = ", NPTEntanglement[n, plist, densityMatrixspecific]]
Print["normalized state = ", cnew]

```

A.6 The End

*What we call the beginning is often the end,
And to make an end is to make a beginning.*

The end is where we start from...

*And the end of all our exploring
Will be to arrive where we started
And know the place for the first time.*

T.S. Eliot

References

- [1] W. H. Zurek, *Complexity, Entropy, and the Physics of Information* (Redwood City, California: Addison-Wesley, 1990)
- [2] C. Beck and F. Schlogl, *Thermodynamics of Chaotic Systems* (Cambridge: Cambridge University Press, 1993)
- [3] B. R. Frieden and B. H. Soffer, “Lagrangians of physics and the game of Fisher-information transfer”, *Phys. Rev. E* **52** (3), (1995) pp. 2274–2286
- [4] B. R. Frieden, *Physics from Fisher Information* (Cambridge: Cambridge University Press, 1998)
- [5] B. R. Frieden, *Science from Fisher Information* (Cambridge: Cambridge University Press, 2004)
- [6] H. S. Leff and A. F. Rex, *Maxwell’s Demons 2: Entropy, Classical and Quantum Information* (Bristol, Philadelphia: Institute of Physics Publishing, 2003)
- [7] S. Curilef, F. Pennini and A. Plastino, “Fisher information, Wehrl entropy, and Landau diamagnetism”, *Phys. Rev. B* **71** (024420), (2005) pp. 1–5
- [8] F. Pennini and A. Plastino, “Power-law distributions and Fisher’s information measure”, *Physica A* **334**, (2004) pp. 132–138
- [9] L. P. Chimento, F. Pennini and A. Plastino, “Naudts-like duality and the extreme Fisher information principle”, *Phys. Rev. E* **62** (5), (2000) pp. 7462–7465

REFERENCES

- [10] F. Pennini and A. Plastino, “Fisher information, canonical ensembles, and Hamiltonian systems”, *Phys. Lett. A* **349**, (2006) pp. 15–20
- [11] S. Lloyd, *Programming the Universe* (London: Jonathan Cape, 2006)
- [12] S. Lloyd, V. Giovannetti and L. Maccone, “Physical Limits to Communication”, *Phys. Rev. Lett* **93 (100501)**, (2004) pp. 1–4
- [13] S. Lloyd, “Computational capacity of the universe”, *Phys. Rev. Lett.* **88 (237901)**, (2002) pp. 1–4
- [14] S. Lloyd, “Ultimate physical limits to computation”, *Nature* **406 (6799)**, (2000) pp. 1047–1054
- [15] A. Daffertshofer, A. R. Plastino and A. Plastino, “Classical No-Cloning Theorem”, *Phys. Rev. Lett.* **88 (210601)**, (2002) pp. 1–4
- [16] A. R. Plastino and A. Daffertshofer, “Liouville Dynamics and the Conservation of Classical Information”, *Phys. Rev. Lett.* **93 (138701)**, (2004) pp. 1–4
- [17] S. Lloyd, “Rolf Landauer (1927-99)”, *Nature* **400 (6746)**, (1999) p. 720
- [18] R. Landauer, “Irreversibility and Heat Generation in the Computing Process”, *IBM J. Res. Develop.* **5 (3)**, (1961) p. 183
- [19] A. Daffertshofer and A. R. Plastino, “Landauer’s Principle and the Conservation of Information”, *Phys. Lett. A* **342 (3)**, (2005) pp. 213–216
- [20] B. Piechocinska, “Information erasure”, *Phys. Rev. A* **61 (062314)**, (2000) pp. 1–9
- [21] M. B. Plenio and V. Vitelli, “The physics of forgetting: Landauers erasure principle and information theory”, *Contemp. Phys.* **42 (1)**, (2001) pp. 25–60
- [22] A. Daffertshofer and A. R. Plastino, “Forgetting and Gravitation: From Landauer’s Principle to Tolman’s Temperature”, *Phys. Lett. A* **362 (4)**, (2007) pp. 243–245

REFERENCES

- [23] A. Peres, *Quantum Theory: Concepts and Methods* (Dordrecht: Kluwer, 1993)
- [24] N. Gisin, “Quantum cloning without signaling”, *Phys. Lett. A* **242** (1), (1998) pp. 1–3
- [25] A. Rényi, “On Measures of Entropy and Information”, *Proc. 4th Berkeley Symp. Math. Stat. and Prob.* **1**, (1961) pp. 547–561
- [26] E. T. Jaynes, “Information Theory and Statistical Mechanics”, *Phys. Rev.* **106** (4), (1957) pp. 620–630
- [27] E. T. Jaynes, “Information Theory and Statistical Mechanics II”, *Phys. Rev.* **108** (2), (1957) pp. 171–190
- [28] E. T. Jaynes, *Probability Theory: The Logic of Science* (Cambridge: Cambridge University Press, 2003)
- [29] C. Tsallis, “Possible generalization of Boltzmann-Gibbs statistics”, *J. Stat. Phys.* **52**, (1988) pp. 479–487
- [30] A. R. Plastino and A. Plastino, “Tsallis’ entropy, Ehrenfest theorem and information theory”, *Phys. Lett. A* **177**, (1993) pp. 177–179
- [31] J. A. S. Lima, R. Silva and A. R. Plastino, “Nonextensive Thermostatistics and the H Theorem”, *Phys. Rev. Lett.* **86** (14), (2001) pp. 2938–2941
- [32] M. Gell-Mann and C. Tsallis, *Nonextensive Entropy: Interdisciplinary Applications* (Oxford: Oxford University Press, 2004)
- [33] M. A. Nielsen and I. L. Chuang, *Quantum Computation and Quantum Information* (Cambridge: Cambridge University Press, 2000)
- [34] H. Barnum, M. A. Nielsen and B. Schumacher, “Information transmission through a noisy quantum channel”, *Phys. Rev. A* **57** (6), (1998) pp. 4153–4175
- [35] A. Ekert, “Quantum cryptography based on Bell’s theorem”, *Phys. Rev. Lett.* **67** (6), (1991) pp. 661–663

REFERENCES

- [36] C. H. Bennett, G. Brassard, C. Crepeau, R. Jozsa, A. Peres and W. K. Wootters, “Teleporting an unknown quantum state via dual classical and Einstein-Podolsky-Rosen channels”, *Phys. Rev. Lett.* **70** (13), (1993) pp. 1895–1899
- [37] C. H. Bennett and S. J. Wiesner, “Communication via one- and two-particle operators on Einstein-Podolsky-Rosen states”, *Phys. Rev. Lett.* **69** (20), (1992) pp. 2881–2884
- [38] A. Ekert and R. Jozsa, “Quantum computation and Shor’s factoring algorithm”, *Rev. Mod. Phys.* **68** (3), (1996) pp. 733–753
- [39] H.-K. Lo, S. Popescu and T. Spiller, *Introduction to Quantum Computation and Information* (River Edge: World Scientific, 1998)
- [40] A. Ekert and P. L. Knight, “Entangled quantum systems and the Schmidt decomposition”, *Am. J. Phys.* **63** (5), (1995) pp. 415–423
- [41] S. Popescu and D. Rohrlich, “Thermodynamics and the measure of entanglement”, *Phys. Rev. A* **56** (5), (1997) pp. R3319–R3321
- [42] P. M. Ainsworth, “Untangling Entanglement”, *Found. Phys.* **37** (1), (2007) pp. 144–158
- [43] C. H. Bennett, H. J. Bernstein, S. Popescu and B. Schumacher, “Concentrating partial entanglement by local operations”, *Phys. Rev. A* **53** (4), (1996) pp. 2046–2052
- [44] W. K. Wootters, “Entanglement of Formation of an Arbitrary State of Two Qubits”, *Phys. Rev. Lett.* **80** (10), (1998) pp. 2245–2248
- [45] C. H. Bennett, D. P. DiVincenzo, J. Smolin and W. K. Wootters, “Mixed-state entanglement and quantum error correction”, *Phys. Rev. A* **54** (5), (1996) pp. 3824–3851
- [46] A. Peres, “Separability Criterion for Density Matrices”, *Phys. Rev. Lett.* **77** (8), (1996) pp. 1413–1415

REFERENCES

- [47] P. Horodecki, “Separability criterion and inseparable mixed states with positive partial transposition”, *Phys. Lett. A* **232**, (1997) pp. 333–339
- [48] K. Życzkowski, P. Horodecki, A. Sanpera and M. Lewenstein, “Volume of the set of separable states”, *Phys. Rev. A* **58 (2)**, (1998) pp. 883–892
- [49] I. D. K. Brown, S. Stepney, S. Sudbery and S. L. Braunstein, “Searching for highly entangled multi-qubit states”, *J. Phys. A: Math. Gen.* **38 (5)**, (2005) pp. 1119–1131
- [50] C. Zander, A. R. Plastino, A. Plastino and M. Casas, “Entanglement and the speed of evolution of multi-partite quantum systems”, *J. Phys. A: Math. Theor.* **40 (11)**, (2007) pp. 2861–2872
- [51] A. Borrás, A. R. Plastino, J. Batle, C. Zander, M. Casas and A. Plastino, “Multi-qubit systems: highly entangled states and entanglement distribution”, *J. Phys. A* **preprint (2007)**
- [52] N. Margolus and L. B. Levitin, “The maximum speed of dynamical evolution”, *Physica D* **120**, (1998) pp. 188–195
- [53] V. Giovannetti, S. Lloyd and L. Maccone, “The role of entanglement in dynamical evolution”, *Europhys. Lett.* **62 (5)**, (2003) pp. 615–621
- [54] L. Mandelstam and I. Tamm, “The uncertainty relation between energy and time in nonrelativistic quantum mechanics”, *J. Phys. (USSR)* **9**, (1945) pp. 249–254
- [55] L. Vaidman, “Minimum time for the evolution to an orthogonal quantum state”, *Am. J. Phys.* **60 (2)**, (1992) pp. 182–183
- [56] W. K. Wootters and W. H. Zurek, “A single quantum cannot be cloned”, *Nature* **299**, (1982) pp. 802–803
- [57] D. Dieks, “Communication by EPR devices”, *Phys. Lett.* **92A (6)**, (1982) pp. 271–272

REFERENCES

- [58] A. R. Plastino and C. Zander, “Would Closed Timelike Curves Help to Do Quantum Cloning?”, *AIP Conf. Proc.: A century of relativity physics, ERE* **841**, (2005) pp. 570–573
- [59] D. Deutsch, “Quantum mechanics near closed timelike lines”, *Phys. Rev. D* **44 (10)**, (1991) pp. 3197–3217
- [60] D. Bacon, “Quantum computational complexity in the presence of closed timelike curves”, *Phys. Rev. A* **70 (032309)**, (2004) pp. 1–7
- [61] C. Tsallis, M. Gell-Mann and Y. Sato, “Asymptotically Scale-Invariant Occupancy of Phase Space Makes the Entropy S_q Extensive”, *Proceedings of the National Academy of Sciences of the USA (PNAS)* **102**, (2005) p. 15,377
- [62] C. Zander and A. R. Plastino, “Composite systems with extensive S_q (power-law) entropies”, *Physica A* **364**, (2006) pp. 145–156
- [63] C. Tsallis, “Nonextensive Statistics: Theoretical, Experimental and Computational Evidences and Connections”, *Braz. J. Phys.* **29 (1)**, (1999) pp. 1–35
- [64] B. Boghosian, “Thermodynamic description of the relaxation of two-dimensional turbulence using Tsallis statistics”, *Phys. Rev. E* **53 (5)**, (1996) pp. 4754–4763
- [65] A. R. Plastino, “ S_q Entropy and Self-Gravitating Systems”, *Europhysics News* **36 (6)**, (November/December 2005) pp. 208–210
- [66] A. Taruya and M. Sakagami, “Antonov problem and quasi-equilibrium states in an N-body system”, *Mon. Not. R. Astron. Soc.* **364 (3)**, (2005) pp. 990–1010
- [67] C. Beck, “Dynamical Foundations of Nonextensive Statistical Mechanics”, *Phys. Rev. Lett.* **87 (180601)**, (2001) pp. 1–4
- [68] H. Uys, H. G. Miller and F. C. Khanna, “Generalized statistics and high- T_c superconductivity”, *Phys. Lett. A* **289**, (2001) pp. 264–272

REFERENCES

- [69] A. Upadhyaya, J.-P. Rieu, J. Glazier and Y. Sawada, “Anomalous diffusion and non-Gaussian velocity distribution of *Hydra* cells in cellular aggregates”, *Physica A* **293**, (2001) pp. 549–558
- [70] L. Borland, “Option Pricing Formulas Based on a Non-Gaussian Stock Price Model”, *Phys. Rev. Lett.* **89 (098701)**, (2002) pp. 1–4
- [71] A. R. Plastino and A. Plastino, “Non-extensive statistical mechanics and generalized Fokker-Planck equation”, *Physica A* **222**, (1995) pp. 347–354
- [72] T. D. Frank, *Nonlinear Fokker-Planck Equations* (Berlin: Springer-Verlag, 2005)
- [73] Z. Chen, “Wigner-Yanase skew information as tests for quantum entanglement”, *Phys. Rev. A* **71 (052302)**, (2005) pp. 1–5
- [74] S. Curilef, C. Zander and A. R. Plastino, “Two particles in a double well: illustrating the connection between entanglement and the speed of quantum evolution”, *Eur. J. Phys.* **27**, (2006) pp. 1193–1203
- [75] J. J. Sakurai, *Modern Quantum Mechanics* (Menlo Park, Calif.: Benjamin, 1985)
- [76] R. P. Feynman, R. B. Leighton and M. L. Sands, *The Feynman Lectures on Physics*, vol.3 (New York: Addison-Wesley, 1969)
- [77] G. B. Roston, M. Casas, A. Plastino and A. R. Plastino, “Quantum entanglement, spin-1/2 and the Stern-Gerlach experiment”, *Eur. J. Phys.* **26**, (2005) pp. 657–672
- [78] M. Razavy, “An exactly soluble Schrödinger equation with a bistable potential”, *Am. J. Phys.* **48**, (1980) pp. 285–288
- [79] V. Giovannetti, S. Lloyd and L. Maccone, “Quantum limits to dynamical evolution”, *Phys. Rev. A* **67 (052109)**, (2003) pp. 1–8

REFERENCES

- [80] J. Batle, M. Casas, A. Plastino and A. R. Plastino, “Connection Between Entanglement and the Speed of Quantum Evolution”, *Phys. Rev. A* **72 (032337)**, (2005) pp. 1–5
- [81] D. McHugh, M. Ziman and V. Buzek, “Entanglement, purity, and energy: Two qubits versus two modes”, *Phys. Rev. A* **74 (042303)**, (2006) pp. 1–13
- [82] M. Taut, “Two electrons in an external oscillator potential: Particular analytic solutions of a Coulomb correlation problem”, *Phys. Rev. A* **48 (5)**, (1993) pp. 3561–3566
- [83] J. Batle, M. Casas, A. R. Plastino and A. Plastino, “Entanglement, mixedness, and q -entropies”, *Phys. Lett. A* **296 (6)**, (2002) pp. 251–320
- [84] S. Lloyd, “The power of entangled quantum channels”, *arXiv quant-ph/0112034 v1*, (2001) pp. 1–14
- [85] L. S. Braunstein and P. van Loock, “Quantum information with continuous variables”, *Rev. Mod. Phys.* **77**, (2005) pp. 513–577
- [86] A. J. Scott, “Multipartite entanglement, quantum-error-correcting codes, and entangling power of quantum evolutions”, *Phys. Rev. A* **69 (052330)**, (2004) pp. 1–10
- [87] D. A. Meyer and N. R. Wallach, “Global entanglement in multiparticle systems”, *J. Math. Phys.* **43 (9)**, (2002) pp. 4273–4278
- [88] G. K. Brennen, *Quantum Inf. Comput.* **3**, (2003) p. 619
- [89] Y. S. Weinstein and C. S. Hellberg, “Entanglement Generation of Nearly Random Operators”, *Phys. Rev. Lett.* **95 (030501)**, (2005) pp. 1–4
- [90] Y. S. Weinstein and C. S. Hellberg, “Matrix-element distributions as a signature of entanglement generation”, *Phys. Rev. A* **72 (022331)**, (2005) pp. 1–6

REFERENCES

- [91] M. Cao and S. Zhu, “Thermal entanglement between alternate qubits of a four-qubit Heisenberg XX chain in a magnetic field”, *Phys. Rev. A* **71** (034311), (2005) pp. 1–4
- [92] A. Lakshminarayan and V. Subrahmanyam, “Multipartite entanglement in a one-dimensional time-dependent Ising model”, *Phys. Rev. A* **71** (062334), (2005) pp. 1–12
- [93] A. R. R. Carvalho, F. Mintert and A. Buchleitner, “Decoherence and Multipartite Entanglement”, *Phys. Rev. Lett.* **93** (230501), (2004) pp. 1–4
- [94] L. Aolita and F. Mintert, “Measuring Multipartite Concurrence with a Single Factorizable Observable”, *Phys. Rev. Lett.* **97** (050501), (2006) pp. 1–4
- [95] J. Anandan and Y. Aharonov, “Geometry of Quantum Evolution”, *Phys. Rev. Lett.* **65** (14), (1990) pp. 1697–1700
- [96] D. C. Brody and D. W. Hook, “On optimum Hamiltonians for state transformations”, *J. Phys. A: Math. Gen.* **39** (11), (2006) pp. L167–L170
- [97] A. Borras, M. Casas, A. R. Plastino and A. Plastino, “Entanglement and the lower bounds on the speed of quantum evolution”, *Phys. Rev. A* **74** (022326), (2006) pp. 1–8
- [98] N. Gisin, G. Ribordy, W. Tittel and H. Zbinden, “Quantum cryptography”, *Rev. Mod. Phys.* **74** (1), (2002) pp. 145–195
- [99] A. Higuchi and A. Sudbery, “How entangled can two couples get?”, *Phys. Lett. A* **273**, (2000) pp. 213–217